

**Key Roles of Ubiquitination and Phosphorylation in
RIG-I/MAVS Viral Sensing Pathway**

APPROVED BY SUPERVISORY COMMITTEE

Dr. Zhijian “James” Chen

Dr. George DeMartino

Dr. Nicolai Van Oers

Dr. Eric N Olson (Chair)

DEDICATION

I would like to thank my parents, especially my mother, Jinyan Si, for her endless and unconditional love, care and support throughout my life. Her insistence, strength, thoughtfulness and confidence about life have always been the inspiration for me to chase my dream. I also would like to thank Xin Cai, for his support, love and enormous help, both personally and professionally. Without them, I would have been nowhere close to today's achievement.

I would also like to thank my mentor, Dr. James Chen for his mentoring and support, both personally and professionally. He has been my role model.

I thank my thesis committee, Dr. Eric N. Olson, Dr. Nicolai Van Oers and Dr. George DeMartino, for their support and care professionally.

I thank all the present and past Chen lab members for their help and inspiring ideas, especially Dr. Lijun Josh Sun, who has offered me enormous help throughout my graduation school and Beethoven Ramirez, the lab manager and a good friend, who has used his selflessness and care to make my life smooth and full of joy.

I thank Dr. Jose Rizo-Rey, as my rotation mentor and a good friend, for his effort and kindness to boost my confidence at the beginning and for his care along the way.

This thesis is only a beginning of my journey.

**KEY ROLES OF UBIQUITINATION AND PHOSPHORYLATION IN
RIG-I/MAVS VIRAL SENSING PATHWAY**

by

SIQI LIU

DISSERTATION THESIS

Presented to the Faculty of the Graduate School of Biomedical Sciences

The University of Texas Southwestern Medical Center at Dallas

In Partial Fulfillment of the Requirements

For the Degree of

DOCTOR OF PHILOSOPHY

The University of Texas Southwestern Medical Center at Dallas

Dallas, Texas

May, 2013

Copyright

by

SIQI LIU, 2013

All Rights Reserved

Key Roles of Ubiquitination and Phosphorylation in RIG-I/MAVS Viral Sensing Pathway

Publication No. _____

SIQI LIU, Ph.D

The University of Texas Southwestern Medical Center at Dallas, 2012

Supervising Professor: Dr. Zhijian “James” Chen

RNA virus infections are detected by the RIG-I family of receptors, which induce the production of type-I interferons (IFNs) and other antiviral molecules through the mitochondrial membrane protein MAVS. We have recently shown that MAVS forms large prion-like aggregates in response to virus infection and that these aggregates are highly potent in activating the cytosolic kinases IKK and TBK1, which in turn activate NF- κ B and IRF3, respectively, to induce IFNs. However, the mechanisms remain unknown. Here I showed that MAVS aggregates recruited several TRAF proteins, including TRAF2, TRAF3, TRAF5 and TRAF6, through two distinct TRAF binding motifs. Mutations of both motifs in

MAVS that disrupted its binding to the TRAF proteins were necessary to abrogate its ability to activate IRF3 and induce IFN β . These antiviral responses were also abolished in cells lacking TRAF2, 5, and 6, but not in those lacking individual TRAF protein. These TRAF proteins catalyze ubiquitination reactions that recruit NEMO to the MAVS signaling complex, leading to the activation of IKK and TBK1. MAVS phosphorylation by the recruited kinases then brings IRF3 to the complex, where IRF3 is phosphorylated by TBK1. These results reveal that MAVS, through the recruitment of multiple E3 ligases, not only activate downstream kinases but also specifies IRF3 phosphorylation by TBK1.

TABLE OF CONTENTS

| | |
|-------------------------------|----|
| ABSTRACT | v |
| CHAPTER I. INTRODUCTION | 1 |
| CHAPTER II. RESULTS | 21 |
| CHAPTER III. DISCUSSION | 63 |
| CHAPTER IV. METHODS..... | 77 |
| CHAPTER V. BIBLIOGRAPHY..... | 86 |

PRIOR PUBLICATIONS

Liu, S., and Chen, Z.J. (2011). Expanding role of ubiquitination in NF-kappaB signaling. **Cell Res** *21*, 6-21.

Sun, L., **Liu, S.**, and Chen, Z.J. (2010). SnapShot: pathways of antiviral innate immunity. **Cell** *140*, 436-436 e432.

Zeng, W., Xu, M., **Liu, S.**, Sun, L., and Chen, Z.J. (2009). Key role of Ubc5 and lysine-63 polyubiquitination in viral activation of IRF3. **Mol Cell** *36*, 315-325.

Dulubova, I., Khvotchev, M., **Liu, S.**, Huryeva, I., Sudhof, T.C., and Rizo, J. (2007). Munc18-1 binds directly to the neuronal SNARE complex. **Proc Natl Acad Sci U S A** *104*, 2697-2702.

Fang, Z., Miao, Y., Ding, X., Deng, H., **Liu, S.**, Wang, F., Zhou, R., Watson, C., Fu, C., Hu, Q., *et al.* (2006). Proteomic identification and functional characterization of a novel ARF6 GTPase-activating protein, ACAP4. **Molecular & cellular proteomics : MCP** *5*, 1437-1449.

LIST OF FIGURES

| | |
|-----------------|----|
| FIGURE 1 | 2 |
| FIGURE 2 | 7 |
| FIGURE 3 | 13 |
| FIGURE 4 | 17 |
| FIGURE 5 | 22 |
| FIGURE 6 | 23 |
| FIGURE 7 | 25 |
| FIGURE 8 | 26 |
| FIGURE 9 | 28 |
| FIGURE 10 | 29 |
| FIGURE 11 | 30 |
| FIGURE 12 | 31 |
| FIGURE 13 | 33 |
| FIGURE 14 | 34 |
| FIGURE 15 | 35 |
| FIGURE 16 | 37 |
| FIGURE 17 | 38 |
| FIGURE 18 | 40 |
| FIGURE 19 | 42 |
| FIGURE 20 | 43 |
| FIGURE 21 | 46 |

| | |
|-----------------|----|
| FIGURE 22 | 47 |
| FIGURE 23 | 48 |
| FIGURE 24 | 49 |
| FIGURE 25 | 51 |
| FIGURE 26 | 53 |
| FIGURE 27 | 54 |
| FIGURE 28 | 56 |
| FIGURE 29 | 57 |
| FIGURE 30 | 59 |
| FIGURE 31 | 60 |
| FIGURE 32 | 65 |
| FIGURE 33 | 69 |
| FIGURE 34 | 71 |
| FIGURE 35 | 74 |

LIST OF TABLES

| | |
|---------------|----|
| TABLE 1 | 4 |
| TABLE 2 | 58 |
| TABLE 3 | 60 |
| TABLE 4 | 68 |

CHAPTER I

INTRODUCTION

The Immune System

The immune system is a biologically structured system for living organisms to defend against various exogenous pathogens throughout their lifespan. The complexity and essential roles of the immune system can be traced from the rudimentary defense barriers in metazoans to the more sophisticated, layered defense mechanisms in vertebrates (Beck and Habicht, 1996; Hornung et al., 2009). The most elementary level of pathogenic protection includes passive surface barriers such as the outside skin and the internal mucosa, bodily fluid with antimicrobial peptides, and commensal flora that compete with pathogenic bacteria for food and space. On a more complex level, the immune system has further evolved to form two separate but intimately related branches of innate and adaptive immunity. Generally, pathogens that have successfully penetrated the surface barriers are first detected and mostly resolved by the host innate immune system within hours. If the response is insufficient, the more potent adaptive immune system, activated through innate immunity, will continue to fight against the particular pathogen for days or even years (Figure 1).

Innate Immune System and Pattern recognition receptors (PRRs)

The innate immune system is the first line of host defense against pathogens through recognition of various pathogen-associated molecular patterns (PAMPs), which are

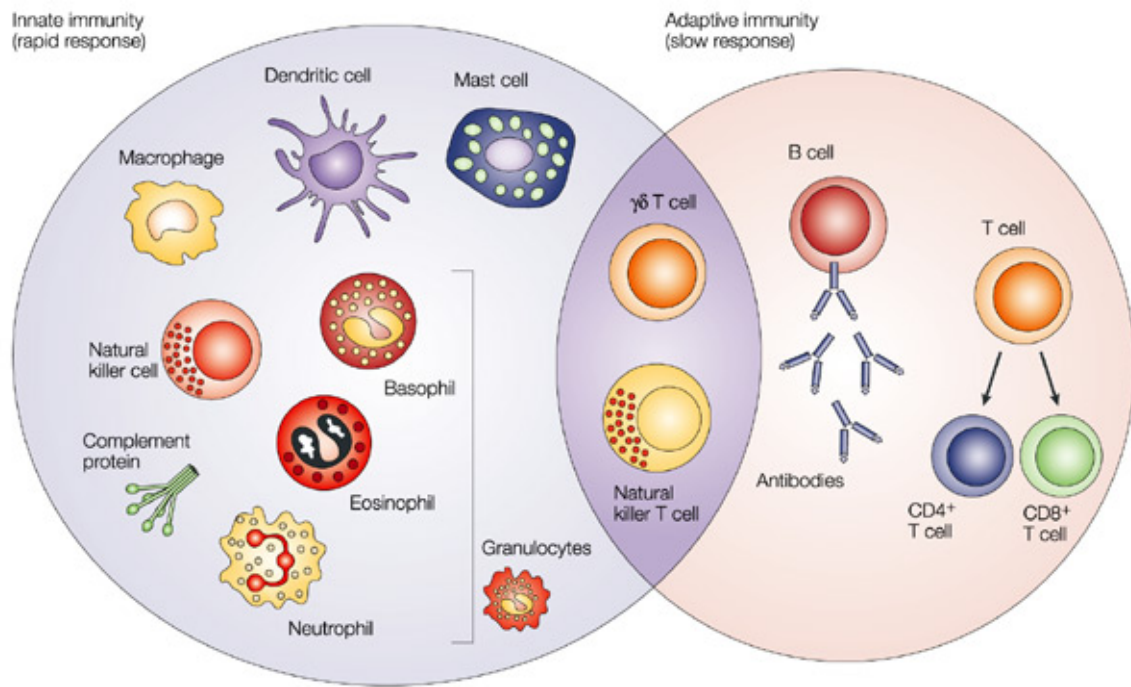


Figure 1. Schematic Representation of Innate and Adaptive Immune Systems (Dranoff, 2004)

The innate immune response is the first line of defense, which consists of soluble factors and diverse types of cells such as neutrophils, mast cells, macrophages, dendritic cells and natural killer cells. It further activates the adaptive immunity, which mounts slower, but lasts months to years, to target an antigen more effectively and specifically. The adaptive immunity consists of antibodies, B cells, and CD4+ and CD8+ T lymphocytes. Natural killer T cells and $\gamma\delta$ T cells are cytotoxic lymphocytes that are in between innate and adaptive immunity.

conserved molecular patterns produced broadly by pathogens but not by the host (Mushegian and Medzhitov, 2001). For example, lipopolysaccharides (LPS) from Gram-negative bacteria, double-stranded (dsRNA) or single-stranded RNA (ssRNA) from viruses, unmethylated CpG DNA from bacteria or viruses are some of the well-characterized PAMPs that potently activate the host pattern recognition receptors (PRRs, Table 1). The PRRs reside either on plasma/endosomal membranes or in the cytosol and their activation upon PAMP recognition in turn triggers downstream signaling to produce type-I interferons (e.g. IFN- α and IFN- β)

and other inflammatory cytokines (e.g. IL-6). These cytokines will alert neighboring cells of pathogenic invasion while up-regulating a set of genes that have potent anti-pathogen functions and thereby rapidly contain the infection before further activating the adaptive immune system (Pichlmair and Reis e Sousa, 2007; Stetson and Medzhitov, 2006).

As some of the best characterized PRRs, the Toll-like receptors (TLRs) are an ancient family of transmembrane PRRs that play essential roles in host defense from flies to humans. In mammals, TLRs are widely expressed in most of the immune cells including epithelial cells, macrophages, dendritic cells and certain types of B and T lymphocytes. To date, 10 members of TLRs in human, 12 in mouse, 9 in *Drosophila* and a single member in *Caenorhabditis elegans* have been identified. All the TLRs possess a leucine-rich ligand-binding domain facing the extracellular side and a Toll/interleukin-1 (IL-1) receptor (TIR) domain facing the cytoplasm for transducing the outside signal across the membrane and further signaling downstream (Mushegian and Medzhitov, 2001; O'Neill and Bowie, 2007; Takeuchi and Akira, 2010). Evolutionarily, TLRs can be grouped into six families, TLR1, TLR3, TLR4, TLR5, TLR7, and TLR11 (Roach et al., 2005). The TLR1 family consists of TLR1/2/6/10/14, which are localized on the plasma membrane. TLR2 forms a heterodimer with other members in this family to detect lipopeptides from fungi, bacteria or protozoa. The TLR4 family includes TLR4 and TLR5, which are also localized on the plasma membrane initially and eventually traffic to endosomal membrane after recognizing bacterial LPS. Members of the other TLR families are localized on the endosomal membrane. TLR3 detects

Table 1. PRRs and Their Ligands

| PRRs | Localization | Ligand | Origin of the Ligand |
|-------------------|-----------------|-----------------------------------|------------------------------------|
| TLR | | | |
| TLR1 | Plasma membrane | Triacyl lipoprotein | Bacteria |
| TLR2 | Plasma membrane | Lipoprotein | Bacteria, viruses, parasites, self |
| TLR3 | Endolysosome | dsRNA | Virus |
| TLR4 | Plasma membrane | LPS | Bacteria, viruses, self |
| TLR5 | Plasma membrane | Flagellin | Bacteria |
| TLR6 | Plasma membrane | Diacyl lipoprotein | Bacteria, viruses |
| TLR7 (human TLR8) | Endolysosome | ssRNA | Virus, bacteria, self |
| TLR9 | Endolysosome | CpG-DNA | Virus, bacteria, protozoa, self |
| TLR10 | Endolysosome | Unknown | Unknown |
| TLR11 | Plasma membrane | Profilin-like molecule | Protozoa |
| TLR13 | Endolysosome | sequence specific 23S rRNA | Bacteria |
| RLR | | | |
| IG-I | Cytoplasm | Short dsRNA, 5'triphosphate dsRNA | RNA viruses, DNA virus |
| MDA5 | Cytoplasm | Long dsRNA | RNA viruses (Picornaviridae) |
| LGP2 | Cytoplasm | Unknown | RNA viruses |
| NLR | | | |
| NOD1 | Cytoplasm | iE-DAP | Bacteria |
| NOD2 | Cytoplasm | MDP | Bacteria |
| CLR | | | |
| Dectin-1 | Plasma membrane | β -Glucan | Fungi |
| Dectin-2 | Plasma membrane | β -Glucan | Fungi |
| MINCLE | Plasma membrane | SAP130 | Self, fungi |

Table 1. A List of PRRs and Their Ligands (updated from (Takeuchi and Akira, 2010))

viral dsRNA. TLR7 and TLR8 of the TLR7 family detect ssRNA whereas TLR9 in this family recognizes unmethylated CpG DNA. The TLR11 family includes mouse-specific TLR11-13 and TLR21-23 in fish and frogs. TLR11 recognizes a profiling-like protein from the parasite *Toxoplasma gondii* and an unknown ligand from uropathogenic *E. coli*. Notably, studies from our lab and others have recently identified the ligand for mouse TLR3 as a 13-residue sequence within the bacterial-specific 23S ribosomal RNA. Unlike the other TLRs that recognize specific molecular motifs, TLR13 recognizes a specific sequence, which triggers robust IL1- β and other cytokine production in mouse (Li and Chen, 2012; Oldenburg et al., 2012).

In addition to TLRs residing on membranes, two groups of cytosolic PRRs have been intensively studied in the past decade. One group of PRRs is the nucleotide-binding domain

(NBD), leucine-rich repeat (LRR)-containing proteins (NLR; also known as NOD-like receptors). All NLR proteins contain NBD and LRR domains. In addition, they are classified into different subfamilies depending on whether they possess CARD, pyrin or baculovirus inhibitor of apoptosis protein repeat (BIR) domains. Among the 20 or so NLR proteins, NOD1 and NOD2, which activate NF- κ B, are the most extensively studied. NOD1 senses the dipeptide γ -d-glutamyl-meso-diaminopimelic acid (iE-DAP), whereas NOD2 is reported to detect muramyl dipeptide (MDP). Both of the ligands are peptidoglycans from the bacterial cell wall (Franchi et al., 2009; Inohara et al., 1999; Ogura et al., 2001).

The other group of cytosolic PRR is RIG-I like receptors (RLRs), including Retinoic acid-inducible gene I (RIG-I), melanoma differentiation-associated gene 5 (MDA5), and laboratory of genetics and physiology 2 (LGP2) (Yoneyama and Fujita, 2008; Yoneyama et al., 2004). This group of cytosolic proteins detects different forms of viral and bacterial RNA present in the host cytosol during invasion and replication (Li et al., 2011b; Takeuchi and Akira, 2008). Additionally, DNAs from some DNA viruses (e.g. adenovirus, herpes simplex virus 1 (HSV-1), and Epstein-Barr virus (EBV)) can be sensed by RNA-polymerase III (pol-III) and transcribed into RNA, which is in turn recognized by RIG-I (Chiu et al., 2009). In addition to TLRs, these cytosolic nucleic acid sensors have provided complementary protection against pathogen invasion.

Viral Sensing Pathways

Viruses are one group of the highly infectious pathogens, which utilize the host machinery to survive and replicate. Many viruses like influenza cause common human illnesses whereas other high virulence ones such as Ebola, AIDS, SARS, hepatitis C virus (HCV) and human immunodeficiency virus (HIV) cause more severe and life-threatening illnesses. Viruses carry their genetic information in the form of DNA or RNA inside nucleocapsids. Some viruses also contain an outer membrane or lipid bilayer. To defend against viral infections, the host innate immune system has developed multiple ways to sense viral infection through recognition of different viral components, such as viral nucleic acids or envelope proteins.

Firstly, TLRs (TLR3, TLR7, TLR8, TLR9) on both the plasma and endosomal membranes recognize viral DNAs or RNAs (O'Neill and Bowie, 2010). Such recognition triggers the activation of these receptors, which recruits downstream TIR-containing adaptor proteins such as myeloid differentiation factor (Myd88) by TLR7-9 or TIR-domain-containing adaptor protein inducing IFN- β (TRIF) by TLR3 to eventually trigger the production of type-I interferons such as IFN- α and IFN- β or inflammatory cytokines such as IL1- β . These pathways are predominant in immune specific cells such as macrophages, T, and B lymphocytes.

Secondly, the cytosolic sensors RIG-I and MDA5 can differentially recognize viral RNAs in the cytoplasm based on their length. Unlike the TLRs, RIG-I is expressed and functional in most if not all cells. RIG-I and MDA5 both contain a DEAD/H-box RNA helicase domain, which binds to double-stranded RNA (Yoneyama et al., 2004). In addition,

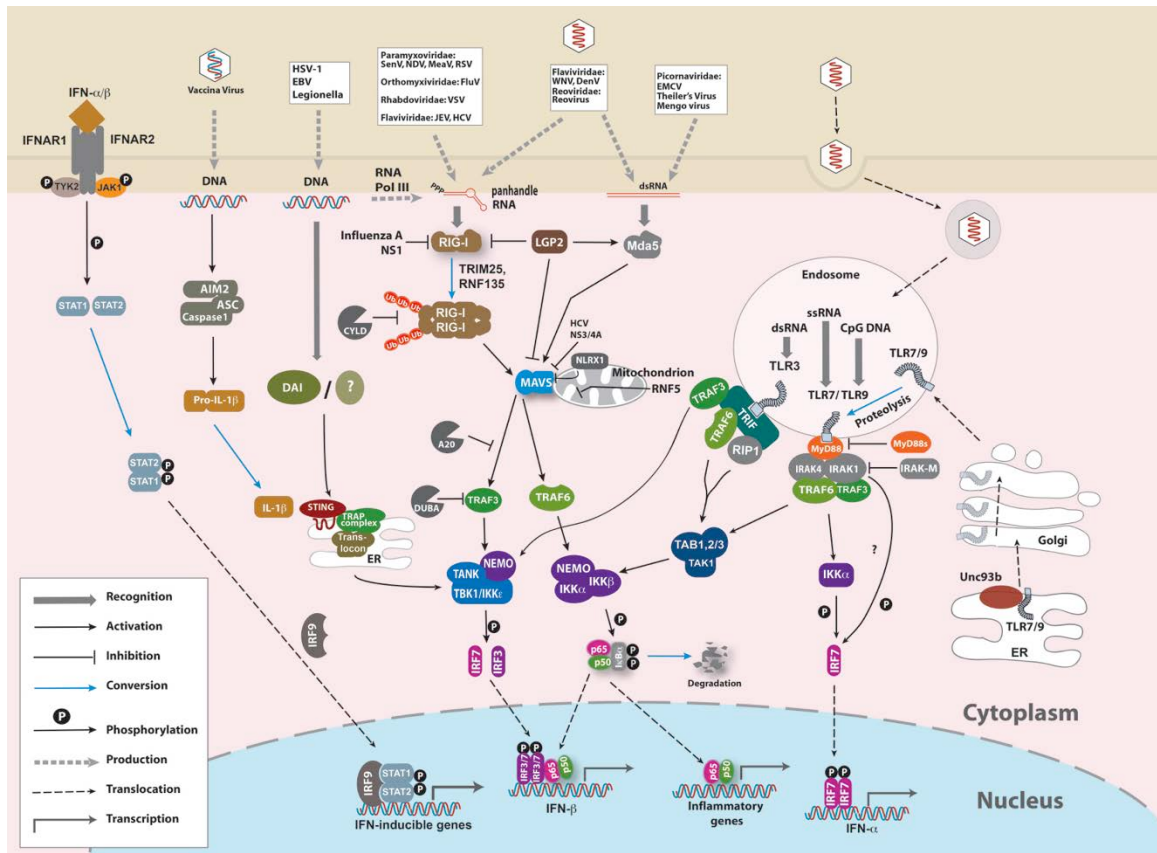


Figure 2. Role of PRRs in Viral Sensing (Adapted from (Sun et al., 2010)).

Innate signaling pathways are triggered by viral nucleic acids that are delivered to the cytosol and endosomes of mammalian host cells. Many viral infections, especially those of RNA viruses, result in the delivery and replication of viral RNA in the cytosol of infected host cells. These cytosolic RNA are recognized by members of the RLR family, which activate mitochondrial localized adaptor protein, MAVS, to further trigger activation of NF-κB targets genes and type-I interferons. Alternatively, when viruses enter cells through endocytosis, their nucleic acids are detected in the lumen of the endosomes by a subset of TLRs including TLR3, TLR7/8, and TLR9. These TLRs are synthesized in the ER, where they associate with the transmembrane protein Unc93b1, which escorts the TLR proteins to endosomes. Activation of TLR7, 8, and 9 recruits cytosolic adaptor protein MyD88, which activates IKK and TBK1 through TRAF6 and TRAF3, respectively. In plasmacytoid dendritic cells (pDC), the MyD88-IRAK1-TRAF6 complex recruits and activates IRF7, which induces production of IFN- α . Binding of dsRNA to TLR3 activates downstream kinases through the adaptor protein TRIF, which in turn recruits TRAF3 and TRAF6.

RIG-I and LGP2 have a C-terminal regulatory domain that specifically binds to RNA bearing 5' triphosphates (Cui et al., 2008; Hornung et al., 2006; Pichlmair et al., 2006). Studies have shown that RIG-I and MDA5 recognize different viruses. MDA5 is required for innate

immunity against picornaviruses such as encephalomyocarditis virus (EMCV), whereas RIG-I is critical in sensing HCV, vesicular stomatitis virus (VSV), Sendai virus (SeV) and influenza A virus (Gitlin et al., 2006; Kato et al., 2008; Takeuchi and Akira, 2008). As for LGP2, the lack of tandem CARD domains for downstream activation may potentially restrict its function to a regulatory role. Some studies have suggested the LGP2 functions as a positive regulator of both RIG-I and MDA5 (Satoh et al., 2010) whereas some have proposed it as a negative regulator of RIG-I (Rothenfusser et al., 2005; Venkataraman et al., 2007; Yoneyama et al., 2005). Thus, the function of LGP2 may be more complex, which requires further investigation.

Thirdly, cytosolic DNA can be detected by the host in several ways (Barber, 2011). In addition to pol-III, which senses some viral DNA to generate intermediate RNA species recognized by RIG-I, PYHIN (pyrin and HIN domain-containing protein) family member absent in melanoma 2 (AIM2) was found to be a cytoplasmic DNA sensor that triggers inflammasome activation, eventually leading to the production of IL1- β (Hornung et al., 2009). Additionally, STING (Stimulator of Interferon genes, also known as MITA or MPYS), was found to be critical for DNA triggered type-I interferon production (Ishikawa and Barber, 2008; Zhong et al., 2008). MEF cells from *Sting*^{-/-} mice failed to induce type-I IFNs in response to infection with HSV-1 or *L. monocytogenes*, or to transfection of ISD (interferon stimulatory DNA), a synthetic double-stranded 45-base pair DNA lacking CpG sequences. Moreover, it is also responsible for the interferon response triggered by DNA derived from HIV in *Trex1*^{-/-} cells, in which the cytosolic HIV DNA fails to be removed by the host exonuclease TREX1 for evading the innate immunity (Yan et al., 2010). Interestingly, the

fact that STING itself doesn't harbor a DNA-binding domain in its structure has suggested the existence of a yet-to-be identified upstream DNA sensor. Recently, a study has suggested that STING recognizes cyclic di-nucleotides generated by Listeria to activate interferon production, which is critical for the host innate immunity in defense against Listeria infection (Sauer et al., 2011). Thus, it is possible that to sense cytosolic DNA, STING is activated through recognition of other second-messengers generated by the unknown upstream DNA sensor that are similar to cyclic di-nucleotides. Future studies on such molecules will shed more light on DNA-sensing innate immunity and causes of certain autoimmune diseases.

Fourthly, viral structures other than nucleic acids can also be sensed by host innate immunity. TRIM5, a RING domain-E3 ligase, has been reported to restrict infection by human immunodeficiency virus (HIV)-1 and other retroviruses. Recently, a study showed that TRIM5 activates NF- κ B and AP-1 by synthesizing K63-linked polyubiquitin chains after directly sensing retroviral capsid (Pertel et al., 2011). The dual role of TRIM5 as both a PRR and a kinase activator has provided an excellent example to demonstrate the agility of host defense against pathogens during the evolution.

Activation of NF- κ B

NF- κ B is a family of heterodimeric transcription factors that regulate genes involved in immunity, inflammation and cell survival (Hayden and Ghosh, 2008). The NF- κ B family has five members, including p50, p52, p65 (RelA), c-Rel and RelB, all of which share an N-

terminal Rel homology domain (RHD) in mediating their dimerization, nuclear localization and DNA binding. The RHD also binds to inhibitory proteins of κB family (IκBs), which sequester NF-κB in the cytoplasm in unstimulated cells. Additionally, a transcription activation domain (TAD) is present in p65, c-Rel and RelB to activate gene transcription, but not in p50 and p52, which are generated from p105 and p100, respectively. p50 and p52 further bind to a TAD-containing member to generate a functional NF-κB dimer.

The activation of NF-κB requires the degradation of IκB proteins or the processing the NF-κB precursors to the mature subunits (Pomerantz and Baltimore, 2002; Spencer et al., 1999). In canonical NF-κB pathways, IκB degradation is the hallmark of NF-κB activation. This includes pathways activated by cytokines such as tumor necrosis factor (TNF) α and IL-1 β , bacterial products such as LPS, and RNA virus such as Sendai virus. The stimulation of these ligands usually leads to the activation of the IκB kinase (IKK) complex, which is composed of catalytic subunits IKK α and IKK β , and the essential regulatory subunit NEMO (also known as IKK γ or IKKAP). The IKK complex phosphorylates IκB α at serine 32 and 36, which is subsequently recognized and polyubiquitinated on lysine 21 and 22 by a ubiquitin ligase complex consisting of Skp1, Cul1, Roc1 and βTrCP (Spencer et al., 1999) (Chen et al., 1995; Scherer et al., 1995; Traenckner et al., 1995). Polyubiquitinated IκB is then degraded by the 26S proteasome, releasing NF-κB into nucleus to activate target genes. Notably, in response to stimulation of a subset of receptors on B cells, such as CD40, NF-κB can also be activated through a noncanonical pathway in which p100 is processed into p52 by the proteasome. In this pathway, IKK α is activated to phosphorylate P100. Phosphorylated

P100 is subsequently polyubiquitinated and partially degraded by the proteasome, releasing p52 and RelB dimer as the active transcription factor (Lin and Ghosh, 1996; Piwko and Jentsch, 2006).

IRF3 and Interferons

As the first series of cytokines to be characterized molecularly, interferons (IFNs) have been extensively studied as the signature of the innate immune defense against viral infection. There are two types of IFNs, type I IFNs (multiple IFN- α proteins and IFN- β) and type II IFN (IFN- γ). Type I IFNs are produced by a variety of cells upon viral infection, whereas IFN- γ is produced only by activated T lymphocytes (T cells) and natural killer (NK) cells. IFNs show broad biological activities, but they most importantly lead to the production of thousands of interferon-stimulated genes to evoke an antiviral response in their target cells through the stimulation of homologous receptors (Taniguchi et al., 2001). Secreted IFNs bind to IFNAR1 and IFNAR2 heterodimer receptor on the cell surface, leading to the recruitment and activation of two downstream kinases, Tyk2 and Jak1 to the receptor. The kinases subsequently phosphorylate STAT1/2, which then form a heterotrimeric transcription factor in combination with IRF9, and translocate into nucleus to turn on the transcription of a large array of genes. The expression of these genes evokes an “antiviral” state, which exhibits antiviral, anti-inflammatory and immuno-modulatory functions in host cells. Additionally, type I IFNs link innate immunity to adaptive immunity through their functions in dendritic cell maturation (Le Bon and Tough, 2002). The IFNs also enhance viral-antigen cross-

presentation through induction of major histocompatibility complex class I (MHC-I).

Interferon regulatory factors consist of a family of 9 transcription factors including IRF1, IRF2, IRF3, IRF4 (also known as PIP, LSIRF, or ICSAT), IRF5, IRF6, IRF7, IRF8 (also known as ICSBP), and IRF9 (also known as ISGF3 γ). These transcription factors share a conserved helix-turn-helix DNA-binding domain (DBD) at their N-terminal for the recognition of a DNA sequence corresponding to the IFN-stimulated response element (ISRE, A/GNGAAANNGAAACT)(Tamura et al., 2008). Among these members, IRF3 and IRF7 are closely related to each other based on their structures and have been studied most extensively for their role in IFN- α/β gene regulation in virus infected cells (Taniguchi et al., 2001). Both IRF3 and IRF7 are ubiquitously expressed, but the expression of IRF7 is completely dependent on type-I IFN signaling whereas that of IRF3 is constitutive, consistent with the fact that IRF3 is the primary transcription factor in viral-induced type-I IFN production. IRF3 contains an activation domain that includes the nuclear export signal (NES) and the IRF association domain (IAD), which is flanked by two autoinhibitory elements that interact with each other. Upon upstream activation of its kinase TBK1 or IKK ϵ by signals such as viral nucleic acids or bacterial LPS, IRF3 is sequentially phosphorylated at two serine-threonine clusters at its C-terminal serine-rich region (SRR), including S385/S386 and S396/S398/S402/T404/S405. Structural studies have shown that the massive phosphorylation reorganizes the autoinhibitory elements, leading to unmasking of a hydrophobic active site and realignment of the DNA binding domain for transcriptional activation (Qin et al., 2003; Takahasi et al., 2003). The phosphorylated IRF3 forms a dimer and subsequently translocates into the nucleus, together with NF- κ B, to activate the transcription of IFN- α/β .

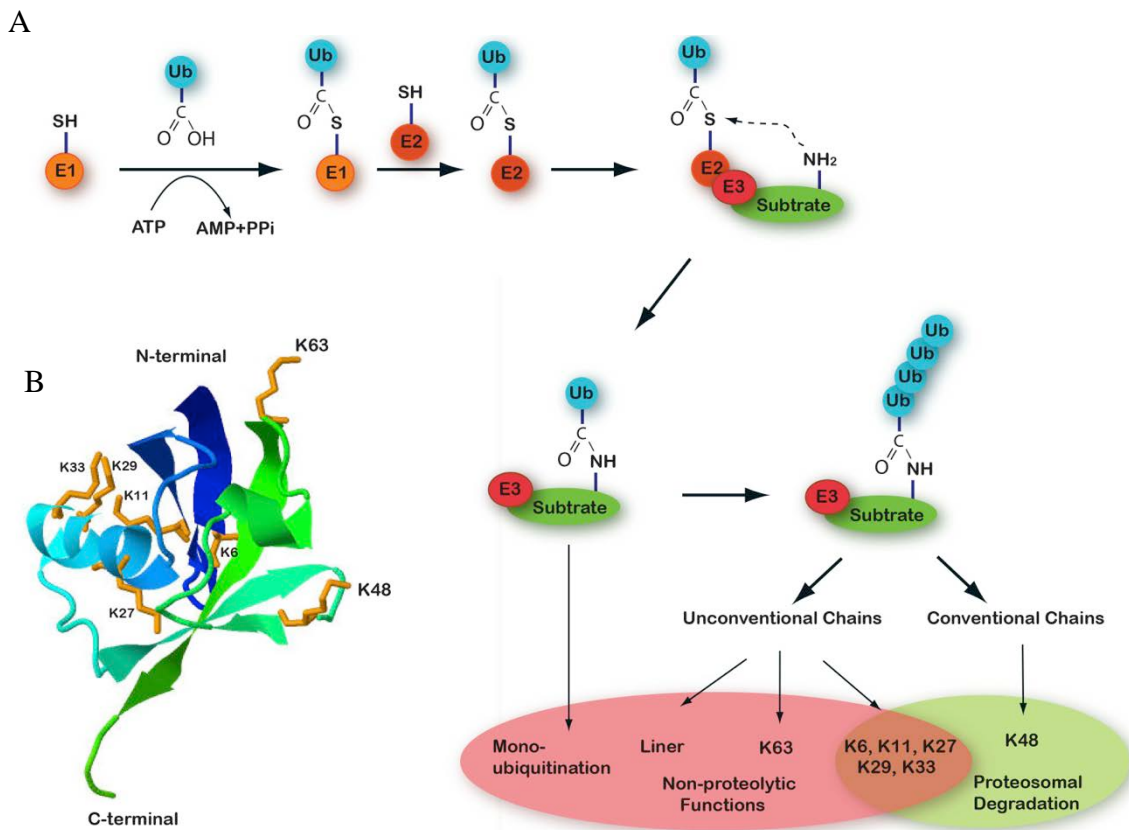


Figure 3. Ubiquitination in Protein Function Regulations (Adapted from (Liu and Chen, 2011))
(A) Schematic representation of the three-step ubiquitination cascade. Mono- and K63-linked ubiquitination generally serve non-proteolytic functions, whereas polyubiquitination of other linkages mostly target proteins for degradation by the proteasome.
(B) Structure of ubiquitin (PDB: 1UBQ), highlighting its seven lysine residues.

Ubiquitination in the Antiviral Signaling Pathways

Ubiquitination is a post-translational modification that attaches one or more ubiquitin molecules, a 76-amino-acid protein, onto target proteins, through a stepwise enzymatic reaction involving three classes of enzymes - E1, E2 and E3 (Figure 3). The human genome encodes two E1s, ~50 E2s and over 700 E3s, underscoring the complexity of the ubiquitin

system (Iwai and Ishikawa, 2006). Ubiquitin has seven lysines (K6, K11, K27, K33, K48 and K63), all of which can be conjugated to ubiquitin molecules to form a polyubiquitin chain. Additionally, the amino terminus of one ubiquitin can be conjugated to the carboxyl terminus of another ubiquitin to form a linear ubiquitin chain (Kirisako et al., 2006). Generally, the ubiquitin chains linked through different lysine residues serve distinct functions in cell signaling. For example, ubiquitin is known for its role in targeting proteins for degradation by the 26S proteasome through the recognition of K48-linked or K11-linked polyubiquitin. In the recent decade, K63-linked polyubiquitin has emerged as important mechanism to regulate cell signaling through a proteasome-independent mechanism, which is best illustrated in the activation of NF- κ B.

In NF- κ B signaling, the activation of the I κ B α kinase, IKK, is one of the best-studied examples, where IKK activation is tightly regulated by polyubiquitination in a proteasome-independent manner. Recent studies have revealed that ubiquitination-mediated kinase activation is a common mechanism underlying NF- κ B activation by diverse stimuli. In vitro, a study in our lab has shown that the polyubiquitin chains can directly activate the TAK1 kinase complex and the IKK kinase complex through binding to the UBDs (Ubiquitin binding domain) on kinase regulatory subunit, TAB1 and NEMO, respectively (Xia et al., 2009). The same mechanism could potentially apply to other IKK related kinases such as TBK1 and IKK ϵ .

Several ubiquitin E3 ligases are common regulators of IKK activation, including TRAF2/5, TRAF6, TRAF3, cIAP1/2 and LUBAC. The tumor necrosis factor (TNF) receptor

associated factors (TRAFs) consists of a family of conserved adaptor proteins in mammals (TRAF1-7) and they have been extensively studied as the major signal transducers in NF- κ B activation by various stimuli (Chung et al., 2002). TRAFs are characterized by the presence of TRAF domain at their C-terminal, consisting of a coiled-coil domain and a conserved TRAF-C domain. Structural studies have suggested that the TRAF domain is critical in TRAF function by mediating self-association and interaction with upstream receptors containing conserved TRAF-binding motif(s) (Park et al., 1999; Ye et al., 2002a; Ye et al., 2002b). Except for TRAF1, all other TRAFs contain a N-terminal RING finger, most of which have been suggested to precipitate the ubiquitination-regulated signaling cascade (e.g. activation of TAK1 and IKK in NF- κ B pathways). For example, TRAF6 has been shown to synthesize unanchored K63-linked polyubiquitin chain together with the E2 complex Ubc13/Uev1A to regulate Myd88-mediated TAK1 and IKK activation. As the sole TRAF in the pathway, its RING domain is required for the activity (Cao et al., 1996; Deng et al., 2000; Lomaga et al., 1999; Xia et al., 2009; Yeh et al., 1997). In contrast, TRAF2 and TRAF5 are important in TNF α -induced IKK activation, but their E3 ligase activity is dispensable (Yeh et al., 1997). Some structural studies have compared the RING domains of TRAF2 and TRAF6 and concluded that TRAF2 doesn't function as an E3 ligase due to the lack of interaction with E2 in its structure (Yin et al., 2009), whereas others have proposed that it undergoes K63-linked autoubiquitination and it needs a co-factor to stimulate the E3 ligases activity (Alvarez et al., 2010; Li et al., 2009). Nevertheless, TRAF2/5 also recruits another family of E3 ligases, cIAP1/2 (cellular inhibitors of apoptosis), which are important in polyubiquitinating RIP1 to trigger downstream kinase activation. Thus, whether TRAF2 and

5 serve only as scaffold proteins or they function redundantly with cIAPs still needs further investigation. LUBAC (Linear Ubiquitin Chain Assembly Complex) is an E3 complex composed of Sharpin, HOIL and HOIP that has been first identified to synthesize head-to-tail linear ubiquitin chains in vitro (Kirisako et al., 2006). Both HOIP and HOIL contain RING-between-RING fingers and HOIP is suggested as the catalytic subunit as its RING mutant abolished the E3 ligase activity of the complex. Surprisingly, this complex was later identified as another key component that regulates the kinase activation in various NF- κ B pathways (Gerlach et al., 2011; Haas et al., 2009; Ikeda et al., 2011; Tokunaga et al., 2011; Tokunaga et al., 2009). However, to equate LUBAC activity to linear ubiquitination for kinase activation, more convincing evidence is still required.

The Molecular Mechanism of RIG-I and MAVS-mediated Viral Sensing Pathway

The cytosolic RNA sensor RIG-I is composed of N-terminal tandem CARDs, a middle DexD/H-Box helicase domain and a repressor domain in its C-terminus. Several recent structural and biochemical analyses have suggested that activation of RIG-I by viral RNAs is likely to be mediated by two sequential events. Firstly, RIG-I is suppressed due to the intramolecular interaction between its CARD and repressor domain. Upon RNA-binding to its repressor domain, CARDs of RIG-I is released from auto-repression, allowing them to bind to other signaling molecules such as ubiquitin (Gack et al., 2007; Kowalinski et al., 2011; Luo et al., 2011; Yoneyama et al., 2004). Secondly, the RNA binding to RIG-I further stimulates an E3 ligase, TRIM25 to synthesize K63-linked free polyubiquitin chains that are

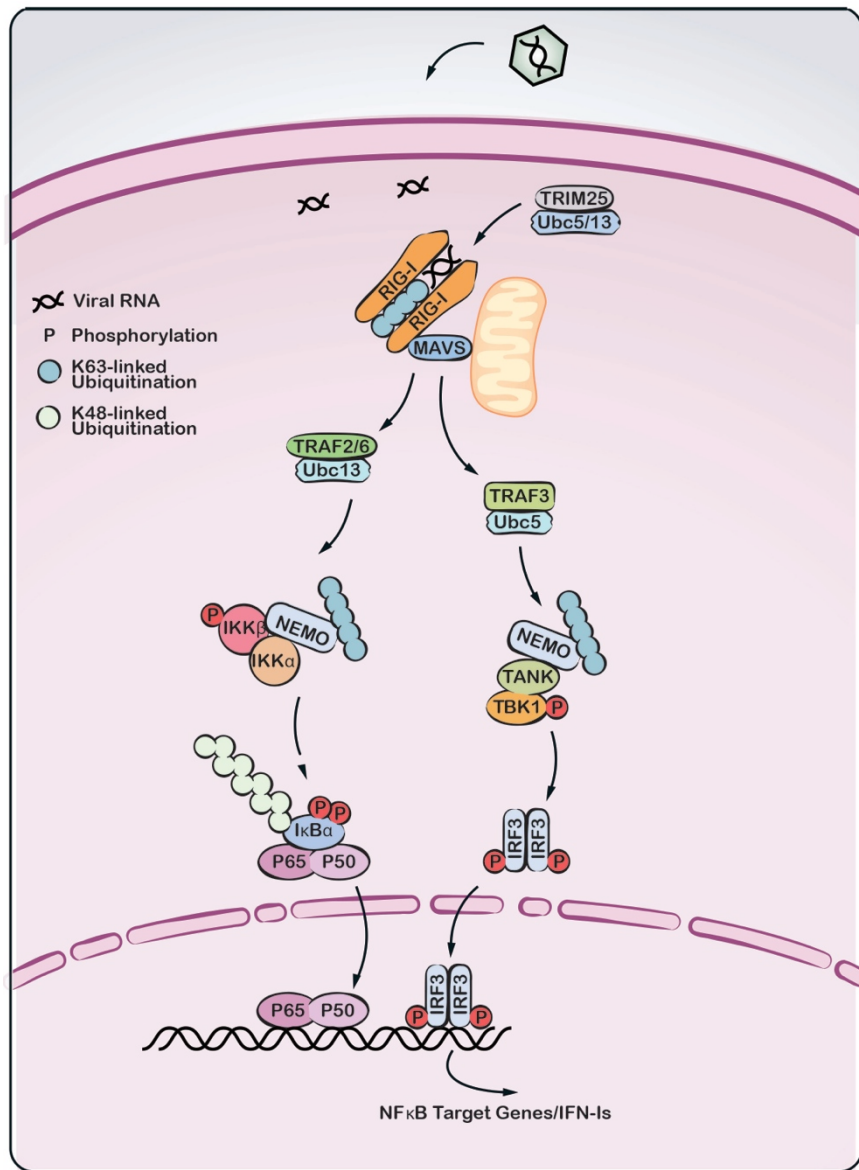


Figure 3. RLR and MAVS Mediate Cytosolic Viral Sensing Pathway.

Upon recognition of cytosolic dsRNA, RIG-I recruits Ubc13 and TRIM25 to synthesize unanchored Lys63-linked polyubiquitin chains. The binding to dsRNA and polyubiquitin drives RIG-I into oligomeric state, which turns the mitochondrial localized adaptor proteins MAVS into prion-like aggregates. Active form of MAVS in turn recruits E3 ligases such as TRAF3 and TRAF6 to activate downstream kinases IKK and TBK1, which subsequently lead to the activation of NF-κB and IRF3, respectively. IRF3 dimer and NF-κB heterodimer, together with other transcription factors, such as AP-1 and c-Jun, turn on the production of type-I interferons and other inflammatory cytokines.

not anchored to any proteins. The subsequent binding of CARDs to the ubiquitin chains creates an oligomerized complex consisting of RIG-I, RNA, and polyubiquitin, which is competent in activating the downstream CARD-containing protein, mitochondrial antiviral signaling protein (MAVS, also known as IPS-1, VISA and CARDIF), presumably through CARD-CARD interaction. MAVS is a mitochondrial-localized protein whose overexpression in 293 cells triggers the activation of its downstream pathways (Kawai et al., 2005; Meylan et al., 2005; Seth et al., 2005; Xu et al., 2005). Recently, a study from our lab has unveiled the mechanism of how MAVS is activated. Namely, the active RIG-I oligomer triggers MAVS to form large polymers though a prion-like mechanism, through which the small portion of MAVS activated by RIG-I is capable of catalytically converting other native MAVS into fibril-like, detergent and protease resistance polymers (Hou et al., 2011). The MAVS polymers further propagate antiviral signaling through the activation of cytosolic kinases IKK and TBK1, which in turn activate the transcription factors, IRF3 and NF- κ B, respectively (Fitzgerald et al., 2003; McWhirter et al., 2005; Sharma et al., 2003) (Figure 4).

The ubiquitin system has been suggested to be important both upstream and downstream of MAVS signaling. Upstream of MAVS, unanchored polyubiquitin binding to RIG-I is required for RIG-I activation as described above. Downstream of MAVS, K63-linked polyubiquitin and the E2 Ubc5 are required for IRF3 activation (Zeng et al., 2009). NEMO has also been shown as an adaptor protein and a ubiquitin sensor important for activation of both IKK and TBK1 (Zeng et al., 2009; Zhao et al., 2007). Additionally, several proteins, including STING, TANK, SINTBAD and NAP1, have been found to associate with TBK1 (Guo and Cheng, 2007; Ishikawa and Barber, 2008; Jin et al., 2008; Ryzhakov and

Randow, 2007; Sasai et al., 2006). Several E3 ligases including TRAF3, TRAF5, cIAP1/2 and MIB1/2 were proposed to regulate IRF3 activation downstream of MAVS (Li et al., 2011a; Mao et al., 2010; Saha et al., 2006; Tang and Wang, 2010; Wang et al., 2012). Notably, LUBAC, the E3 ligase complex that specifically synthesizes linear ubiquitin chains, has been suggested to negatively regulate the viral pathway both upstream and downstream of MAVS (Belgnaoui et al., 2012; Inn et al., 2011). However, direct evidence and biochemical mechanisms of how ubiquitination regulates the activation of the downstream kinases and transcription factors are still lacking.

We have previously described a cell-free system that mimics viral infection in cells (Zeng et al., 2009). In my thesis project, I dissected the mechanism of how MAVS propagates downstream signaling. Conventional purification strategies unveiled TRAF6 as a potent IRF3 activator in the presence of activated MAVS. Moreover, by introducing shRNA against TRAF6 into TRAF2/5 deficient cells, I found that TRAF2 and TRAF5 act redundantly with TRAF6 to activate both IRF3 and NF- κ B in response to virus. Additionally, I provide evidence that the E3 ligase activity of TRAF6 is essential in the TRAF6-dependent activation of IRF3 and NF- κ B, whereas the E3 ligase activity of TRAF2 is redundant with that of HOIP in the TRAF2-depedent pathway downstream of MAVS. Furthermore, mutation of TRAF2/5/6 binding sites on MAVS abolished the ability of MAVS to activate downstream signaling after virus infection, without affecting its ability to form prion-like aggregates. Meanwhile, MAVS aggregation mutants that are defective in downstream signaling failed to bind and bring TRAFs into high molecular weight fractions in response to virus, suggesting that the prion-like conformational change of MAVS enables the recruitment

and activation of TRAF proteins. Finally, I found that through its ubiquitin-binding domains, NEMO, along with TBK1 and IKK, forms a ubiquitination-dependent complex with TRAFs and MAVS both in vitro and in cells. Meanwhile, IRF3 also forms a similar complex with MAVS and TRAF after stimulation. I also provide evidence that MAVS is phosphorylated by recruited kinases and the phosphorylation may be important for recruiting IRF3 to the complex, where IRF3 is then phosphorylated by adjacent TBK1. Taken together, these results demonstrate a key role of MAVS, TRAF2/5 and TRAF6, in the formation of a ubiquitin-dependent signalosome with NEMO and the kinases, to activate IRF3 through a ubiquitination-coupled phosphorylation event.

CHAPTER II RESULTS

Establishment of Biochemical Assay for IRF3 Activation

To dissect the biochemical mechanism of MAVS-dependent IRF3 Activation, we used a previously established a cell-free IRF3 dimerization assay that mimics IRF3 activation in virus-infected cells (Zeng et al., 2009). Briefly, when crude mitochondria fraction (P5) from Sendai virus infected 293 cells was incubated with cytosolic extracts (S5 or S100) from uninfected cells, along with [³⁵S]-IRF3 and ATP, IRF3 dimerization can be visualized by autoradiography of gels following native poly-acrylamide gel electrophoresis (Figure 5, A and B). Later, we found that virus-activated mitochondrial fraction contained an active, polymerized form of MAVS, which can be replaced by recombinant MAVS lacking its transmembrane domain (MAVS Δ TM) (Hou et al., 2011).

The authenticity of the in vitro assay has been fully investigated. Consistent with activation of IRF3 by virus in vivo, the dimerization of IRF3 in the in vitro assay is fully dependent on TBK1 in the S5 and MAVS in the virus-activated P5 (data not shown). Moreover, P5 isolated from cells overexpressing RIG-I (N) or MAVS without virus infection, could potently activate IRF3 in vitro. These findings suggest that the in vitro assay faithfully recapitulated the epistasis of several components of virus induced IRF3 activation in cells. Thus, this robust system served as a powerful tool for the identification of new players and the dissection of the biochemical mechanism responsible for the MAVS-mediated IRF3 activation.

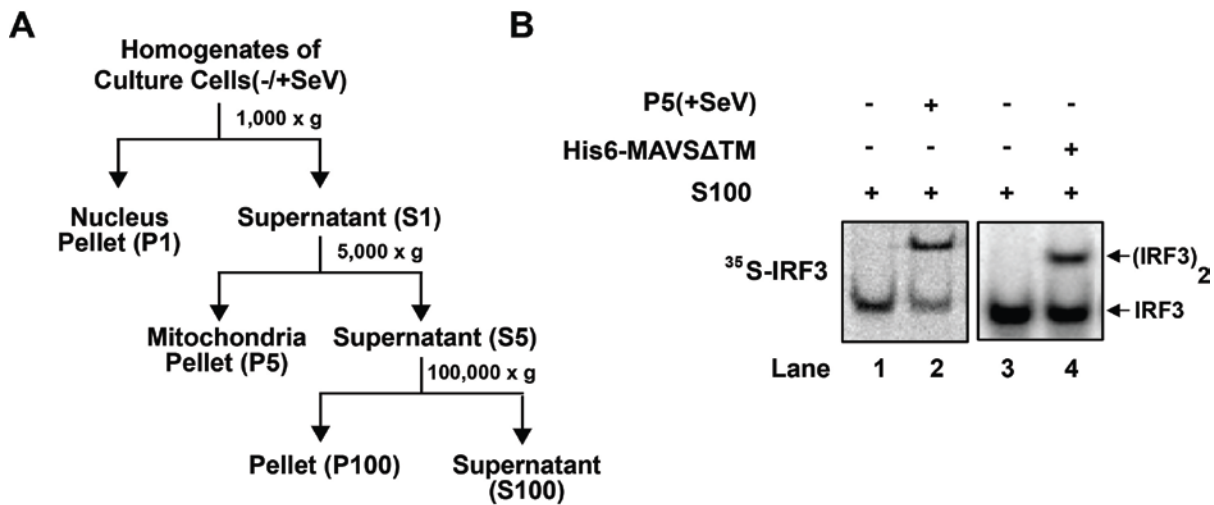


Figure 5. Establishment of Biochemical Assay for IRF3 Activation

(A) Diagram of the fractionation procedure of cell homogenates. Culture cells infected with Sendai virus (+SeV) or mock treated (-SeV) were homogenized in hypotonic buffer, followed by sequential centrifugation to separate crude mitochondrial (P5) from cytosolic supernatant (S5 and S100) as described previously.

(B) IRF3 activation in vitro. Mitochondrial fraction (P5) from Sendai virus-infected HEK293T cells or purified His₆-tagged MAVS without the transmembrane domain was incubated with cytosolic extract (S5) from uninfected cells in the presence of ATP and ³⁵S-IRF3.

Identification of TRAF6 as an IRF3 Activator in vitro

By taking advantage of the in vitro system, we fractionated the Hela S100 protein extract on an anion exchange column (Q-Sepharose) into Q-A containing the flow through in 0.1M NaCl and Q-B containing proteins eluted with 0.3M NaCl. Interestingly, we found that both Q-A and Q-B fractions were required to support IRF3 activation in our in vitro assay. The key factor in Q-A was further identified as Ubc5 (Zeng et al., 2009), indicating the ubiquitination system is involved in MAVS-mediated IRF3 activation.

When we tried to purify the factor responsible for IRF3 activation in Q-B, we found that it has a complex composition with IKK α , IKK β , NEMO, and TBK1 all co-purified in this fraction (data not shown). Of note, *Ikka*/ $\beta^{-/-}$ MEF cells respond normally to VSV in IRF3 activation (Figure 6A). Moreover, NEMO lacking its N-terminal IKK binding site

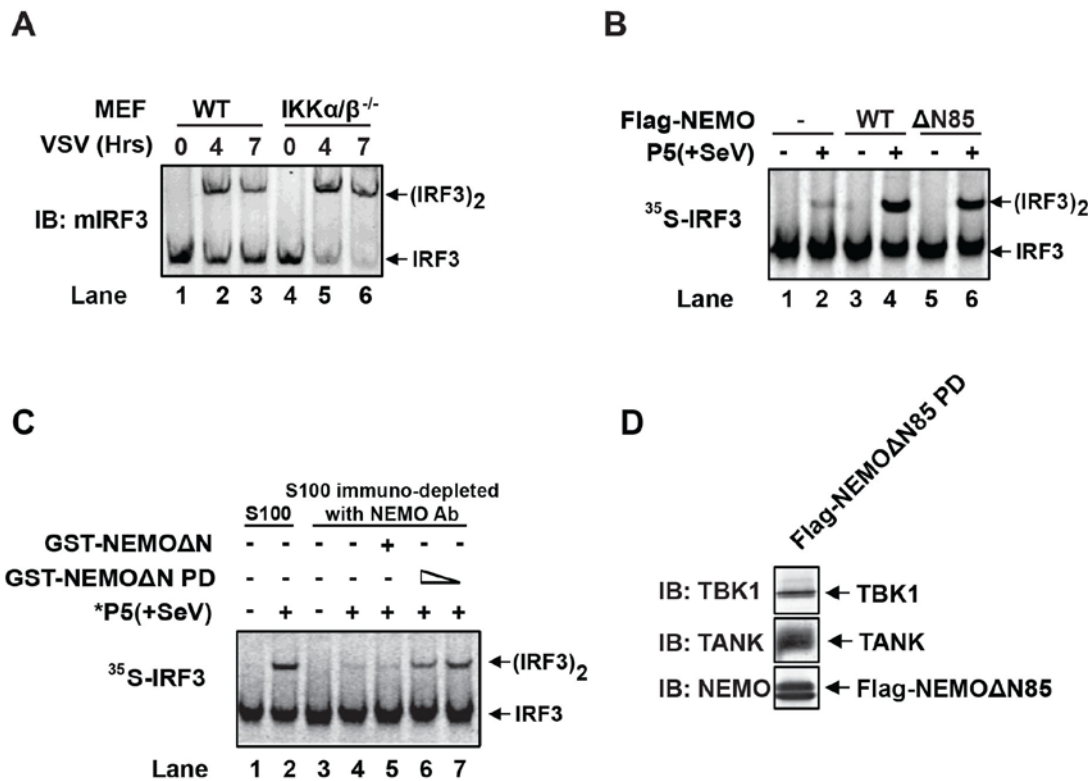


Figure 6. NEMO-TBK1 Complex is Required for IRF3 Activation

(A) Wild-type and $\text{Ikka}/\beta^{-/-}$ MEF cells were infected with VSV for indicated period of time. IRF3 dimerization was analyzed by immunoblotting.

(B) Flag-tagged wild-type and $\Delta\text{N}85$ NEMO were tested for their ability to rescue IRF3 dimerization in $\text{Nemo}^{-/-}$ S5 in the presence or absence of virus activated P5.

(C) NEMO-interacting complex is required for IRF3 activation in vitro. Cytosolic extract (S100) from HeLa cells was depleted by NEMO antibody. Meanwhile, GST-tagged NEMO without its N-terminal IKK binding region (GST-NEMO Δ N) was mixed with cytosolic extract from $\text{Nemo}^{-/-}$ MEF cells to collect GST-NEMO Δ N pull down (NEMO Δ N PD). The supernatant after NEMO depletion was tested in the IRF3 dimerization assay, with or without either GST-NEMO or GST-NEMO Δ N PD.

(D) Flag-NEMO Δ N85 PD contains NEMO, TANK and TBK1. $\text{Nemo}^{-/-}$ MEF cells stably expressing Flag-NEMO Δ N85 were used to isolate endogenous NEMO-TBK1 complex. NEMO, TANK and TBK1 were analyzed by immunoblotting. Flag-NEMO Δ N85 PD was later used to replace the GST-NEMO Δ N PD described in Fig.1 in the cell-free assay.

(NEMO Δ N85) rescued the defect of IRF3 activation in $\text{Nemo}^{-/-}$ cell extracts (Figure 6B), indicating an IKK-independent role of NEMO in virus induced IRF3 activation. Furthermore, after depletion NEMO with a NEMO specific antibody, S100 lost its ability to support IRF3 dimerization in vitro. IRF3 dimerization could not be rescued by adding back NEMO alone,

suggesting that other NEMO-associating proteins are important in the pathway (Figure 6C, lane 2, 3, and 5). NEMO has been reported to interact with TBK1 through TANK (Zhao et al., 2007). Consistent with this, a pull-down of flag tagged NEMO Δ N (NEMO Δ N PD), expressed in *Nemo*^{-/-} cells, associate with endogenous TANK and TBK1 (Figure 6D). And when added back to S100 after NEMO antibody depletion, the NEMO Δ N PD sample rescued IRF3 activation by virus-activated P5 (Figure 6C, lane 6 and 7). Further analysis of NEMO Δ N PD confirmed that it contained only NEMO, TANK and TBK1 (data not shown). This suggests that NEMO and the TBK1 complex function together in IRF3 activation.

However, NEMO Δ N PD does not fully replace Q-B in IRF3 activation in vitro even in the presence of ubiquitin and E3 (data not shown), indicating that additional factor(s) might be required for IRF3 activation. We further fractionated Q-B on Heparin-Sepharose and tested the ability of individual fractions to support IRF3 dimerization in the presence or absence of NEMO Δ N PD. In these reactions, we used purified Ubc5 to replace Q-A and supplemented ubiquitin and E1 to avoid identifying these known factors. Several fractions from heparin column showed IRF3 stimulatory activity, which was dependent on NEMO Δ N PD (e.g. fraction 14 in Figure 7A). Subsequently, five more steps of conventional chromatography were used to purify this activity (figure 7B, left). Fractions from the last monoQ column were subjected to silver staining and tandem mass spectrometry, from which one peptide corresponding to TRAF6 (LTILDQSEAPVR) was identified. Immunoblotting with a TRAF6 antibody confirmed that TRAF6 co-purified with the IRF3 dimerization activity in two independent purifications (Figure 7B, right).

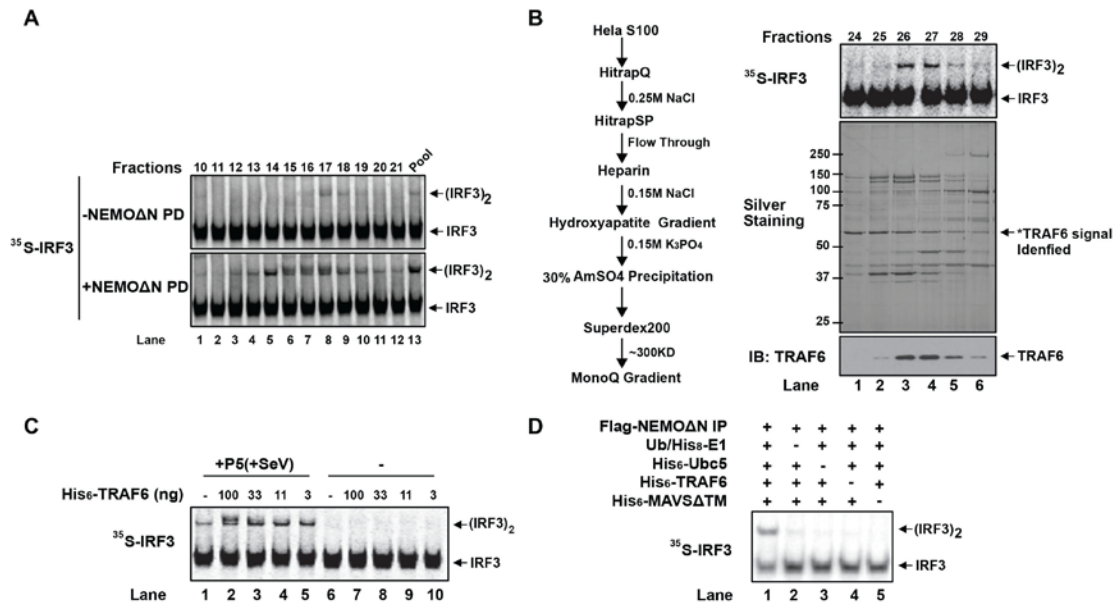


Figure 7. Identification of TRAF6 as an IRF3 Activator

(A) A second activity is required for IRF3 activation in vitro in addition to NEMO Δ N PD. Hela S100 was fractionated on Q-Sepharose column. Eluate by 0.1M-0.3M NaCl was collected and fractionated on Heparin-Sepharose. Fractions from Heparin-Sepharose were analyzed for IRF3 dimerization in vitro in the absence or presence of NEMO PD. In addition, the reactions contain Ubiquitin, His₈-E1, Ubc5, virus-activated P5 and ATP.

(B) Identification of TRAF6 as the active component in Fr14 of Heparin-Sepharose. Scheme of biochemical fractionation of the second activity (right panel). Fractions from the last monoQ were tested for their ability to stimulate IRF3 dimerization in the presence of NEMO-PD and virus-activated P5 (top left) and were analyzed by silver staining (middle left) and immunoblotting with a TRAF6 antibody (bottom left). (Asterisk) BSA overlaps with TRAF6 signal.

(C) Recombinant TRAF6 activates IRF3. Indicated amount of His₆-TRAF6 purified from Sf9 cells was added into the IRF3 dimerization assay to replace the Heparin Fr14.

(D) Reconstitution of IRF3 dimerization in vitro. NEMO Δ N85 PD, Ubiquitin, His₈- E1, Ubc5, His₆-TRAF6, His₆-MAVS Δ TM, His₈-IRF3 and ³⁵S-IRF3 were added or subtracted in the presence of ATP. IRF3 dimerization was analyzed by native gel electrophoresis and followed by autoradiography.

To determine whether TRAF6 is important for IRF3 activation in vitro, we replaced the Heparin fraction with recombinant TRAF6 in the IRF3 assay (figure 7C). A small amount of TRAF6 supported robust IRF3 activation in a MAVS and ubiquitin system dependent manner (Figure 7, C and D). Moreover, the activity from TRAF6 could not be replaced by purified flag-TRAF2 or flag-TRAF3 in vitro (data not shown).

TRAF6 and TRAF2/5 are Important for IRF3 and IKK Activation in vitro

To determine whether TRAF6 is indeed an essential component in IRF3 activation, cell extracts from wild-type and *Traf6*^{-/-} primary MEF cells were tested for their ability to activate IRF3 in vitro. *Traf6*^{-/-} S5 was defective in supporting both IRF3 dimerization and I κ B α phosphorylation in vitro, and these defects were rescued by adding back wild-type TRAF6 (Figure 8, A, B, and E), but not by TRAF6 RING domain mutant (TRAF6C70A), TRAF6 Zinc finger deletion (TRAF6 Δ ZF), or TRAF6 with the TRAF-C domain replaced by a fragment of bacterial gyrase-B (T6RZC) (Wang et al., 2001). This suggests both TRAF6 E3 ligase activity and its ability to interact with other proteins, *e.g.* MAVS (Wang et al., 2001; Xu et al., 2005), are important for IRF3 activation. Interestingly, it has been shown that *Traf6*^{-/-} cells exhibited normal interferon production (Seth et al., 2005; Zeng et al., 2009). *Traf6*^{-/-} primary cells supported IRF3 and NF- κ B activation, as well as cytokine production in response to virus (Figure 9, A-E). Thus, it is possible that other factor(s) that cannot be recovered by the purification is redundant with TRAF6 in cells. We tested extracts from other TRAF deficient cells in vitro and found that S5 from *Traf2*^{-/-}/*Traf5*^{-/-} (*Traf2/5*^{-/-}) MEF cells failed to support both IRF3 dimerization and I κ B α phosphorylation in vitro, which were restored by adding back either wild-type TRAF2 or TRAF5 (Figure 8, A, C, and F). Unlike TRAF6, TRAF2 RING deletion (TRAF2 Δ R) but not its TRAF-C domain deletion (TRAF2 Δ C) restored IRF3 dimerization in S5 from *Traf2/5*^{-/-} cells. Notably, the defect in *Traf2/5*^{-/-} S5 was also restored by adding purified TRAF6 in vitro (Figure 8D), suggesting the presence of abundant TRAF6 can bypass the requirement of TRAF2 for IRF3 activation in

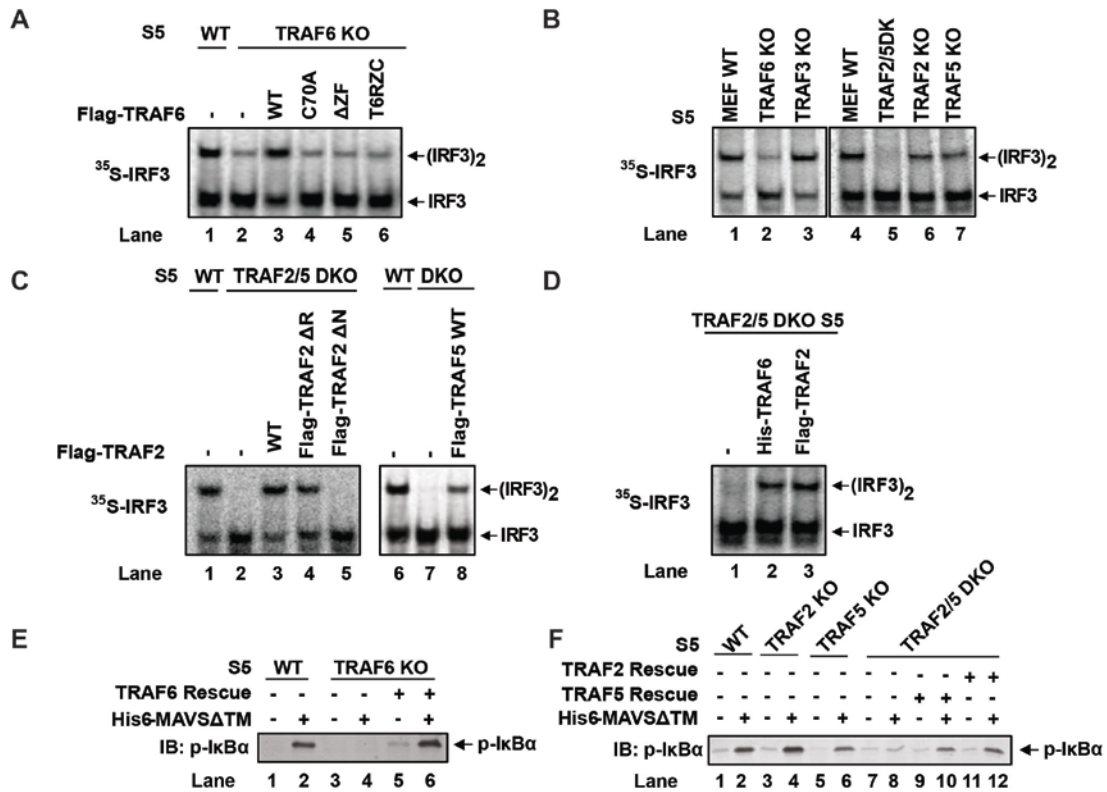


Figure 8. TRAF2/5 and TRAF6 are Important for IRF3 Activation in vitro.

(A) Cell extract without TRAF6 is defective in IRF3 activation in vitro. Cytosolic extracts from wild-type or *Traf6*^{-/-} primary MEF cells were analyzed in IRF3 dimerization assay with virus-activated P5 replaced by purified His₆-MAVSΔTM. Flag-TRAF6 wild-type and mutants were tested for their ability to rescue the IRF3 dimerization in *Traf6*^{-/-} S5.

(B) TRAF2 and 5 are also important for IRF3 activation in vitro. Cytosolic extracts S5 from WT or different TRAF deficient MEF cells were analyzed in IRF3 dimerization assay with His₆-MAVSΔTM.

(C) Either TRAF2 or TRAF5 rescues IRF3 dimerization in Traf2/5 DKO extract. Flag-TRAF2 wild-type and mutants, as well as Flag-TRAF5 wild-type were tested for their ability to rescue IRF3 dimerization in Traf2/5^{-/-} S5.

(D) Recombinant TRAF6 rescues the IRF3 dimerization defect in S5 from TRAF2/5 DKO in vitro. His₆-TRAF6 was incubated with S5 from *Traf2/5* DKO MEF cells. Dimerization of ³⁵S-IRF3 was analyzed by native gel electrophoresis.

(E) Cell extract without TRAF6 is defective in IκBα phosphorylation in vitro. Cytosolic extracts S5 from WT or *Traf6*^{-/-} MEF cells were incubated in vitro with His₆-MAVSΔTM and ATP. Flag-TRAF6 was added into S5 from *Traf6*^{-/-} and phosphorylated IκBα was analyzed by immunoblotting.

(F) Cell extract without TRAF2/5 is defective in IκBα phosphorylation in vitro. Cytosolic extracts S5 from WT, *Traf2*^{-/-}, *Traf5*^{-/-} and *Traf2/5* DKO MEF cells were analyzed in IRF3 dimerization assay in the presence of His₆-MAVSΔTM. Flag-tagged TRAF2 and TRAF5 were tested for their ability to rescue the IκBα phosphorylation in *Traf6*^{-/-} S5. Phosphorylated IκBα was analyzed by immunoblotting (bottom).

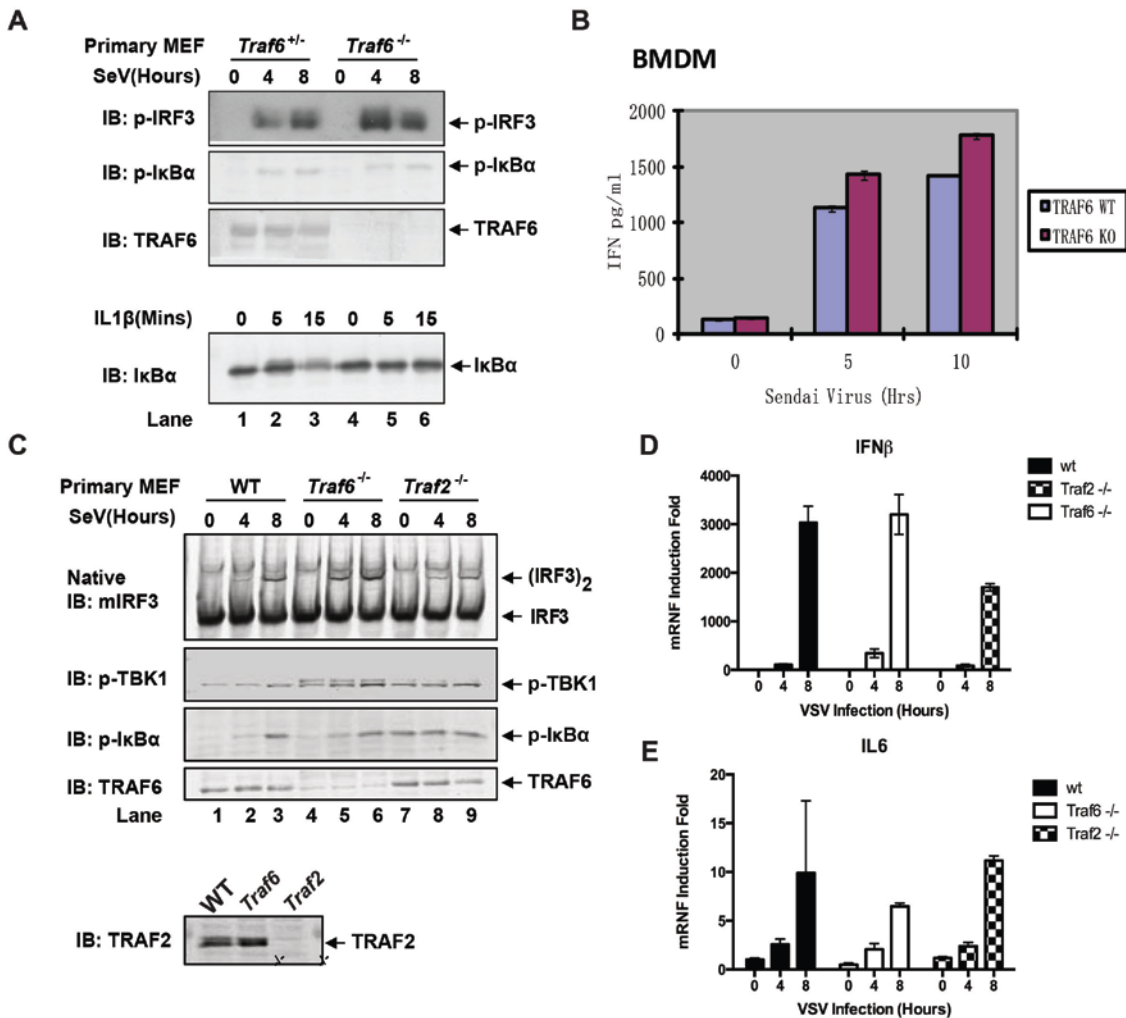


Figure 9. *Traf6*^{-/-} and *Traf2*^{-/-} Cells don't show strong defect in IRF3 and NF-κB Activation by virus.

(A) Wild-type and *Traf6*^{-/-} primary MEF cells were infected with Sendai virus for indicated period of time and phosphorylation of IRF3 and I κ B α was analyzed by immunoblotting (top). As a control, wild-type and *Traf6*^{-/-} primary MEF cells were treated by IL-1 β and total I κ B α was analyzed by immunoblotting (bottom).

(B) Bone marrow cells were isolated from Wild-type and *Traf6*^{-/-} mice and differentiated into Bone marrow derived macrophages in presence of M-CSF. Medium from Sendai virus infected BMDMs was collected and secreted IFN- β was measured by ELISA.

(C) Wild-type, *Traf6*^{-/-} and *Traf2*^{-/-} primary MEF cells were infected by Sendai virus for indicated period of time. Dimerization of IRF3, phosphorylation of TBK1 and I κ B α were analyzed by immunoblotting. Endogenous TRAF6 and TRAF2 were confirmed by immunoblotting.

(D-E) Total RNA was isolated from cells described in (C) and mRNA level of IFN- β and IL-6 was analyzed by qPCR.

crude extract, which is possibly the reason why TRAF2-dependent activity wasn't recovered in the purification.

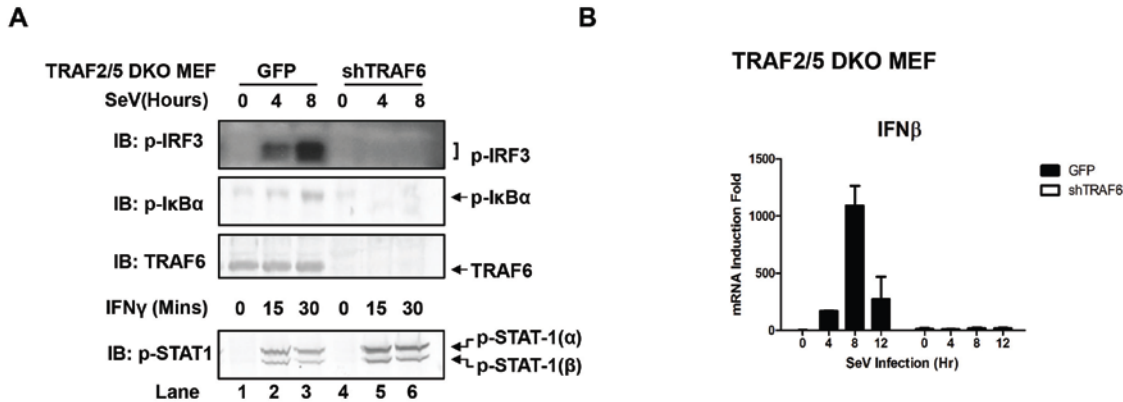


Figure 10. TRAF2/5 and TRAF6 Function Redundantly in both IRF3 and NF-κB Activation by virus.
 (A) Depletion of TRAF6 in *Traf2/5*^{-/-} MEF cells abolishes both IRF3 and NF-κB Activation by virus. Lentiviral vector expressing shRNA against TRAF6 or empty vector was introduced into *Traf2/5*^{-/-} MEF cells and Sendai virus induced phosphorylation of endogenous IRF3 and IκBα were analyzed by immunoblotting (top). IFN-γ induced STAT1 phosphorylation was also analyzed in the same pair of cells as a control (bottom).
 (B) Depletion of TRAF6 in *Traf2/5*^{-/-} cells abolishes IFN-β mRNA induction by virus. The cells described in (A) were treated with Sendai virus for indicated period of time before total RNA was isolated. IFN-β mRNA induction fold was analyzed by quantitative PCR (qPCR).

TRAF6 and TRAF2/5 are Redundant for IRF3 and IKK Activation in vivo

Similar to *Traf6*^{-/-} MEFs, *Traf2*^{-/-} MEFs induced IFNβ and IL6 normally in response to Sendai virus infection, as well as IRF3 dimerization (Figure 9, C, D and E). Moreover, in contrast to the profound defect of *Traf2/5* DKO cell extracts in supporting IRF3 and IKK activation by MAVS, the DKO cells activated IRF3 and induced IFNβ normally after Sendai virus infection (Figure 10, A and B). Importantly, knockdown of TRAF6 expression by short hairpin RNA (shTRAF6) in the DKO cells abolished IRF3 activation and IFNβ induction by Sendai virus, but did not impair STAT1 phosphorylation induced by IFNγ (Figure 10).

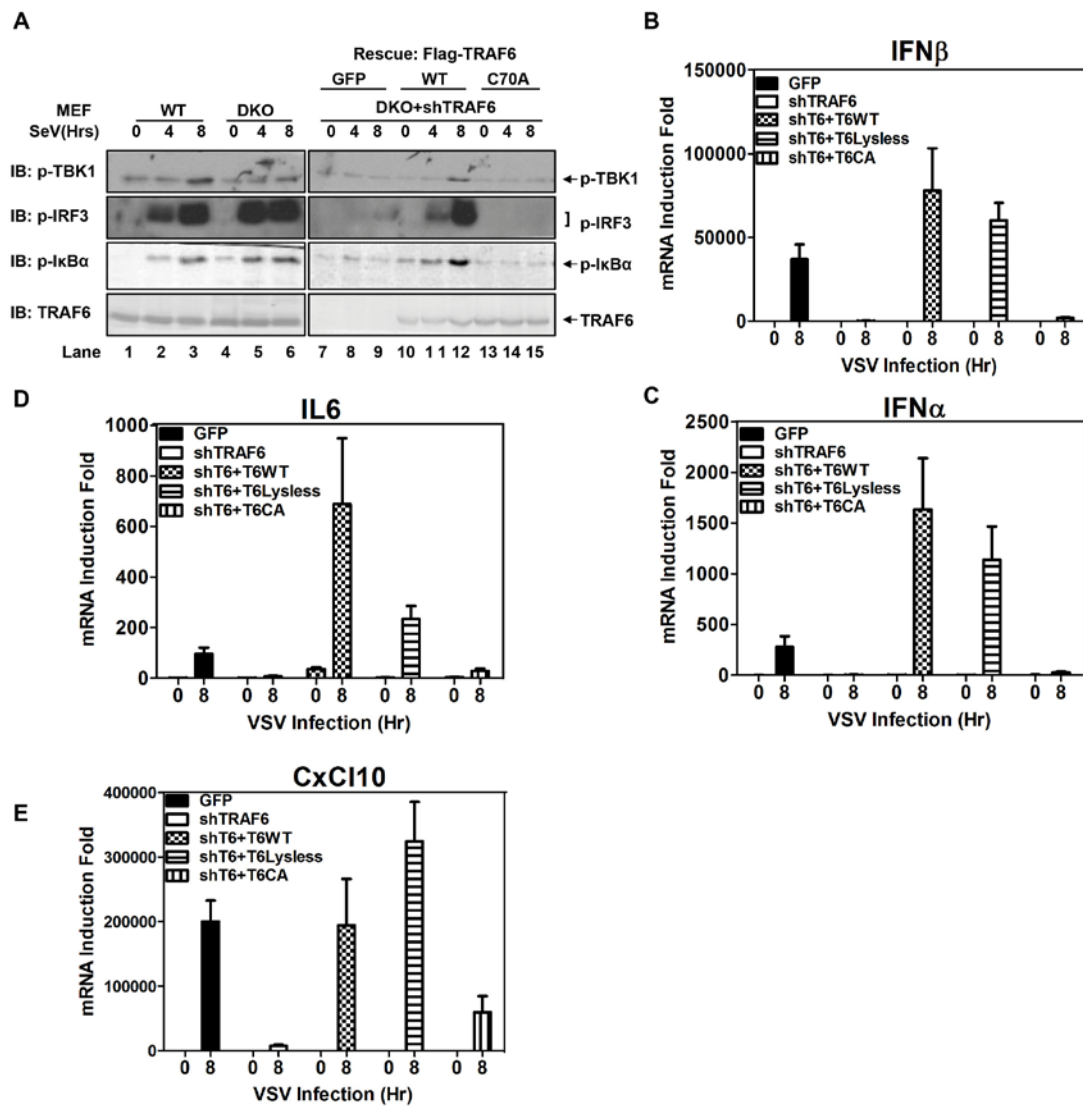


Figure 11. The RING Domain of TRAF6 is Required for TRAF6-dependent IRF3 and NF- κ B Activation by virus.

(A) TRAF6 wild-type but not the RING mutant rescues the downstream defect of the cells in which TRAF2, 5 and 6 are depleted. *Traf2/5^{-/-}* MEF cells stably expressing shRNA against TRAF6 (DKO+shT6) and those in which endogenous TRAF6 was replaced with WT or RING mutant Flag-TRAF6 were stimulated with Sendai Virus for indicated period of time. Phosphorylation of TBK1, IRF3 and I κ B α was analyzed by immunoblotting. (B-E) Total RNA from cells described in (A) was isolated and the induction of the cytokines was analyzed by qPCR.

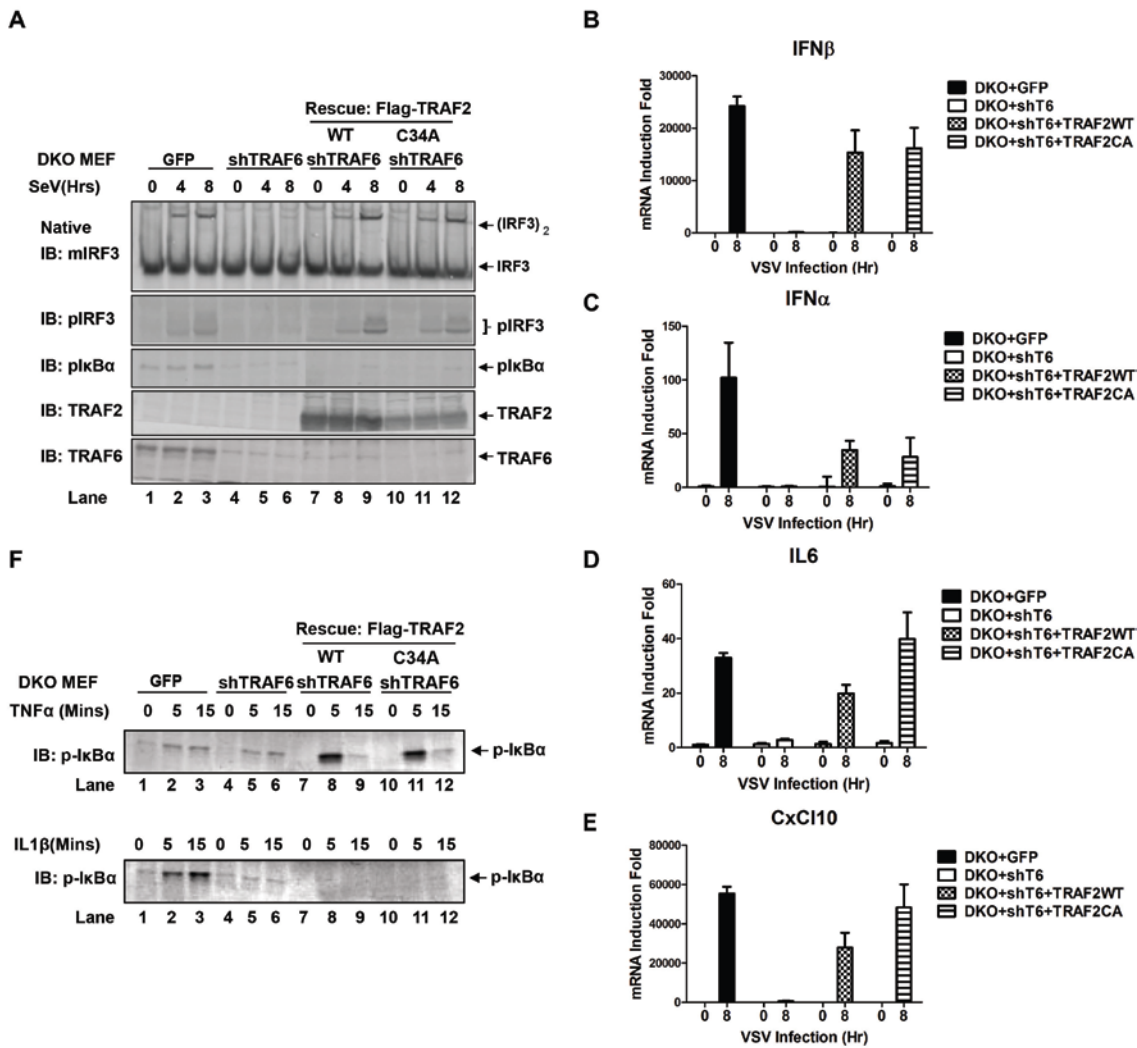


Figure 12. The RING Domain of TRAF2 is Dispensable for TRAF2-dependent IRF3 and NF- κ B Activation by virus.

(A) Both TRAF2 WT and RING mutant rescue the downstream defect of the cells in which TRAF2, 5 and 6 are depleted. *Traf2/5*^{-/-} MEF cells stably expressing WT or RING mutant Flag-TRAF2 were stimulated with Sendai virus for indicated period of time. Dimerization of IRF3, phosphorylation of IRF3 and IkBa were analyzed by immunoblotting.

(B-E) Total RNA from cells described in (A) was isolated and the induction of the cytokines was analyzed by qPCR.

(F) Cells described in (A) were stimulated with either TNF- α or IL-1 β . Phosphorylation of IkBa was analyzed by immunoblotting.

To exclude the off-target effect of shRNA and further investigate the role of TRAF2 and TRAF6 in IRF3 and NF- κ B activation by virus in cells, we performed complementation experiments by expressing different TRAF proteins in DKO+shT6 cells. Consistent with the in vitro rescue experiments, the defects in DKO+shT6 cells were rescued by wild-type TRAF6 but not by RING mutant (C70A) TRAF6 (Figure 11, A-E). Meanwhile, the defects were also rescued by either wild-type TRAF2 or RING mutant (C34A or Δ RING) TRAF2 (Figure 12, A-E). As controls, both wild-type and mutant TRAF2 rescued I κ B α phosphorylation by TNF α , but not by IL-1 β (Figure 12F). These results suggest that the E3 ligase activity of TRAF2 is either dispensable or redundant with that of another E3 ligase, which requires further investigation. Taken together, these data indicate that TRAF2/5 or TRAF6 can independently trigger activation of both IRF3 and NF- κ B downstream of MAVS in response to virus.

The E3 ligase Activity of LUBAC is Redundant with that of TRAF2

The dispensable role of TRAF2's E3 ligase activity implies involvement of another E3 ligase in TRAF2-dependent IRF3 activation. Hence, we tested several other E3 ligases reported to play a role in innate immunity, including TRAF3 and LUBAC complex. In brief, we found that cell extracts from *cpdm* MEF cells, defective in HOIP signaling, and from WT MEF stably expressing shRNA against HOIP are both defective in IRF3 activation in vitro (Figure 13, A and B). This defect can be rescued by adding back wild-type Flag-LUBAC containing Flag-HOIL and Flag-HOIP proteins but not by mutant LUBAC containing a HOIP RING mutant (C693/696S, CS). However, both *cpdm* MEF cells and HOIP (CS)

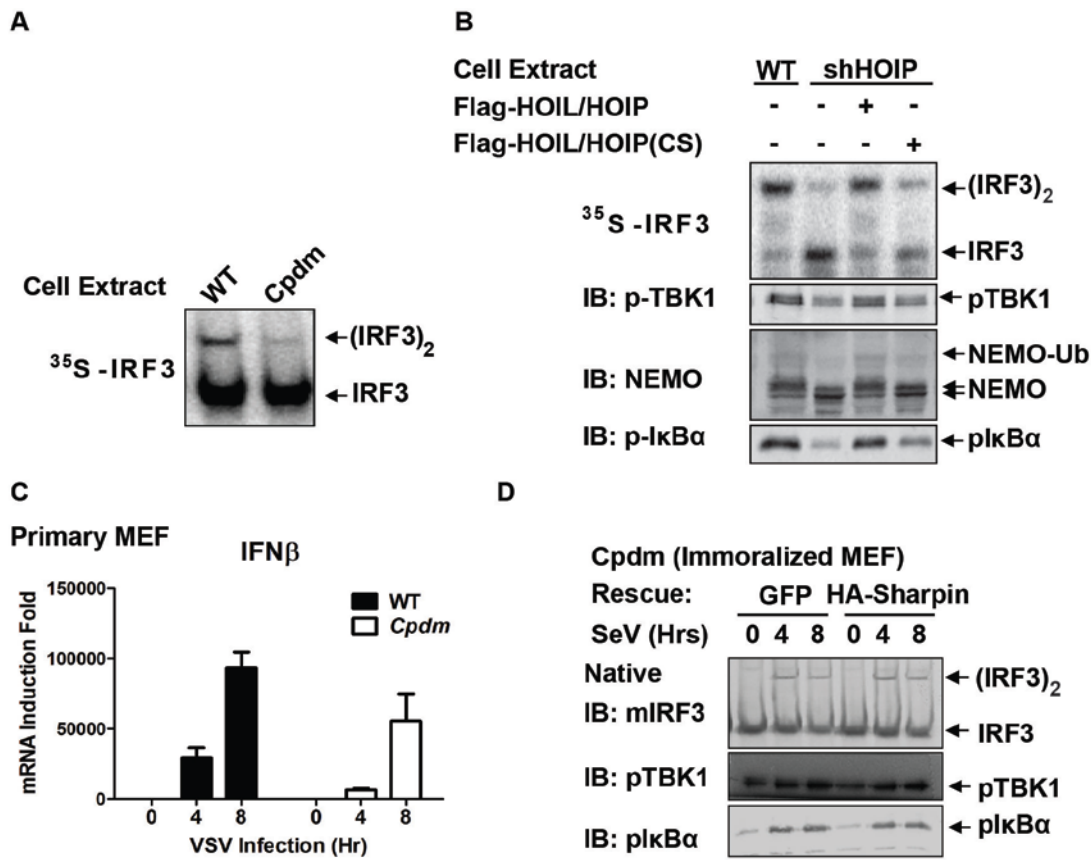


Figure 13. LUBAC Complex is Important for IRF3 Activation In vitro.

(A) Cell extracts from Wild-type and *Cpdm* MEF cells were tested for their ability to support IRF3 dimerization in vitro in the presence of His₆-MAVSΔTM.

(B) Extracts from WT cells or MEF cells stably expressing shRNA against HOIP were tested for their ability to support IRF3 dimerization in vitro in the presence of His₆-MAVSΔTM. Flag-LUBAC complex purified from 293 cells containing wild-type HOIL and Wild-type or RING mutant HOIP were added into the shHOIP extract to test their ability to rescue the IRF3 dimerization defect in vitro.

(C) Primary wild-type or *Cpdm* MEF cells were infected with VSV for indicated period of time. qPCR was performed to examine IFN- β RNA induction.

(D) Immortalized *Cpdm* MEF cells stably expressing GFP or HA-Sharpin were infected with Sendai virus for indicated period of time. Dimerization of IRF3, phosphorylation of TBK1 and I κ B α were analyzed by immunoblotting.

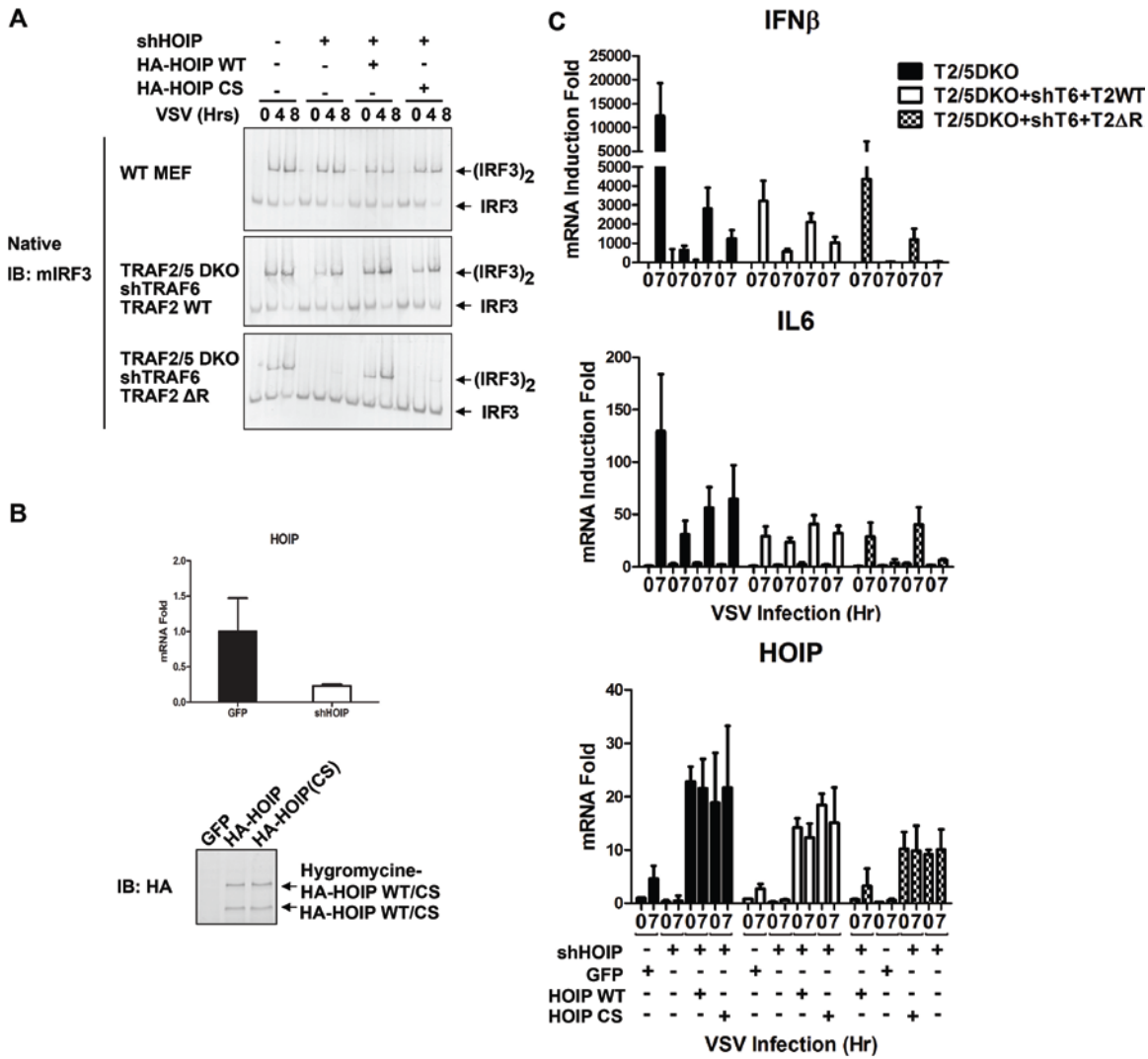


Figure 14. The E3 ligase Activity of HOIP and TRAF2 are Redundant in Cells in Response to Virus

(A) Lentiviral vectors encoding GFP, shRNA against HOIP, HA-HOIP WT and RING mutant were introduced into wild-type MEF cells and DKO+shT6 cells expressing either WT or RING mutant TRAF2 as described in Figure 12A. Dimerization of endogenous IRF3 was analyzed by immunoblotting after cells were infected with VSV for indicated period of time.

(B) Knockdown efficiency of HOIP described in (A) was analyzed by qPCR (top). Expression of HA-HOIP WT and mutant were analyzed by immunoblotting (bottom).

(C) Lentiviral vectors expressing GFP, shRNA against HOIP, HA-HOIP WT and RING mutant were introduced into cells described in Fig.12A. After VSV infection for indicated period of time, IFN- β , IL6 and HOIP mRNA expression were analyzed by qPCR.

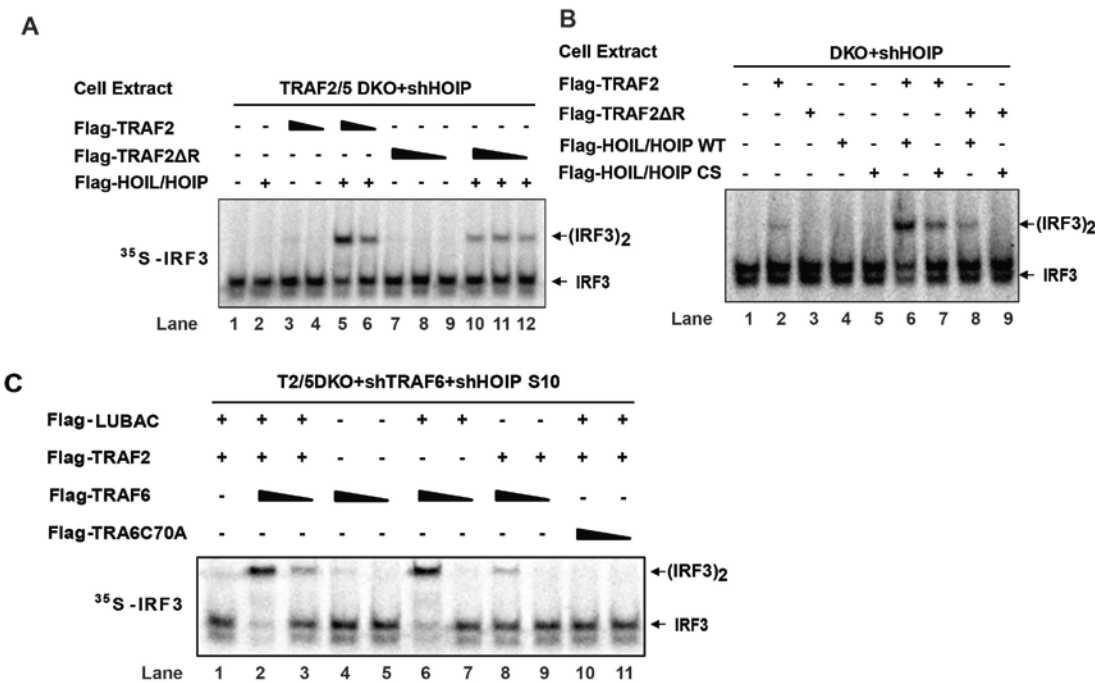


Figure 15. The E3 ligase Activity of HOIP and TRAF2 are Redundant for IRF3 Dimerization in vitro.
 (A-B) Cytosolic extracts from DKO+shHOIP cells were analyzed in IRF3 dimerization assay in the presence of His₆-MAVS Δ TM. Wild-type or Δ RING Flag-TRAF2 and wild-type or CS mutant Flag-LUBAC were tested in combination for their ability to rescue the IRF3 dimerization in the same extract.
 (C) Cytosolic extracts from DKO+shHOIP+shTRAF6 cells were analyzed in IRF3 dimerization assay in the presence of His₆-MAVS Δ TM. Wild-type or Δ RING Flag-TRAF2, wild-type or CS mutant Flag-LUBAC and Wild-type or CA mutant Flag-TRAF6 were tested in combination for their ability to rescue the IRF3 dimerization in the same extract.

knock-in cells exhibited only very mild defect in IFN- β induction by virus (Figure 13C).

Moreover, no obvious defect was observed in either IRF3 dimerization or I κ B α phosphorylation (Figure 13D). Strikingly, further knocking down of HOIP in DKO+shT6 cells stably expressing different TRAF2 proteins specifically abolished virus induced IRF3 activation and cytokine production only in the cells expressing the TRAF2 RING mutant, but

not in those expressing wild-type TRAF2 (Figure 14, A-C). Furthermore, the defect caused by depletion of HOIP can be rescued by introducing wild-type HOIP, but not its E3 ligase mutant. Consistently, we also found that IRF3 activation in cell extracts from *Traf2/5*^{-/-} MEF cells stably expressing shRNA against HOIP (DKO+shHOIP) can be rescued by adding either purified TRAF2 or LUBAC in vitro, whereas adding TRAF2 RING mutant and LUBAC together failed to restore the activity (Figure 15, A and B). This, couple with the fact that DKO+shT6 cells are unable to respond to virus, suggests that firstly, TRAF2 functions upstream of HOIP and secondly, the E3 ligase activity of TRAF2 and HOIP are redundant in TRAF2-dependent IRF3 and NF-κB activation.

TRAFs are Directly Recruited to Aggregated MAVS through its TRAF-binding Motifs

MAVS has binding motifs for TRAF2, TRAF3 and TRAF6 (Paz et al., 2011; Saha et al., 2006; Seth et al., 2005; Xu et al., 2005) (Figure 16A). We found that purified TRAF2 and TRAF6 directly interacted with MAVS Δ TM (N460) in vitro, and the binding between TRAF6 and MAVS was abolished by further deletion of TRAF6 binding motif (455-460) on MAVS, whereas TRAF2 binding to MAVS was unaffected (Figure 16B). As a control, IRF3 didn't interact with MAVS Δ TM. This suggests that the active form MAVS indeed has the ability to interact with TRAF proteins directly. Subsequently, we examined the interaction between TRAF proteins and endogenous MAVS in DKO+shT6 cells stably expressing different TRAF2 or TRAF6 proteins. Both TRAF2 and TRAF6 interacted with endogenous MAVS in a virus-dependent manner (Figure 16C). Moreover, to test if the TRAF2/6 and MAVS interacted through the TRAF binding motifs in virus infected

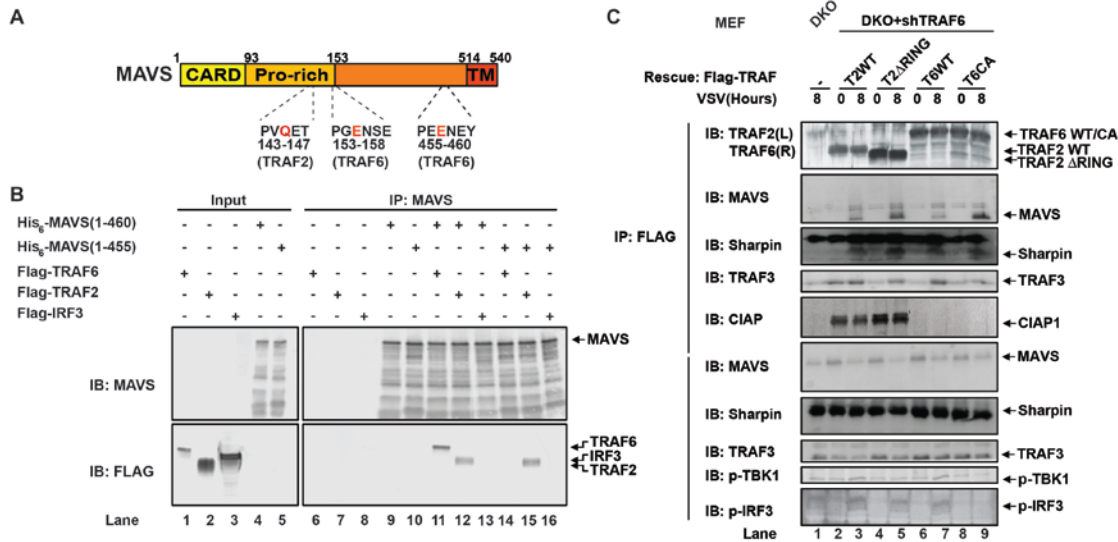


Figure 16. MAVS Recruits Multiple TRAF Proteins upon Virus Infection.

(A) Endogenous MAVS recruits both TRAF2 and TRAF6 in a virus-dependent manner. DKO+shT6 MEF cells stably expressing Wild-type or mutant flag-TRAF proteins were infected with VSV for indicated period of time. TRAF proteins were immunoprecipitated with M2 anti-Flag agarose and co-precipitated proteins were analyzed by immunoblotting.

(B) TRAF binding motifs in human MAVS.

C. In vitro binding assay for MAVS and TRAF proteins. His₆-MAVS (N460) or His₆-MAVS (N455) purified from *E.Coli* was mixed with flag-TRAF6, Flag-TRAF2 or Flag-IRF3 purified from 293 cells, followed by immunoprecipitation using a MAVS antibody. Co-immunoprecipitated proteins were analyzed by immunoblotting.

cells, we introduced MAVS harboring TRAF binding site mutants into MEF cells. Indeed, mutation of TRAF6 binding sites (E155/457D, ΔT6) specifically disrupted binding between MAVS and TRAF6 whereas mutation of the TRAF2 binding site (Q145N, ΔT2) abolished the ability for MAVS to interact with TRAF2 (Data not shown, performed by Jueqi Chen). Furthermore, complementation of these MAVS mutants into *Mavs*^{-/-} cells showed that only MAVS ΔT6+ΔT2 failed to induce IFN-β production in response to virus (Figure 17, performed by Jueqi Chen). Meanwhile, a virus replication assay demonstrated that *Mavs*^{-/-} cells reconstituted with MAVS ΔT6+ΔT2 failed to suppress VSV replication, whereas cells

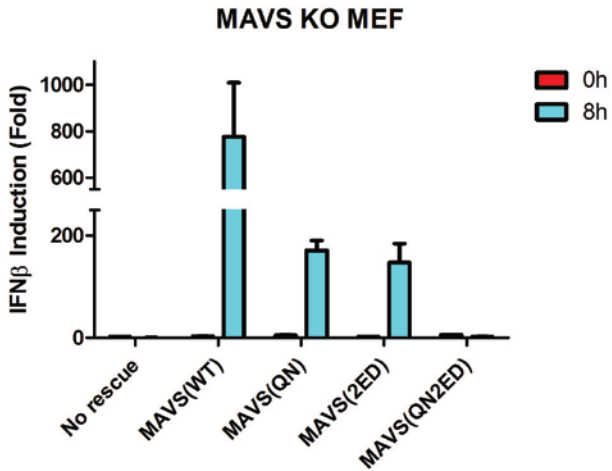


Figure 17. The TRAF Binding Motifs on MAVS are Essential for MAVS-mediated Activation of NF- κ B and IRF3.

Total RNA from cells described in (A) was isolated after Sendai virus infection and mRNA induction of IFN- β was analyzed by qPCR (by Jueqi Chen).

expressing WT or other mutant MAVS contained VSV replication more efficiently (data not shown, performed by Jueqi Chen). To further confirm that the defect of these MAVS mutants is due to disruption of specific TRAF proteins recruitment, we further replaced the endogenous MAVS with these MAVS mutants in *Traf6*^{-/-} and *Traf2/5*^{-/-} MEF cells. MAVS Δ T2 failed to propagate virus-induced signaling in TRAF6 KO MEF, which can be rescued by introducing WT but not RING mutant TRAF6, supporting the conclusion that MAVS Δ T2 can only function through TRAF6. Similarly, MAVS Δ T6 was defective in activating the pathway in *Traf2/5*^{-/-} MEF cells, but the defect was restored by expressing either WT or RING mutant TRAF2 (data not shown, performed by Jueqi Chen). Moreover, introduction of MAVS Δ T6 in neither *Traf2*^{-/-} nor *Traf5*^{-/-} blocked the IFN- β induction by virus, suggesting a redundant function of TRAF2 and TRAF5 (data not shown, performed by Jueqi Chen). Lastly, *Mavs*^{-/-} MEF cells complemented with full-length MAVS mutant proteins that are unable to form MAVS polymer failed to recruit TRAF proteins and to propagate downstream

signaling in response to virus (data not shown, performed by Jueqi Chen). Taken together, these findings indicate that the prion-like conformational switch of MAVS is crucial for the recruitment of TRAF2/5 and TRAF6, which function in parallel downstream of MAVS to activate the transcription factors.

NEMO Forms a Complex with MAVS and TRAF2/6

We have previously shown that the ubiquitin-binding domain of NEMO is required for IRF3 activation both in vitro and in vivo (Zeng et al., 2009). Based on this, NEMO was proposed as a sensor of K63-linked polyubiquitin chains to mediate the activation of TBK1 and IKK in response to virus. In order to identify ubiquitination target(s) that relays upstream signal to NEMO, we incubated flag-tagged NEMO with Hela S100 in the presence of MAVS Δ TM. MAVS and TRAF2 were found to coimmunoprecipitate with flag-NEMO only after incubation at 30°C. Moreover, the MAVS-TRAF2-NEMO interaction was inhibited when viral-OTU (vOTU), a deubiquitinase that removes both conjugated and unanchored ubiquitin chains, was included in the reaction mix (Figure 18A). These results suggest that MAVS and TRAF2 form a MAVS fiber-induced, ubiquitination-dependent signaling complex with NEMO in vitro. We also found the ubiquitin-binding mutant (UBD mut, Y308S/H413A/C417A) NEMO failed to pull down the TRAF2-MAVS complex, suggesting that NEMO binding to ubiquitin might be important for the complex formation (Figure 18B). Moreover, when we incubated flag-NEMO with extracts from various MEF-deficient cells in the presence of MAVS Δ TM, the NEMO-MAVS complex formation

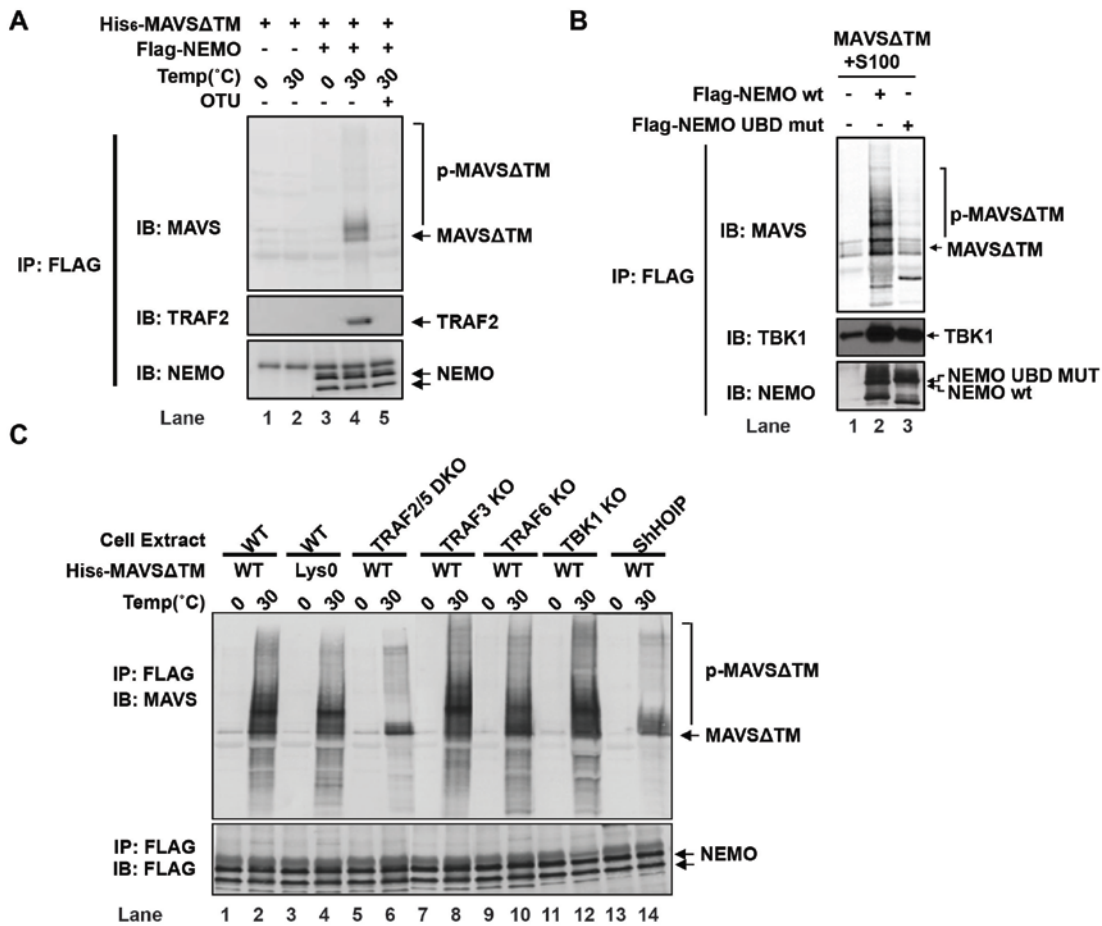


Figure 18. NEMO Forms a Complex with TRAF2 and MAVS in vitro.

(A) NEMO pulls down MAVS and TRAF2 in a DUB-dependent manner. Expression vector for Flag-NEMO was transfected into *Nemo*^{-/-} cells and protein was purified using anti-Flag (M2) agarose. Purified Flag-NEMO was incubated with Hela S100 and His₆-MAVSΔTM in the presence of ATP with or without vOTU and then immunoprecipitated with M2 agarose. Coimmunoprecipitated MAVS and TRAF2 were analyzed by immunoblotting (top and middle).

(B) NEMO ubiquitin binding domain is important for NEMO-MAVS complex formation. Wild-type and UBD mutant Flag-NEMO were tested for their ability to form NEMO-MAVS complex in the assay described in (A).

(C) TRAF2/5 and HOIP are important for the NEMO-MAVS complex formation. Cell extracts (S5) from various deficient MEF cells were incubated with Flag-NEMO and His₆-MAVSΔTM for indicated period of time at 30 °C. NEMO was then immunoprecipitated using M2 agarose and coimmuno precipitated MAVS was analyzed by immunoblotting (top).

dramatically decreased in extracts from *Traf2/5*^{-/-} MEF cells and cells stably expressing shRNA against HOIP (Figure 18C).

To further characterize this complex, we performed two sets of in vitro SILAC experiments as shown in Figure 19A. In the first set, we incubated flag-NEMO with extracts from either heavy or light isotope labeled wild-type MEF cells in the presence or absence of MAVS Δ TM. In the second set of SILAC, we incubated wild-type or UBD mut NEMO with extracts from either heavy or light labeled wild-type MEF cells in the presence of MAVS Δ TM. Heavy labeled, modified forms of MAVS and TRAF2 were enriched in the flag-NEMO Co-IP in both sets of SILAC as shown in Figure 19B. Proteins in the flag-NEMO Co-IP were identified by mass spectrometry and the signal-dependent interactions with NEMO were ranked by the heavy to light ratios (H/L) of signal intensity analyzed by MAXQUANT (Figure 19, C and D).

187 proteins were identified in both sets of SILAC (Figure 19E). In addition to MAVS, heavy labeled TRAF2, PLK1 and cIAP1 were enriched in both sets of SILAC (high H/L ratio) (Figure 19F), suggesting a MAVS-dependent, NEMO ubiquitin-binding dependent interactions between these proteins and NEMO. PLK1 was previously shown as a negative regulator of MAVS (Vitour et al., 2009). cIAP1/2 have also been shown to be important in antiviral pathway downstream of MAVS (Mao et al., 2010). In our studies, cIAP1 interacts with wild-type and Δ RING TRAF2 constitutively and independent of viral infection as shown in Figure 16C, but no obvious signaling defect has been observed by SMAC mimetic treatment either in vitro or in vivo in response to virus (data not shown). Thus, we focused on TRAF2 as one of the putative ubiquitination targets downstream of MAVS in the following study.

Figure 19

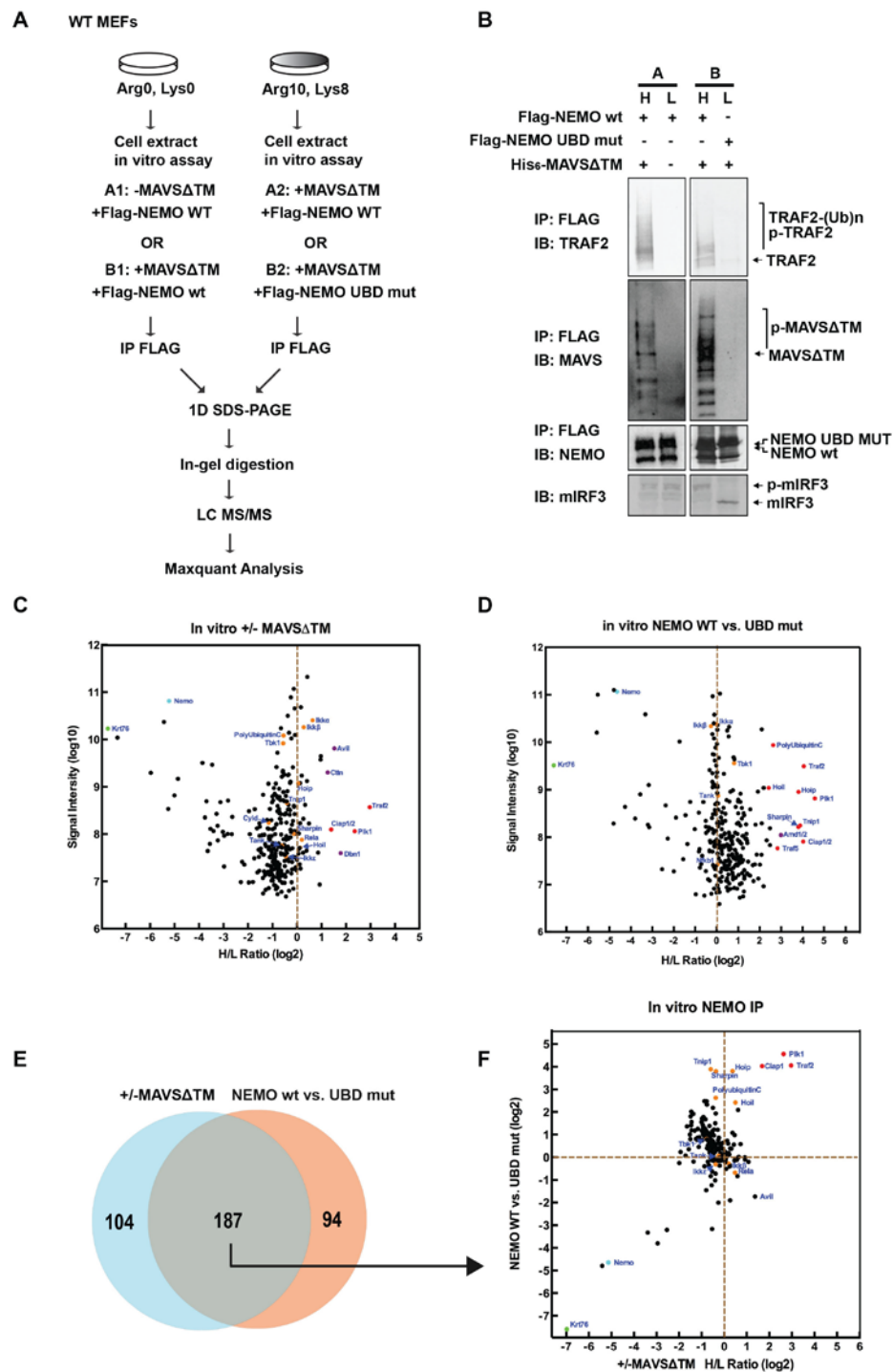


Figure 20

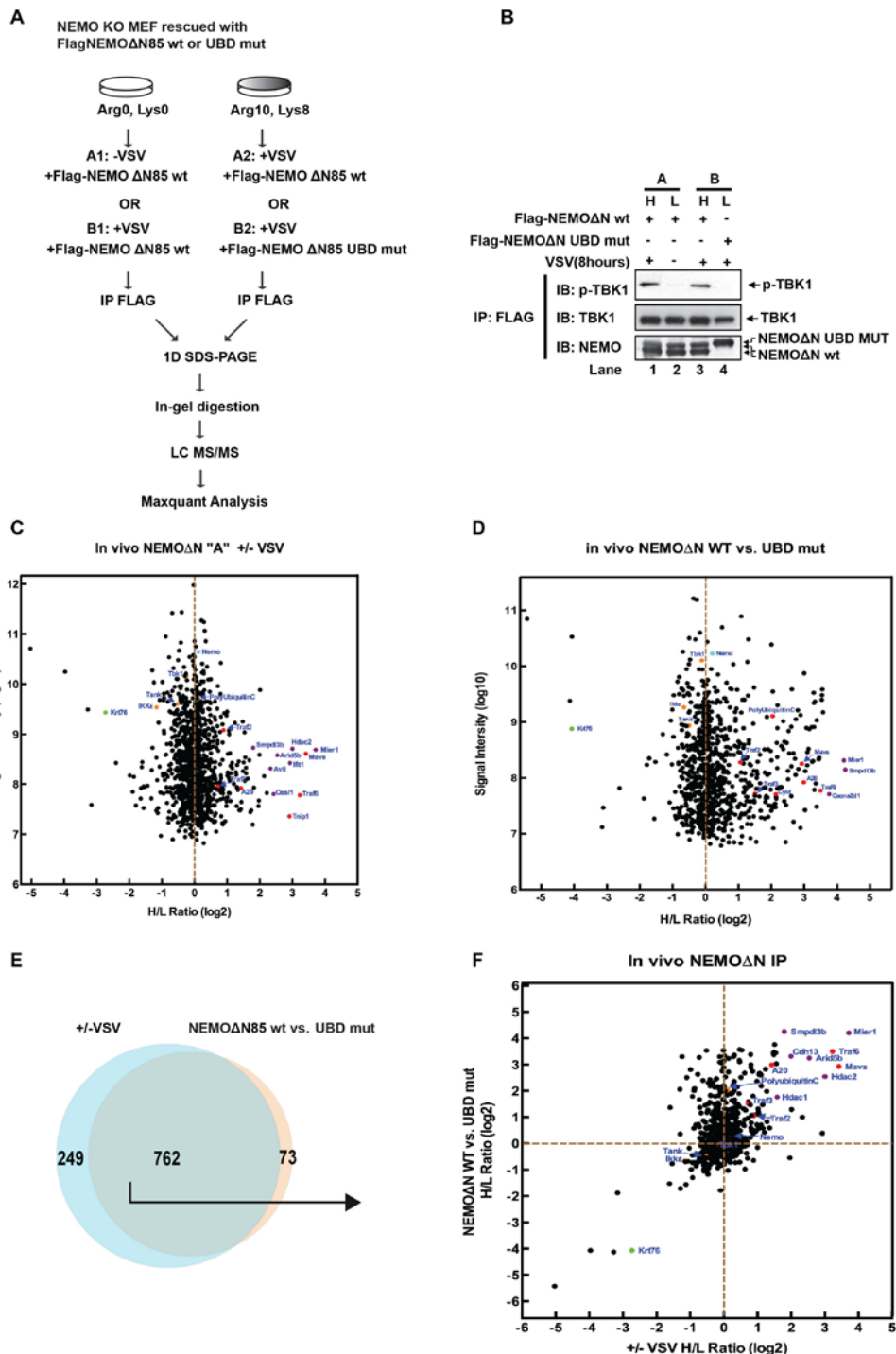


Figure 19. Characterization of NEMO-interacting Proteome in vitro by SLIAC.

(A) Experimental design of the SILAC experiments comparing proteins coimmunoprecipitated with NEMO in vitro:

A: MEF WT S5 (Heavy: Lys8, Arg10) with His₆-MAVSΔTM versus MEF WT S5 (Light: Lys0, Arg0) without His₆-MAVSΔTM, in the presence of Flag-NEMO wt.

B: MEF WT S5 (Heavy: Lys8, Arg10) with Flag-NEMO wt versus MEF WT S5 (Light: Lys0, Arg0) Flag-NEMO UBD mutant, in the presence of His₆-MAVSΔTM.

(B) IRF3 phosphorylation in each SILAC reaction and coimmunoprecipitation of MAVS, TRAF2 in the in vitro SILAC experiments were analyzed by immunoblotting (top and middle).

(C-D) SILAC ratios (H/L) for proteins plotted against the total peptide intensities in both SILAC experiments. Expected signal-dependent NEMO binding proteins with a high H/L ratio were highlighted in red; expected signal-independent NEMO binding proteins with a ratio about 1 were in orange; putative unknown factors with a high H/L ratio were highlighted in purple; NEMO (exogenous proteins without heavy label) was highlighted in cyan whereas Krt76 was in green as an example of exogenous contaminants.

(E-F) Venn diagram showing 187 proteins present in both SILAC experiments (left). Of these proteins, SILAC ratios in SILAC “A” were plotted against that in SILAC “B”. Proteins with high ratios in both experiments were highlighted in red. Other expected NEMO binding proteins were highlighted in orange. NEMO (Cyan) and Krt76 (Green) were also highlighted (right).

Figure 20. Characterization of NEMO-interacting Proteome in Response to Virus by SILAC.

(A) Experimental design of the SILAC experiments comparing proteins coimmunoprecipitated with NEMO in vivo.

A: *Nemo*^{-/-} MEF cells stably expressing Flag-NEMOΔN85 wt (Heavy: Lys8, Arg10) with 8 hour VSV infection versus mock infection (Light: Lys0, Arg0).

B: *Nemo*^{-/-} MEF cells stably expressing Flag-NEMOΔN85 wt (Heavy: Lys8, Arg10) versus *Nemo*^{-/-} MEF cells stably expressing Flag-NEMOΔN85 UBD mutant (Light: Lys0, Arg0), both with 8 hour VSV infection.

(B) TBK1 and p-TBK1 coimmunoprecipitated with flag-NEMO ΔN85 were confirmed by immunoblotting in the SILAC experiments.

(C-D) SILAC ratios (H/L) for proteins plotted against the total peptide intensities in both SILAC experiments as described in Figure 21E.

(E-F) Venn diagram showing 762 proteins present in both SILAC experiments (left). Of these proteins, SILAC ratios in SILAC “A” were plotted against that in SILAC “B” as described in Figure 21F (right).

To determine whether NEMO also forms a complex with MAVS in response to virus in cells, we performed two sets of SILAC experiments in *Nemo*^{-/-} MEF cells stably expressing wild-type or UBD mutant Flag-NEMOΔN85 as shown in Figure 20A. As a control, TBK1 was coimmunoprecipitated with Flag-NEMO constantly whereas phosphorylated TBK1 was only present in the heavy labeled Co-IP samples with viral infection and wild-type NEMO ΔN85 (Figure 20B). Proteins identified in each SILAC

experiments were ranked by H/L ratio (Figure 20, C and D). 762 proteins were present in both sets of SILAC experiments (Figure 20, E and F). MAVS, TRAF6, A20, TRAF2 and TRAF3 are among those associated with NEMO in a virus-dependent and NEMO UBD-dependent manner.

Lysine Mutations of TRAF2 or NEMO did not Affect the Activation of IRF3 or NF-κB by Virus

We have previously suggested a role of lysine 63 (K63)-linked polyubiquitination in IRF3 activation by MAVS using a dominant-negative assay (Zeng et al., 2009). Using U2OS cells stably expressing a tetracycline-inducible shRNA vector targeting ubiquitin (Xu et al., 2009), we tested a panel of ubiquitin mutants, including those containing a point mutation at lysine 63 (K63R), mutations on all lysines but lysine 63 (K63 only), or His-tagged ubiquitin known to block linear ubiquitination, for their ability to rescue IRF3 dimerization and I κ B α phosphorylation in vitro. Consistently, cells extract with its endogenous ubiquitin depleted failed to support both IRF3 activation and I κ B α phosphorylation in vitro. The defects were rescued by adding back wild-type, K63 only and His₆-Ubiquitin but not by K63R ubiquitin (Figure 21).

As for the ubiquitination targets, we focused on MAVS, TRAF2, TRAF6 and NEMO because these proteins interact with NEMO in a signal-dependent, NEMO ubiquitin-binding dependent manner in the SILAC experiments. We have shown that *Mavs*^{-/-} MEF cells stably expressing MAVS with all its lysines mutated into arginines (lys-les) still supported viral-induced cytokine production without much defect (Zeng et al., 2009). Here we also showed

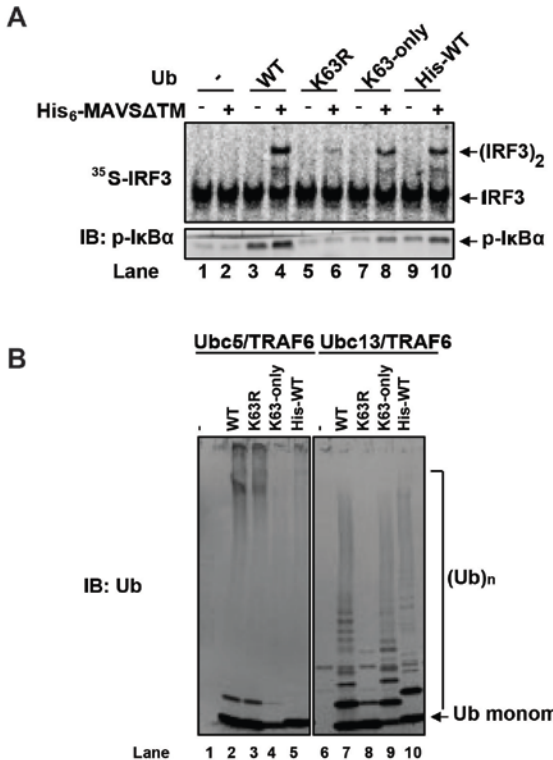


Figure 21. K63-linked Polyubiquitin is Critical for Activation of Both IRF3 and NF-κB in vitro by MAVS.

(A) U2OS cells stably integrated with tetracycline-inducible shRNA against ubiquitin genes were growing in the presence of tetracycline for 48 hours. In vitro assay for IRF3 dimerization was carried out as described, except that 1μg of recombinant ubiquitin and its mutants were added to the S5 from the ubiquitin depleted cells. Phosphorylation of IκBα was analyzed by immunoblotting (top).

(B) As a control, different ubiquitin mutants were tested for their ability to make polyubiquitin chains with either Ubc13 and TRAF6 or Ubc5 and TRAF6 in vitro (bottom).

that DKO+shT6 MEF cells stably expressing a lysine-less form of TRAF6 rescued induction of IFN-β and other cytokines in response to VSV (Figure 11, B-E).

Endogenous TRAF2 was modified in a MAVS-dependent manner in vitro (Figure 22B). In S5 from *Nemo*^{-/-} MEF cells, the TRAF2 modification was lost, which was rescued by adding back wild-type NEMO but not the UBD mutant NEMO (Figure 23F). Moreover, the modification disappeared when vOTU was included in the reaction. To explore whether ubiquitination of TRAF2 is important, we incubated Flag-TRAF2 with S100 from *Traf2/5*^{-/-} MEF cells in the presence of MAVSΔTM, followed by flag immunoprecipitation after denaturing the reaction with SDS. Both linear and Lysine 63-linked ubiquitin were found in the IP product (Table 4). Additionally, six ubiquitination sites on murine TRAF2 were

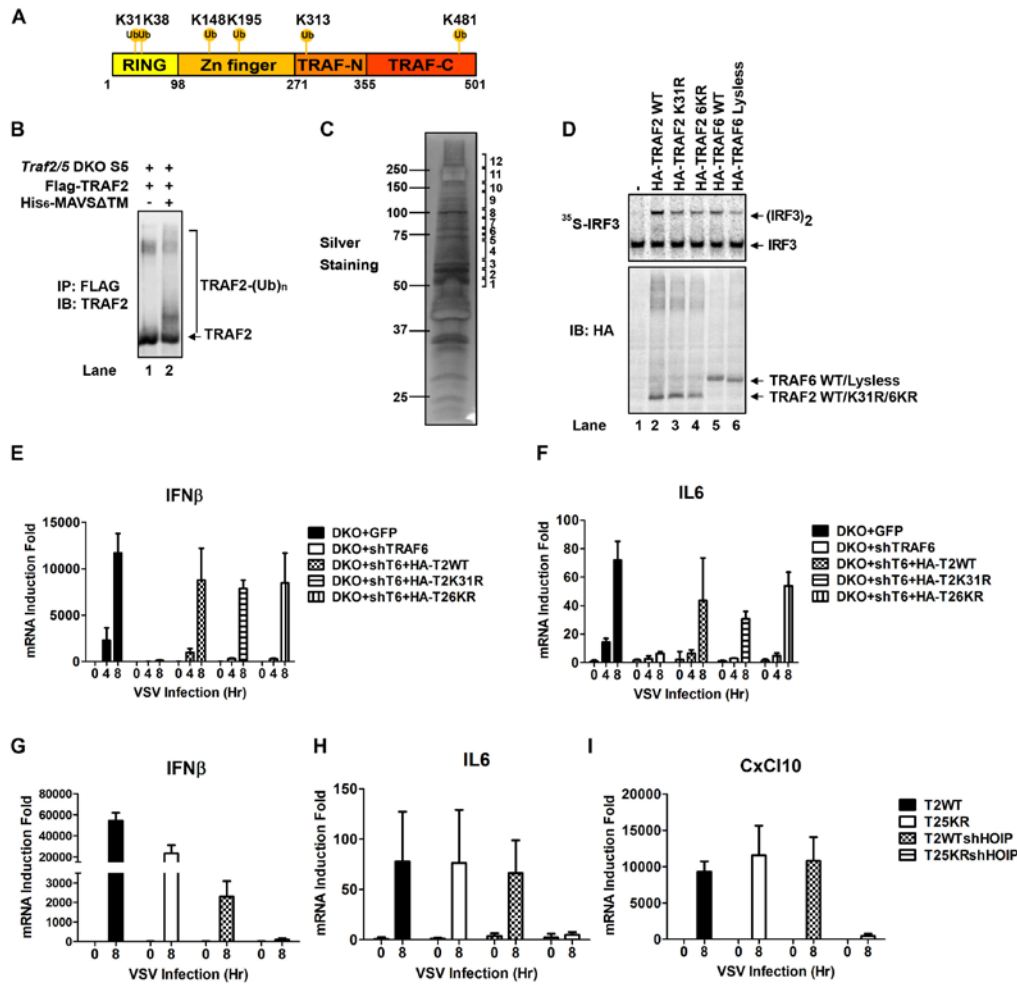


Figure 22. TRAF2 Ubiquitination is Dispensable for IRF3 and NF-κB Activation Induced by Virus.
 (A) A schematic diagram of TRAF2 protein with all the lysines modified by Glycine-Glycine (GlyGly-K) identified by mass spectrometry highlighted.

(B) Flag-TRAF2 was incubated with S5 from *Traf2/5*^{-/-} MEF cells in the presence or absence of MAVSΔTM. Flag-TRAF2 was immunoprecipitated by M2-agarose and eluted by flag peptide after the reaction was terminated with SDS. TRAF2 modification was analyzed by immunoblotting.

(C) Identification of TRAF2 Ubiquitination Sites induced by His₆-MAVSΔTM in vitro. The in vitro reaction described in B was carried out at a large scale and Flag-TRAF2 was eluted by flag peptide after the IP. The eluate was resolved on SDS-PAGE followed by silver staining. Gel slices were cut as indicated and subjected to mass spectrometry analysis.

(D) Vectors encoding HA-tagged proteins were overexpressed in HEK293 cells and proteins were purified by HA agarose followed by HA peptide elution. The purified proteins were then tested for their ability to activate IRF3 dimerization in S5 from *Traf2/5*^{-/-} MEF cells in vitro. Equal amount of protein were added as shown by immunoblotting.

(E-F) Vectors with HA-TRAF2 wildtype or KR mutants were introduced into *Traf2/5* DKO MEF cells stably expressing shRNA against TRAF6. Stable cells were infected with VSV for indicated period of time and total RNA was isolated. The mRNA induction of cytokines was analyzed by qPCR.

(G-I) Lentiviral vectors shRNA against HOIP were introduced into TRAF2 rescuing cells lines described in (D) and the mRNA induction of cytokines was analyzed by qPCR.

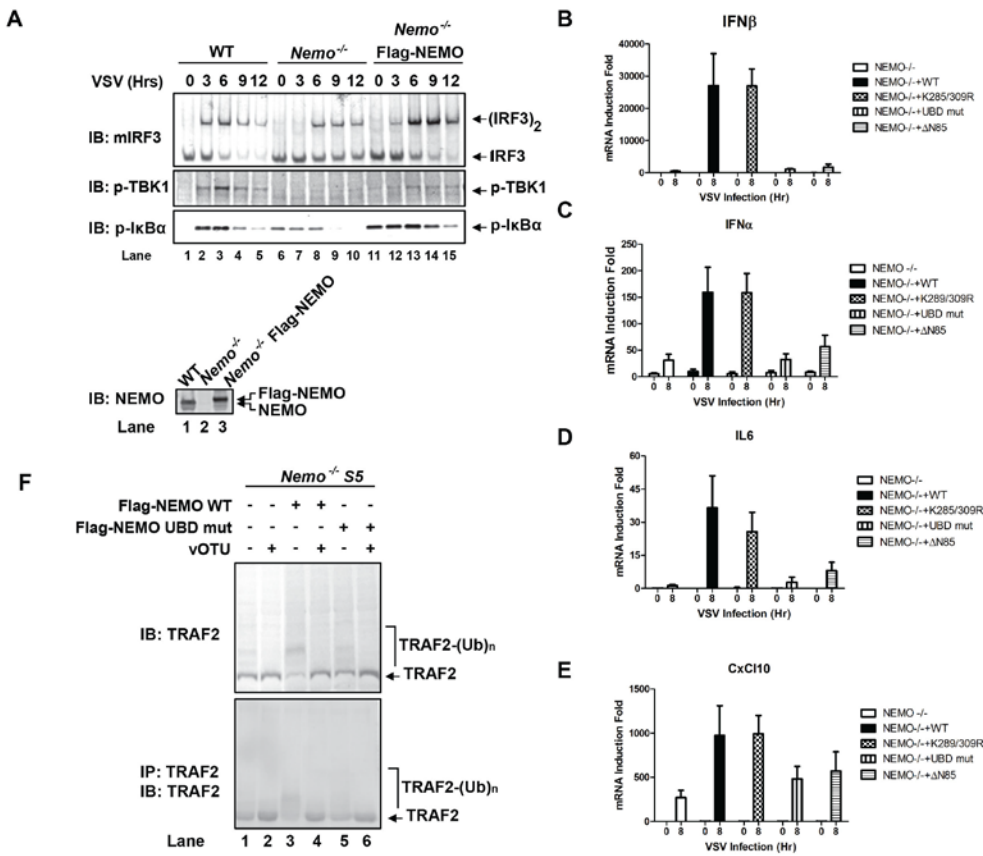


Figure 23. NEMO is Important for both IRF3 and NF-κB Activation by Virus.

(A) Wild-type and *Nemo*^{-/-} MEF cells stably expressing GFP or flag-NEMO were infected with VSV for indicated period of time. IRF3 dimerization, TBK1 and IκB α phosphorylation were analyzed by immunoblotting (top). Flag-NEMO expression was compared to the endogenous NEMO in Wild-type MEF by immunoblotting (bottom).

(B-E) *Nemo*^{-/-} MEF cells stably expressing GFP, flag-NEMO WT or mutants were infected with VSV for indicated period of time. The mRNA level of cytokines was analyzed by qPCR.

(F) NEMO ubiquitin binding activity is important for IRF3 dimerization and TRAF2 ubiquitination in vitro. Flag-NEMO WT and UBD mutant were incubated with *Nemo*^{-/-} S5 with or without vOTU, TRAF2 was then immunoprecipitated after stopping the reaction with SDS. TRAF2 modification and IRF3 phosphorylation were analyzed by immunoblotting.

detected by mass spectrometry, including K31, K38, K148, K195, K313 and K481 as shown in Figure 24A. Among these lysines, K31 was identified as the auto-ubiquitination site of TRAF2 in the TNF pathway and K38 is an arginine in human TRAF2 (Li et al., 2009). However, mutation of all six lysines to arginines (6KR) didn't cause any obvious defect in

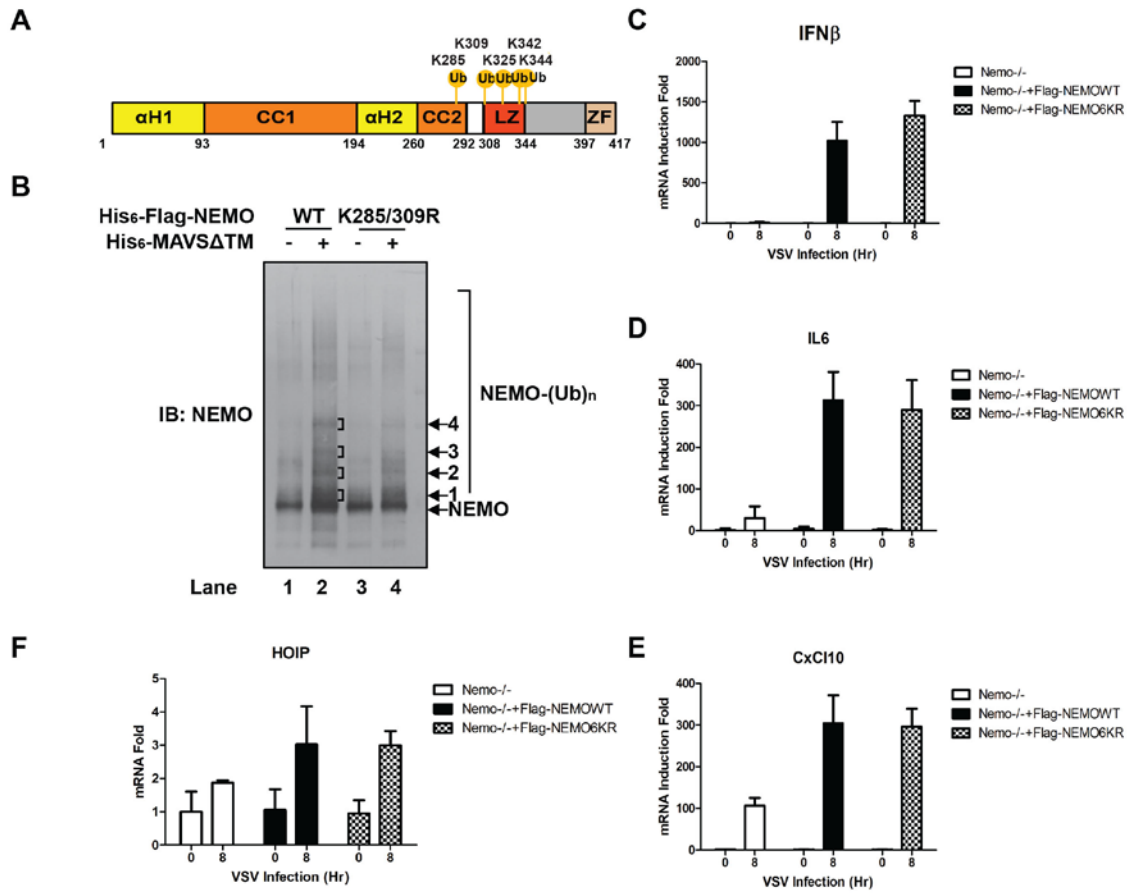


Figure 24. NEMO Ubiquitination is Dispensable for IRF3 and NF-κB Activation Induced by Virus.

(A) A schematic diagram of NEMO protein with all the lysines modified by GlyGly identified by mass spectrometry highlighted.

(B) NEMO Undergoes MAVS Δ TM-dependent Ubiquitination in vitro. Purified His-Flag-NEMO wildtype or K285/309R were incubated with Nemo $^{-/-}$ S5 in vitro. After stopping the reaction with SDS, NEMO was immunoprecipitated with M2 agarose followed by Nickel beads pull down in 6M Urea. Covalently modified NEMO was analyzed by immunoblotting and silver staining. Indicated gel slices were cut out and subjected for mass spectrometry analysis.

(C-F) Nemo $^{-/-}$ MEF cells stably expressing GFP, flag-NEMO WT or K111/285/309/325/342/344R (6KR) were infected with VSV for indicated period of time. The mRNA level of cytokines was analyzed by qPCR.

IRF3 activation in vitro or in cytokine production by virus in cells (Figure 22, E and F).

Interestingly, further knockdown of HOIP dramatically abolished the cytokine production in

DKO+shT6 cells stably expressing 5KR (K31/148/195/313/481R) TRAF2 but not wild-type

TRAF2 (Figure 22, G-I), suggesting that ubiquitination target(s) of HOIP may be redundant with ubiquitinated TRAF2 in activating the TRAF2-dependent pathway *in vivo*.

NEMO is reported to be ubiquitinated by HOIP at lysine 285 and 309 with the modification important for NF-κB activation in the TNF pathway (Tokunaga et al., 2009). *Nemo*^{-/-} MEF cells stably expressing NEMO K285/309R mutant support virus-induced cytokine production similar to those expressing wild-type NEMO (Figure 23, B-E). In order to identify additional ubiquitination sites on NEMO specific to MAVS downstream signaling, endogenous amount of His-flag-NEMO was incubated with S5 from *Nemo*^{-/-} MEF cells in the presence of MAVSΔTM. NEMO was enriched by tandem-tag purification under denaturing conditions. MAVS-induced NEMO ubiquitination was apparent with wild type NEMO but reduced on K285R/K209R mutant NEMO (Figure 24B). Signal-dependent ubiquitination sites on NEMO were detected by mass spectrometry including K285, K325, K342 and K344 as shown in Figure 24A. However, *Nemo*^{-/-} MEF cells stably expressing 5KR (K283/309/325/342/344R) mutant NEMO still supported virus-induced cytokine production similar to those expressing wild-type NEMO (Figure 24 C-F). Taken together, the ubiquitination of TRAF2 or NEMO alone is not required for MAVS-mediated activation of IRF3 and NF-κB. However, it remains possible that the ubiquitination on these proteins are redundant.

IRF3 Forms a Complex with MAVS and TRAF2/6

We have provided evidence that ubiquitination events downstream of MAVS are important for the activation of both TBK1 and IKK, possibly through ubiquitin-mediated

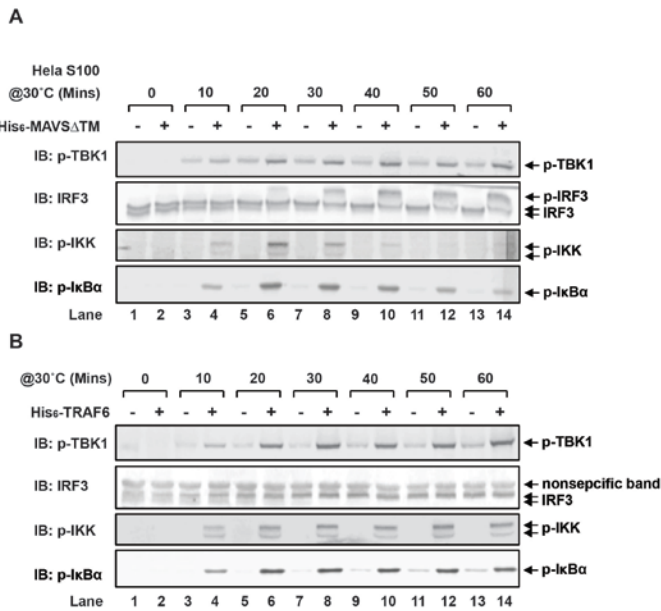


Figure 25. MAVS Specifically Activates IRF3 in Cell Extract.

(A-B) HeLa S100 was incubated with His₈-IRF3 in the presence or absence of either His₆-MAVS Δ TM (A) or His₆-TRAF6 (B). Phosphorylation of IKK, TBK1, I κ B α and IRF3 was analyzed by immunoblotting.

recruitment of NEMO-TBK1 or NEMO-IKK complex to MAVS. Recombinant TBK1 has been shown to be capable of phosphorylating IRF3 at key residues required for its dimerization and activation (Panne et al., 2007). TBK1 kinase activity is regulated by Ser172 phosphorylation within its classical kinase activation loop (Kishore et al., 2002; Ma et al., 2012). However, TBK1 activation is not only limited to pathways that activates IRF3 (Clark et al., 2011; Ou et al., 2011; Xie et al., 2011) and it phosphorylates various substrates (e.g. AKT) by different stimuli. Thus, it is possible that there are additional mechanisms that regulate IRF3 phosphorylation by TBK1 downstream of MAVS.

It is well established that recombinant TRAF6 directly activates IKK and I κ B α in a wild-type cell extract in vitro (Deng et al., 2000). Interestingly, recombinant TRAF6 can also activate TBK1 (Figure 25A) but not IRF3 in vitro. On the other hand, recombinant MAVS Δ TM not only phosphorylates of IKK, I κ B α , and TBK1, it also potently activates

IRF3 in the same cell extract (Figure 25B). These in vitro systems are ideally suited to study the dual role of MAVS in the activation of both TBK1 and IRF3. Indeed, only IRF3 and NEMO, but not IRF7 or I κ B α , pulled down heavily modified MAVS and TRAF2 from Hela S100 after 30°C incubation in the presence of MAVS Δ TM (Figure 26A). Meanwhile, the complex formation was abolished when vOTU was included, indicating the interaction depends on ubiquitination. Additionally, we found that the IRF3 interacts with its kinase TBK1 more efficiently when MAVS Δ TM but not TRAF6 was present in the reaction whereas the interaction between I κ B α and its kinase IKK is independent of the upstream activator (Figure 26C). These results strongly indicate the MAVS uniquely marks IRF3 as the TBK1 substrate. Furthermore, to test if the MAVS-IRF3 complex formation required other components, we tested the extracts from various deficient MEF cells and found that except for *Tbk1*^{-/-} extract, cell extracts lacking ubiquitination E3 ligases or the ubiquitin sensor NEMO which failed to support IRF3 dimerization were also defective in the IRF3-MAVS complex formation (Figure 26B). These findings suggest that, MAVS first forms a complex with IRF3. Second, an upstream ubiquitination event is important for this complex formation. Third, the formation of MAVS-IRF3 complex brings IRF3 and TBK1 into close proximity but is independent of TBK1's kinase activity (data not shown).

Unlike NEMO, IRF3 doesn't possess any ubiquitin-binding domains in its structure (Figure 27A). And unlike TRAF proteins, it doesn't directly interact with MAVS through any binding motifs. To determine which domain of IRF3 is responsible for MAVS-IRF3 complex, different truncated forms of IRF3 were purified and tested for their ability to pull

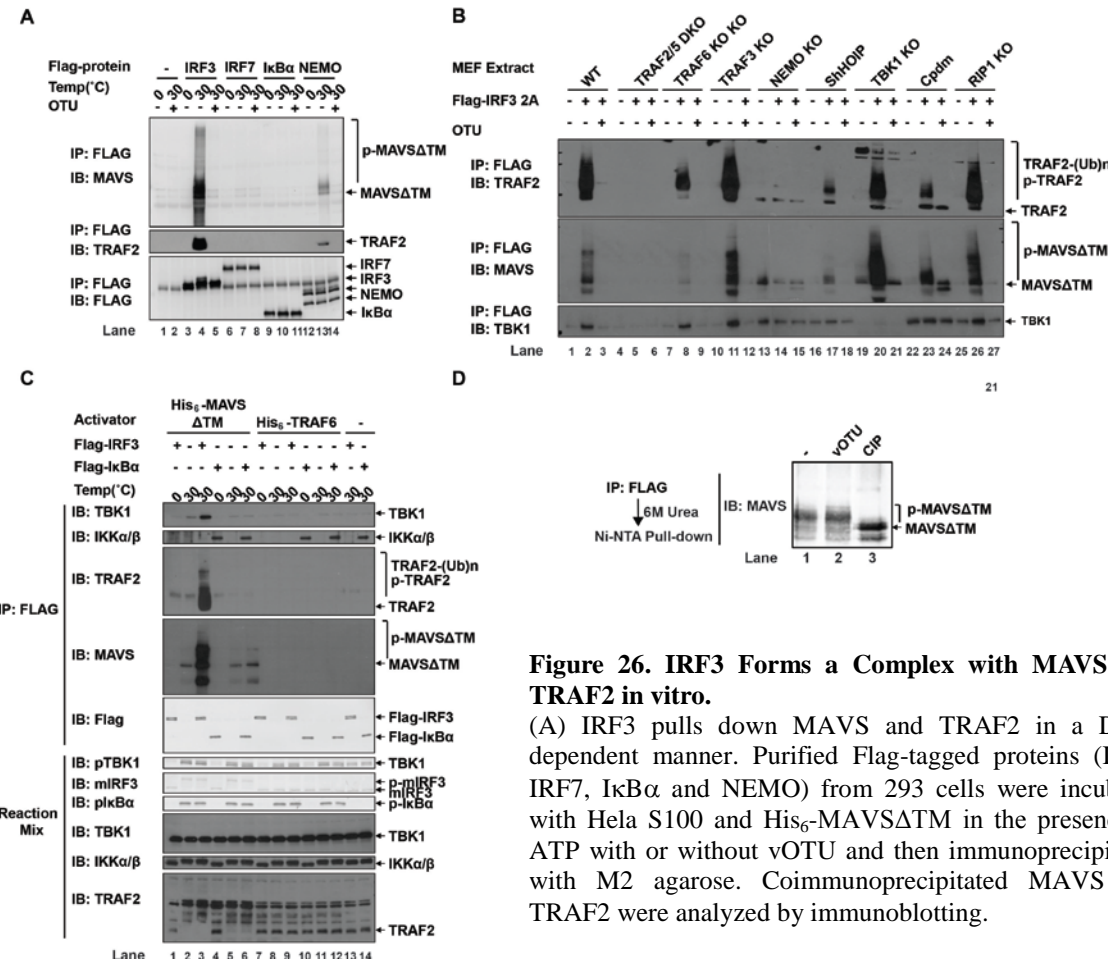


Figure 26. IRF3 Forms a Complex with MAVS and TRAF2 in vitro.

(A) IRF3 pulls down MAVS and TRAF2 in a DUB-dependent manner. Purified Flag-tagged proteins (IRF3, IRF7, I κ B α and NEMO) from 293 cells were incubated with Hela S100 and His₆-MAVSΔTM in the presence of ATP with or without vOTU and then immunoprecipitated with M2 agarose. Coimmunoprecipitated MAVS and TRAF2 were analyzed by immunoblotting.

(B) TRAF2/5, TRAF6, NEMO and HOIP are important for the IRF3-MAVS complex formation. Cell extracts (S5) from various deficient MEF cells were incubated with Flag-IRF3 (2A) and His₆-MAVSΔTM for indicated period of time at 30 °C. IRF3 was then immunoprecipitated with M2 agarose and coimmunoprecipitated proteins were analyzed by immunoblotting.

(C) MAVS specifically brings IRF3 and TBK1 into proximity. Purified Flag-tagged IRF3 and I κ B were incubated with wild-type MEF S100 in the presence of His₆-MAVSΔTM or His₆-TRAF6 as the activator and then immunoprecipitated with M2 agarose. Coimmunoprecipitated proteins were analyzed by immunoblotting.

down the complex. The entire C-terminal region of IRF3, including the transactivation domain and the serine-rich region are required for the IRF3-MAVS complex formation (Figure 27, B and C). Notably, the structure of this region has been suggested to exhibit similarity to the MH2 domain of the Smad protein family and the FHA domain, which are known to bind a phosphorylated peptide in mediating protein-protein interactions (Qin et al.,

2003; Takahasi et al., 2003).

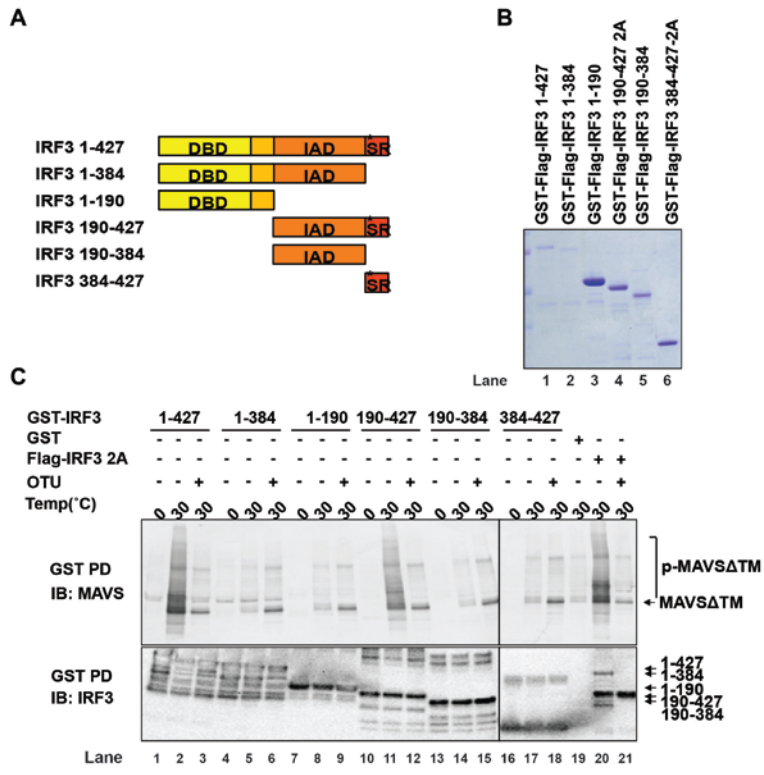


Figure 27. IRF3 C-terminal is Responsible for the IRF3-MAVS Complex Formation.

(A) IRF3 deletion mutants. Top, 427aa human IRF3: 1-112aa, DNA-binding domain (DBD); 190-384aa, IRF-associating domain (IAD) and 385-427aa, serine-rich region (SRR). Bottom, deletion mutants: 1-384, lacking SRR; 1-190, lacking IAD and SRR; 190-427, lacking DBD; 190-384, only having IAD; 384-427, only having SRR. Mutants with SRR contain S385A/S386A (2A) (B) Coomassie blue staining for GST-IRF3 full-length and deletion mutants purified from *E. Coli*. (C) GST-IRF3 proteins described in (A) and (B) were incubated with Wild-type MEF S100 His₆-MAVSΔTM in the presence or absence of OTU and then pulled down with Glutathione agarose. Proteins on the agarose were analyzed by immunoblotting.

Noting that MAVSΔTM pulled down by IRF3 was heavily phosphorylated and sensitive to CIP treatment (Figure 27D), we hypothesized that IRF3 binding to phosphorylated MAVS might be important for IRF3 activation by TBK1. To examine this model, the ability of purified TBK1 to phosphorylate IRF3 was studied in a simplified in vitro system in the presence or absence of MAVSΔTM. We found that although purified TBK1 is constitutively active, it only phosphorylates IRF3 efficiently with the addition of MAVSΔTM (Figure 28, A and B). Moreover, only with the addition of MAVSΔTM is IRF3

able to pull down both TBK1 and MAVS Δ TM, the interaction of which was abolished with the addition of CIP to the reaction (Figure 28, C and D). However, single serine mutations on MAVS have not affected its ability to activate IRF3 in vitro so far (data not shown). Given the fact that the MH2 domain of the Smad proteins interacts with protein peptides with multiple phosphorylated sites, it is likely that the IRF3c (aa190-427) binds to MAVS through several phosphorylation sites. Thus, additional evidence is needed to support the model of phosphorylation-induced interaction between IRF3 and MAVS.

To further characterize the IRF3-MAVS interaction, we performed in vitro SILAC experiments as shown in Figure 29A. We incubated extracts from either heavy or light labeled wild-type MEF cells in the presence or absence of MAVS Δ TM. GST-IRF3c was added at 0°C after the reaction. Proteins in the subsequent GST pull-down were identified by mass spectrometry and the signal-dependent interactions with IRF3c were ranked by the heavy to light ratios (H/L) of signal intensity analyzed by MAXQUANT (Figure 29, B and C). Strikingly, multiple positive and negative regulators reported in MAVS-IRF3 pathway were present in this MAVS-dependent super-complex (Figure 29C), including MAVS, E3 ligases (TRAF1/2/3/5, cIAP1/2 and Sharpin/HOIL/HOIP), kinases (TBK1/IKK ϵ , IKK α/β and PLK1), negative regulators (A20/Abin1/Abin2/Taxbp1, Optineurin and CYLD), and ubiquitin chains (linear linkage, Table 2). Additionally, MAVS was found to be heavily phosphorylated at multiple sites including S222 and S366, whereas TRAF2 was both phosphorylated and ubiquitinated. Notably, we didn't see TRAF6 in the complex, which could be due to the transient nature of the interaction between endogenous TRAF6 and MAVS. In a separate experiment, purified TRAF6 was added into the extract from *Traf2/5*^{-/-}

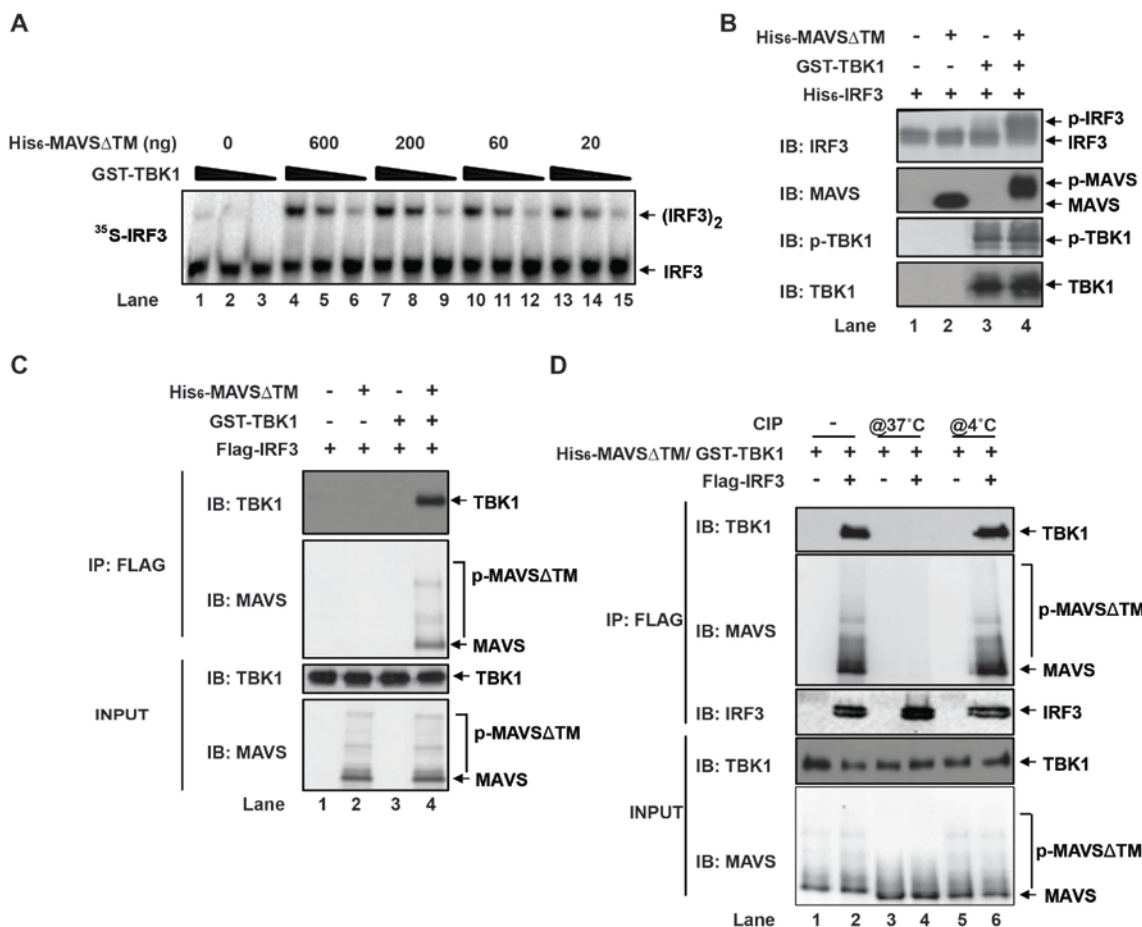


Figure 28. Purified TBK1 Still Needs MAVS to Activate IRF3 Efficiently.

(A) Different concentration of GST-TBK1 purified from Sf9 cells were tested for their ability to activate IRF3 in vitro with ATP in the presence or absence of different concentration of His₆-MAVSΔTM.

(B) Different combination of GST-TBK1 and His₆-MAVSΔTM were tested for their ability to phosphorylate His₈-IRF3 in the presence of ATP in vitro. After the reaction, proteins were analyzed by immunoblotting.

(C) Different combinations of GST-TBK1, His₆-MAVSΔTM were incubated in vitro in the presence of ATP. After the reaction, Flag-IRF3 2A was added on ice and immunoprecipitated with M2 anti-FLAG agarose and co-immunoprecipitated proteins were then analyzed by immunoblotting.

(D) GST-TBK1, His₆-MAVSΔTM were incubated in vitro in the presence of ATP. CIP was included in the 30°C reaction for Lane 3 and 4 or was added on ice after the reaction for Lane 5 and 6. Flag-IRF3 2A was added on ice after the reaction and immunoprecipitated with M2 agarose. Co-immunoprecipitated proteins were analyzed by immunoblotting.

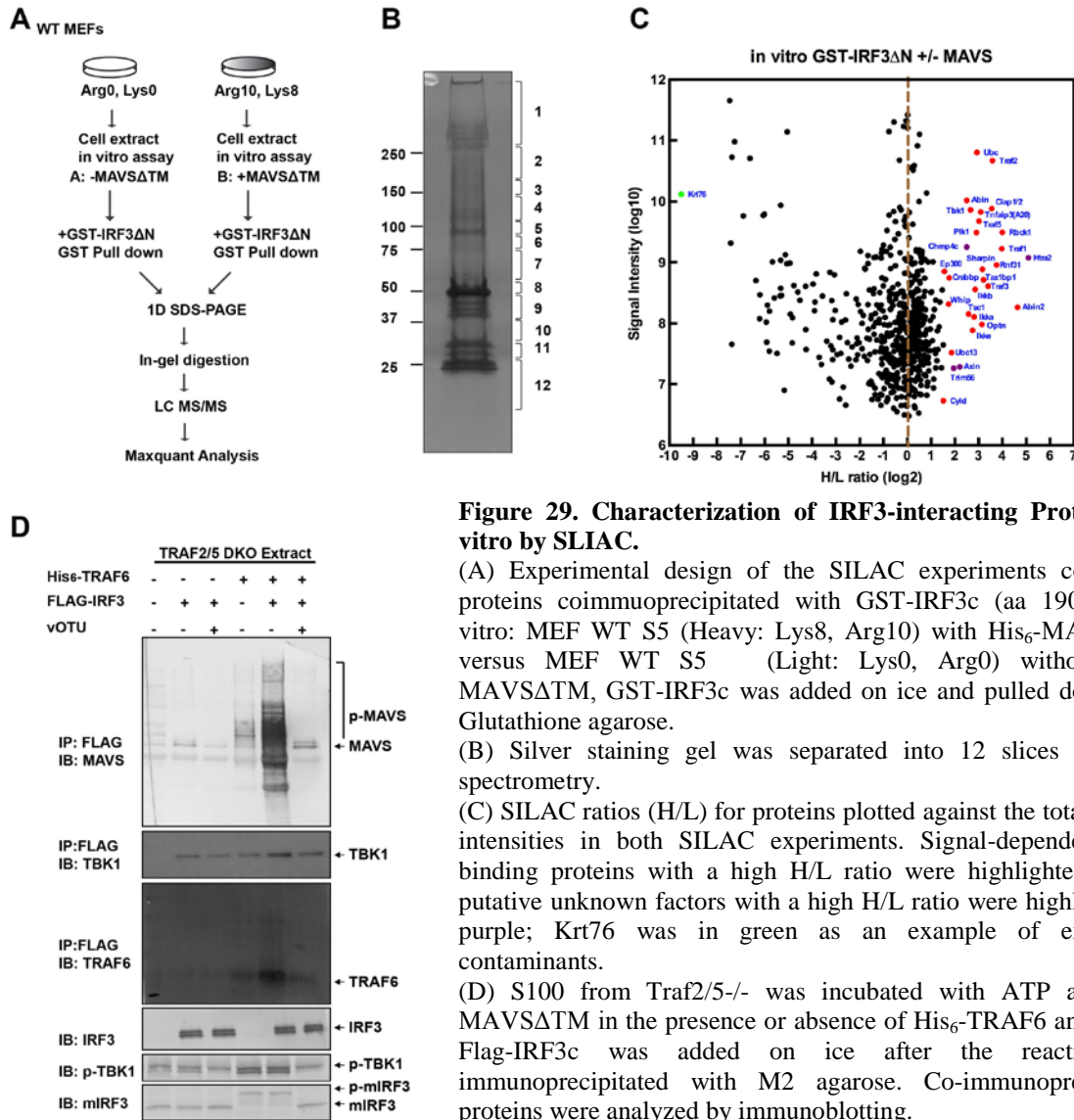


Figure 29. Characterization of IRF3-interacting Proteome in vitro by SLIAC.

(A) Experimental design of the SILAC experiments comparing proteins coimmunoprecipitated with GST-IRF3c (aa 190-427) in vitro: MEF WT S5 (Heavy: Lys8, Arg10) with His₆-MAVS Δ TM versus MEF WT S5 (Light: Lys0, Arg0) without His₆-MAVS Δ TM, GST-IRF3c was added on ice and pulled down with Glutathione agarose.

(B) Silver staining gel was separated into 12 slices for mass spectrometry.

(C) SILAC ratios (H/L) for proteins plotted against the total peptide intensities in both SILAC experiments. Signal-dependent IRF3 binding proteins with a high H/L ratio were highlighted in red; putative unknown factors with a high H/L ratio were highlighted in purple; Krt76 was in green as an example of exogenous contaminants.

(D) S100 from Traf2/5 $^{-/-}$ was incubated with ATP and His₆-MAVS Δ TM in the presence or absence of His₆-TRAF6 and vOTU. Flag-IRF3c was added on ice after the reaction and immunoprecipitated with M2 agarose. Co-immunoprecipitated proteins were analyzed by immunoblotting.

MEF cells as described in Figure 3D, lane 3, and flag-IRF3 IP was carried out after the reaction. With the addition of TRAF6, IRF3-TRAF6-MAVS-TBK1 complex was captured in the absence of TRAF2/5 as shown in Figure 29D. Taken together, these results suggest

Table 2. List of Ubiquitin linkages Identified in IRF3-SILAC (Maxquant).

| | Ratio H/L | Modified Sequence | Sample No. | Charge | Mass | Intensity (log10) | Intensity L (log10) | Intensity H (log10) |
|--------|-----------|-------------------|------------|--------|----------|-------------------|---------------------|---------------------|
| Linear | 13.678 | _GGMQIFVK_ | 2 | 2 | 878.4684 | 7.71 | 6.54 | 7.68 |
| | 13.975 | _GGMQIFVK_ | 3 | 2 | 878.4684 | 7.89 | 6.70 | 7.86 |
| | 14.279 | _GGMQIFVK_ | 4 | 2 | 878.4684 | 8.11 | 6.91 | 8.08 |
| | 13.222 | _GGMQIFVK_ | 5 | 2 | 878.4684 | 8.47 | 7.32 | 8.44 |
| | 13.535 | _GGMQIFVK_ | 6 | 2 | 878.4684 | 8.00 | 6.85 | 7.96 |
| | 15.042 | _GGMQIFVK_ | 7 | 2 | 878.4684 | 7.98 | 6.71 | 7.96 |
| | 15.15 | _GGMQIFVK_ | 10 | 2 | 878.4684 | 7.42 | 6.21 | 7.39 |
| | 22.606 | _GGMQIFVK_ | 12 | 2 | 878.4684 | 7.09 | 5.81 | 7.06 |
| | 13.868 | _GGM(ox)IFVK_ | 4 | 2 | 894.4633 | 7.14 | 6.01 | 7.10 |
| | 4.5806 | _GGM(ox)IFVK_ | 6 | 2 | 894.4633 | 7.10 | 6.09 | 7.05 |
| K48 | 2.5382 | _LIFAGK(g)QLEDGR_ | 1 | 2 | 1459.778 | 7.21 | 6.64 | 7.07 |
| | 2.5748 | _LIFAGK(g)QLEDGR_ | 1 | 3 | 1459.778 | 7.12 | 6.50 | 7.00 |
| | 4.6074 | _LIFAGK(g)QLEDGR_ | 2 | 2 | 1459.778 | 7.31 | 6.58 | 7.22 |
| | 8.8062 | LIFAGK(g)QLEDGR | 8 | 3 | 1459.778 | 8.00 | 7.24 | 7.91 |

the active form of MAVS first recruits E3 ligases, kinases and substrates to form a core signalosome that leads to kinase activation and specifies substrate phosphorylation. Second, the signalosome further bring together positive and negative regulators of the pathway; and third, TRAF2 and TRAF6 are each capable of forming a complex with MAVS, IRF3 and TBK1, which may be crucial for MAVS-dependent IRF3 phosphorylation by TBK1.

To test if IRF3, MAVS, and other proteins form a similar complex in vivo after virus infection, HEK293 cells transiently overexpressing flag-IRF3 (2A) were infected with Sendai virus and complex formation was examined by Flag-IP. Consistent with the in vitro system, IRF3 also pulled down MAVS, TBK1, TRAF2 and TRAF6 in a virus-dependent manner in cells (Figure 30A). To further characterize this virus-induced complex formation, we performed a SILAC experiment as described in Figure 30, B and C. IRF3 interacted with MAVS, E3 ligases TRAF2/6, kinases TBK1/IKK ϵ , negative regulators A20/Abin, and other

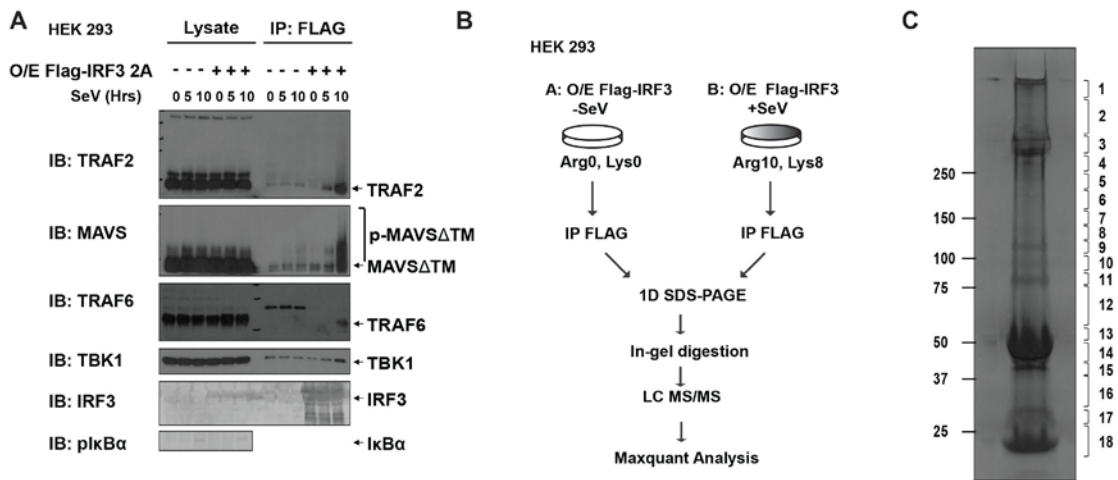


Figure 30. IRF3 Forms a Complex with Endogenous MAVS, TRAF2, TRAF6 and TBK1 In Response to Virus.

(A) HEK293 cells transiently overexpressing Flag-IRF3 (2A) were infected with Sendai virus for 12 hours. Flag-IRF3 was immunoprecipitated with M2 anti-FLAG agarose. Co-immunoprecipitated proteins were analyzed by immunoblotting.

(B) Experimental design of the SILAC experiments comparing proteins coimmunoprecipitated with FLAG-IRF3 in HEK293 cells with or without Sendai virus infection:

HEK293 cells expressing Flag-IRF3 (Heavy: Lys8, Arg10) with Sendai virus infection versus HEK293 cells expressing Flag-IRF3 uninfected (Light: Lys0, Arg0). Flag-IRF3 was immunoprecipitated with M2 anti-FLAG agarose.

(C) Silver staining gel was separated into 18 slices for mass spectrometry.

proteins (Table 3). Some components identified in the in vitro SILAC were not present in the in vivo experiment. For example, although the LUBAC complex was not identified in the in vivo SILAC, we have provided strong genetic evidence for their role in the pathway. The difference between the MAVS-IRF3 complex in vivo and in vitro could be explained by the more dynamic nature of MAVS-IRF3 signaling in vivo, which would require testing multiple infection time points. It could also be due to the in vivo abundance of other proteins that affects protein identification by mass spectrometry. Overall, the IRF3-MAS complexes from in vitro and in vivo greatly resemble each other.

Table 3. Putative IRF3 Interacting Proteins Identified in the *in vivo* SILAC.

A Model for MAVS-Mediated IRF3 and NF-κB Activation

Based on current evidence, a working model is proposed for MAVS-mediated IRF3 activation (Fig 31). Upon virus infection, the sequential binding of RIG-I to viral RNA and unanchored lysine-63 (K63) polyubiquitin chains promotes RIG-I to form higher order oligomers, which then rapidly induce MAVS polymerization. The polymerized MAVS further recruits and activates E3 ligases TRAF2/5 (possibly also LUBAC) and TRAF6. These E3 ligases in turn synthesize K63-linked or linear polyubiquitin chains (presumably on TRAF2 and other proteins), which recruit the NEMO-IKK α/β -TANK-TBK1 kinase complex to MAVS for their activation. In addition to the I κ B α phosphorylation by IKK, these activated kinases further phosphorylate MAVS at multiple sites. Phosphorylated MAVS specifically recruits IRF3 and eventually allows IRF3 phosphorylation by the proximal TBK1.

Conclusion of Research Project

In summary, my current study has unveiled a novel mechanism of MAVS-mediated IRF3 activation through ubiquitination-coupled phosphorylation events, which will facilitate further investigation into the regulation of IRF3 in other innate immunity pathways.

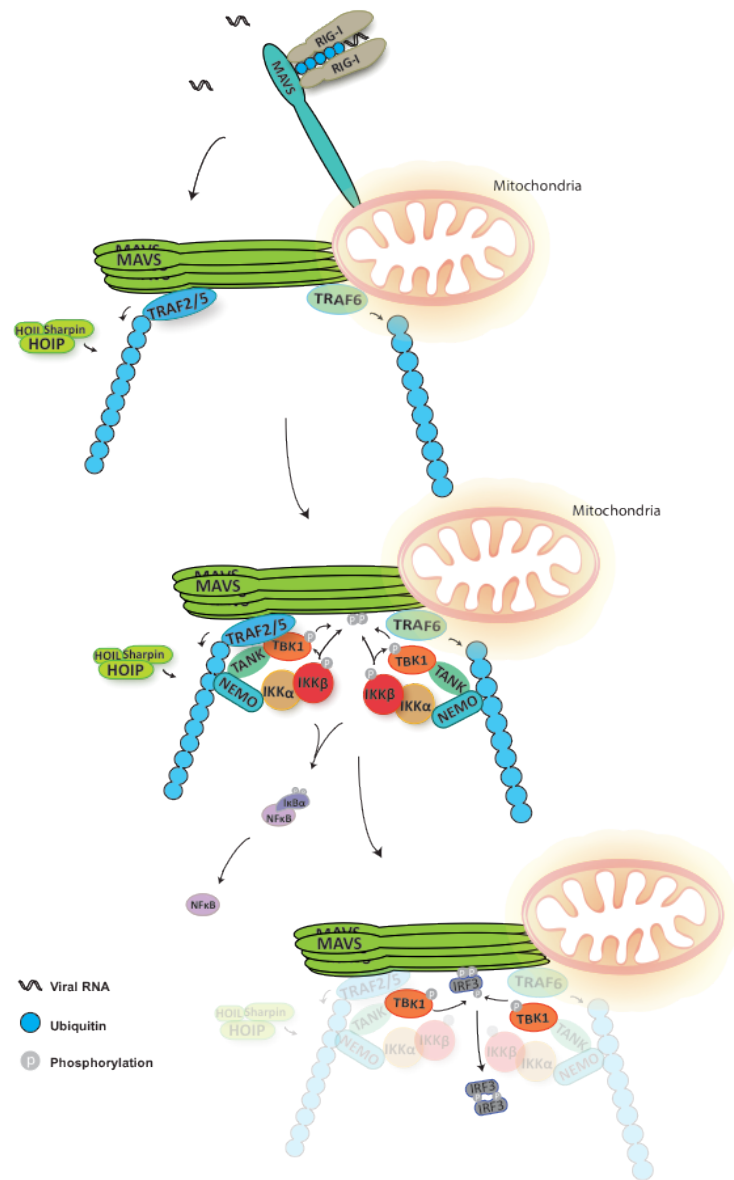


Figure 31. A Model for MAVS-mediated IRF3 and NF-κB Activation in Response to Virus.

CHAPTER III

DISCUSSION

By taking advantage of a cell-free system that faithfully recapitulates virus induced IRF3 activation, we provide insight into the unknown factors and the underlying mechanisms that are responsible for virus induced IRF3 activation downstream of MAVS. Starting with the identification of TRAF6 as an E3 ligase required for IRF3 activation through conventional purification strategies, we provide convincing biochemical and genetics evidence that aggregated MAVS directly employs both TRAF2/5 and TRAF6 in parallel to propagate downstream signaling. Additionally, we found that the E3 ligase activity of TRAF2 is redundant with that of HOIP in TRAF2-dependent IRF3 activation, whereas the E3 ligase activity of TRAF6 is essential for TRAF6-dependent IRF3 activation. Furthermore, we found that NEMO-containing IKK and TBK1 kinase complexes are recruited to MAVS and TRAF proteins though the ubiquitin-binding domain of NEMO, suggesting a key role of polyubiquitin chain as a scaffold for MAVS-induced kinase activation. Finally, we found that after kinase activation, MAVS was subsequently phosphorylated, which then recruits IRF3 and allows IRF3 phosphorylation by TBK1. Taken together, we delineate the mechanism of MAVS signaling as a ubiquitination-mediated phosphorylation cascade that specifies the activation of both NF- κ B and IRF3.

Multiple E3 Ligases Recruited to MAVS

Proteins in the TRAF family have been intensively studied and presented as key regulators in most innate immune signaling pathways, including TLR/IL-1 and TNF pathways (Chung et al., 2002). Notably, most of these pathways engage different TRAF proteins to fulfill different signaling cascades. For example, the IL-1 receptor and some of the TLRs recruit TRAF6 as the sole E3 ligase through the adaptor protein Myd88 to activate NF- κ B. The TNF receptor, on the other hand, employs TRAF2/5 through TRADD, not only to activate NF- κ B and JNK, but also to protect cells from apoptosis. However, MAVS on mitochondria recruits TRAF2/5, TRAF3, and TRAF6 to activate both IRF3 and NF- κ B upon viral infection. Although MAVS is capable of utilizing either TRAF2/5 or TRAF6 to produce comparable amount of interferon- α/β and other inflammatory cytokines, the binding sites for TRAF2 and TRAF6 are surprisingly conserved across mammals (Figure 32), suggesting that downstream of MAVS certain non-redundant functions for these TRAF proteins are yet to be discovered.

In our vitro assay, although both purified TRAF6 and MAVS Δ TM activate kinases TBK1 and IKK in cell extracts, the activation showed very different kinetics: IKK phosphorylation by MAVS Δ TM was rapidly turned off whereas TRAF6 induced IKK activation was more persistent (Figure 25). This raises a possibility that TRAF2/5 and TRAF6-mediated pathways, although both activate NF- κ B, may recruit different positive and negative regulators. For example, A20 can be recruited to TRAF6 through Taxbp1 or to K63-linked polyubiquitin chains, whereas DUBA was proposed to interact with TRAF3 to

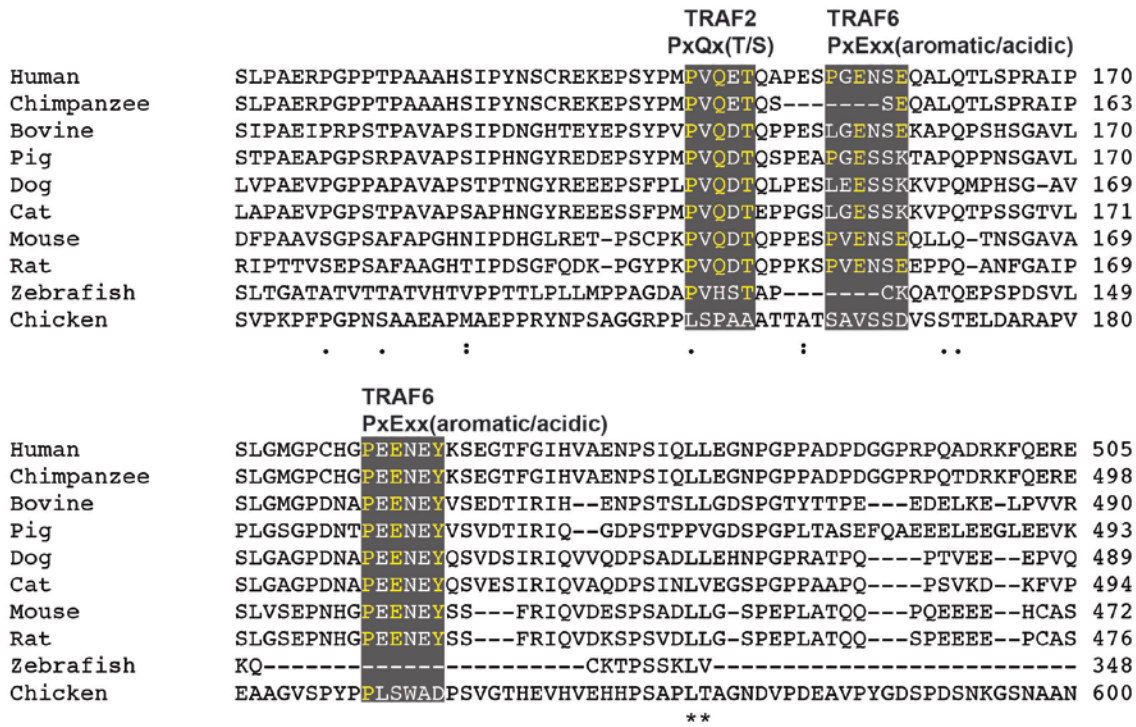


Figure 32. The TRAF Binding Sites on MAVS are Conserved in Mammals.

Across-species Alignment of the TRAF Binding Motifs on MAVS. The conserved binding motifs for TRAF2 and TRAF6 are highlighted in grey boxes. Conserved key residues in the binding sites are in yellow letters.

negatively regulate the MAVS-mediated IRF3 activation (Kayagaki et al., 2007; Ling and Goeddel, 2000; Maelfait et al., 2012). And this differential regulation may lead to different kinetics in the activation of both IRF3 and NF- κ B, which subsequently turn on the transcription of an overlapping but not identical set of genes.

Another possible role of TRAF redundancy could be to compensate for the myriad activity in different signaling pathway for which these non-abundant proteins are responsible for. The recruitment of multiple E3 ligases to MAVS could ensure a rapid interferon response to defend against viral infection for cells that are constantly engaged in other inflammatory response. The recruitment of multiple TRAFs into a complex would ensure

quick and robust polyubiquitin chain synthesis at the site of their recruitment while allowing the ubiquitin chains to efficiently engage downstream signaling proteins. Further investigation on the anti-viral response in TRAF-deficient cells pre-challenged with various cytokines (e.g. TNF α) could be very informative in this regard. It would also be interesting to test if *Traf6*^{-/-} mice exhibit a more profound defect in viral clearance and interferon production comparing to cultured *Traf6*^{-/-} cells. Additionally, viruses are highly adaptive and mutate quickly, which allows them to evolve numerous ways to evade host innate immunity. Having multiple TRAF proteins redundantly could potentially minimize the chance of viral evasion if the viruses happen to inhibit one of the TRAF-mediated pathways.

TRAF3 was proposed to be the E3 ligase responsible for IRF3 activation in TLR and RLR pathways (Oganesyan et al., 2006; Saha et al., 2006; Tseng et al., 2010). The role of TRAF3 in antiviral defense was mostly based on the evidence that *Traf3*^{-/-} cells were severely defective in IFN- α production and partially defective in IFN- β production. However, direct evidence showing defective virus-induced IRF3 dimerization was lacking in these studies. In our study, *Traf3*^{-/-} MEF cells didn't show any profound defect in IRF3 activation either by virus or in vitro through activation by recombinant MAVS Δ TM. However, consistent with the published results, we did observe a partial defect in IFN- β production while the IFN- α production was severely decreased. In contrast, the DKO+shT6 cells are completely defective in both IRF3 activation and IFN α/β induction by virus. These suggest that TRAF2/5 and TRAF6 play a more direct role in virus induced IRF3 and NF- κ B activation, whereas TRAF3 may serve a regulatory function while more directly affecting

IRF7 activation and IFN- α induction. Nonetheless, TRAF2/5, TRAF3 and TRAF6 are all recruited to MAVS and indispensable for the full activation of downstream signaling cascade. Further research on the role of TRAF3 and IRF7 activation will be interesting and informative in understanding the blueprint of MAVS-mediated antiviral pathway.

Linear vs. Lys-63 polyubiquitination

In the last decade, K63-linked polyubiquitination has become well-established for its function in proteasome-independent signaling regulation (Chen and Sun, 2009). One of the best-studied signaling pathways is the K63 ubiquitin mediated activation of the IKK complex, which then phosphorylates I κ B α leading to NF- κ B activation by diverse stimuli such as IL-1 β and TNF α . In the IL-1 pathway, activated TRAF6, together with E2 Ubc13/Uev1A, synthesizes K63-linked polyubiquitin chains that serve as a scaffold that binds TAB1 and NEMO and activates the TAK1 and IKK kinase complexes, respectively (Chen, 2005; Deng et al., 2000; Wang et al., 2001). In the TNF pathway, however, a role of ubiquitin chains of mixed-linkage has been suggested since the replacement of endogenous ubiquitin with K63R ubiquitin still supported NF- κ B activation (Xu et al., 2009). Moreover, the requirement of Ubc5 in addition to the K63-linkage-specific E2, Ubc13, has casted a further mystery on the ubiquitination-regulation in this pathway. Recently, LUBAC, the protein complex that specifically synthesizes head-to-tail linear ubiquitin chains, have been proposed to play an essential role in NF- κ B activation by various

| Sample No. | 1 | 2 | 3 | 4 | 5 | 6 | 7 | 8 | 9 | 10 | 11 | 12 |
|---|--|-----------------------|----------------------------|---------------------------------------|--------------------------|---|-------------------------------------|-------------------------------------|--------------------------------------|------------------------------------|---------------------------------------|--------------------------------------|
| mTRAF2 Sequence Coverage% (Score) | 63% (3162) | 60% (2399) | 41% (1215) | 62% (3754) | 47% (1239) | 34% (453) | 36% (692) | 32% (456) | 53% (1277) | 36% (467) | 47% (1046) | 45% (760) |
| Ubiquitination GlyGly-K Site (modified peptides/ unmodified peptides) | K38 (2/10) K148 (1/22) K148 (7/35) K195 (3/4) | K481 (2/0) | K148 (6/47) K481 (9/13) | K31 (2/1) K38 (2/13) K481 (7/5) | K38 (4/11) K481 (4/2) | K38 (2/5) K148 (1/6) K195 (1/0) K481 (5/8) | K481 (3/0) K148 (2/14) | K38 (2/5) | K481 (2/3) | K481 (5/8) | K481 (5/8) | |
| Ubiquitin Sequence Coverage% (Score) | 47% (118) M1 (2/3) | 49% (115) M1 (4/3) | N/A M1 (6/10) | 52% (262) K48 (2/4) | N/A K48 (2/4) | 42% (185) K48 (2/8) | 49% (251) M1 (11/7) K48 (1/6) | 37% (461) M1 (5/4) K48 (4/11) | 52% (973) M1 (11/12) K48 (4/7) | 38% (310) M1 (8/7) K48 (4/7) | 52% (565) M1 (11/10) K48 (4/15) | 53% (407) M1 (12/11) K48 (6/7) |
| GlyGly-K Linkage (modified peptides/ unmodified peptides) | K48 (3/2) | K48 (2/2) | K63 (3/2) | | | K63 (0/3) | | K63 (4/6) | | K63 (4/2) | K63 (2/2) | |

Table 4. TRAF2 Undergoes MAVS Δ TM-dependent Ubiquitination in vitro.

TRAF2 signal recovered in each slice (top row); Ubiquitination sites (GlyGly-K on TRAF2) Identified on TRAF2 in each slice (middle row); Ubiquitination Linkage (GlyGly-K on Ubiquitin) identified in each slice (bottom row).

stimuli (Damgaard et al., 2012; Gerlach et al., 2011; Haas et al., 2009; Ikeda et al., 2011; Niu et al., 2011; Tokunaga et al., 2011; Tokunaga et al., 2009; Xu et al., 2009). Specifically, linear ubiquitination on NEMO lysine-285 has been suggested to be responsible for linear ubiquitin chain mediated NF- κ B activation, while another structural study showed that linear-di-ubiquitin has a higher binding affinity to NEMO NUB domain than does K63-di-ubiquitin (Rahighi et al., 2009). A definite and systematic study on the role of linear ubiquitination by LUBAC in these pathways is still lacking. Further studies using a ubiquitin mutant that is specifically defective in linear-chain synthesis without affecting K63-linked chain formation will be essential to dissecting the role of linear-ubiquitination in NF- κ B activation.

There are two layers of ubiquitination regulation in MAVS-mediated innate immune

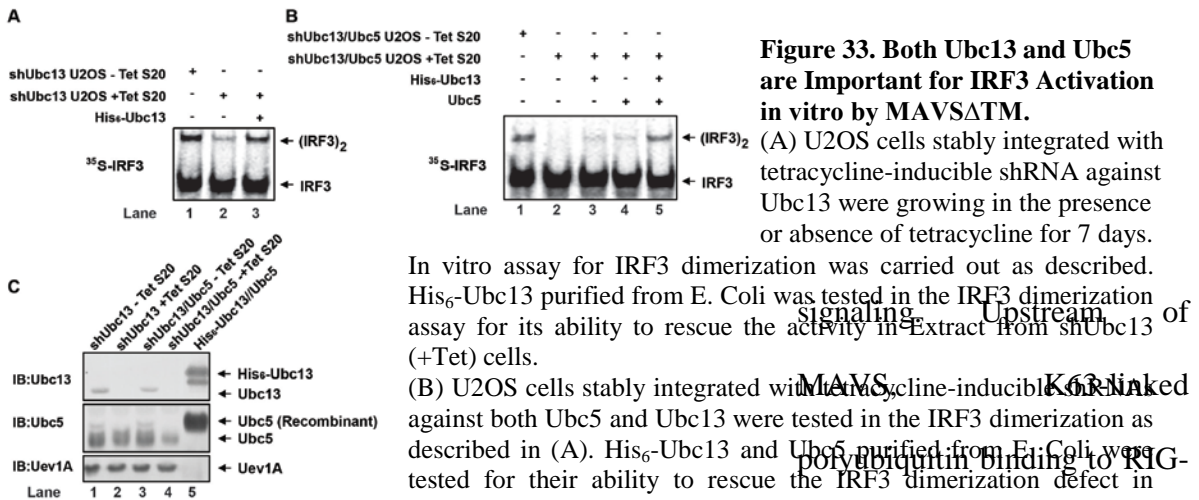


Figure 33. Both Ubc13 and Ubc5 are Important for IRF3 Activation in vitro by MAVS Δ TM.

(A) U2OS cells stably integrated with tetracycline-inducible shRNA against Ubc13 were growing in the presence or absence of tetracycline for 7 days.

In vitro assay for IRF3 dimerization was carried out as described. His₆-Ubc13 purified from E. Coli was tested in the IRF3 dimerization assay for its ability to rescue the activity in Extract from shUbc13 (+Tet) cells.

(B) U2OS cells stably integrated with MAVS Δ TM, tetracycline-inducible shRNA against both Ubc5 and Ubc13 were tested in the IRF3 dimerization as described in (A). His₆-Ubc13 and Ubc5 purified from E. Coli were tested for their ability to rescue the IRF3 dimerization defect in extract from shUbc5/shUbc13 (+Tet) cells.

I is required for its activation by MAVS Δ TM. The knockdown efficiency of Ubc5 and Ubc13, as well as the recombinant proteins, was analyzed by immunoblotting. provided convincing evidence that K63-linked ubiquitination plays an essential role in the activation of TBK1 and IKK. Meanwhile, we found that the depletion of K63-linkage specific E2 Ubc13 from cell extract also abolished MAVS-dependent IRF3 activation in addition to its requirement of Ubc5 (Figure 33). This may indicate that Ubc13 cooperates with Ubc5 to specify the ubiquitin chain linkage. Furthermore, we show an important role of LUBAC in TRAF2-dependent IRF3 and NF- κ B activation both in vitro and in vivo. In support of this, we have found massive linear ubiquitin conjugates (GGMQIFVK) on TRAF2 and NEMO by mass spectrometry after in vitro reaction (Table 4), suggesting a role of linear ubiquitination in this pathway. However, His₆-ubiquitin, known to block linear ubiquitination chain synthesis, still rescued phosphorylation of both IRF3 and I κ B α (Figure 21). Thus, further research on the role of LUBAC and linear ubiquitination in MAVS dependent innate immune signaling is required.

Ubiquitination Target vs. Unanchored Polyubiquitin Chains

Besides ubiquitination linkage specificity, the debate on the role of conjugated ubiquitin vs. unanchored ubiquitin chains in IKK activation is still ongoing. Many studies have provided evidence that ubiquitinated proteins are important for the cell signaling. For example, polyubiquitination of RIG-I on lysine 172 by E3 TRIM25 was first shown to be critical for RIG-I activation (Gack et al., 2007). In contrast, studies from our lab convincingly showed unanchored K63 polyubiquitin chains binding to RIG-I or MDA-5 is responsible for activating this family of RNA sensors (Jiang et al., 2012; Zeng et al., 2010). In another example, polyubiquitination of IRAK4, TRAF6 and NEMO have been proposed to be important for Myd88-mediated TAK1 and IKK activation (Lamothe et al., 2006; Petroski et al., 2007; Sun et al., 2004). In contrast, a study from our lab showed that the unanchored ubiquitin chains synthesized by Ubc13/Uev1A and TRAF6 are capable of activating the TAK1 kinase complex in vitro (Xia et al., 2009). However, the same unanchored ubiquitin chains failed to replace Ubc5 and TRAF6 in our purified assay for IRF3 activation (as described in Figure 7D) in the presence of MAVS Δ TM and NEMO-TBK1 kinase complex (data not shown), suggesting that either free ubiquitin chains are dispensable for IRF3 activation or more complex regulation by polyubiquitin chains that cannot be recapitulated in vitro may be involved.

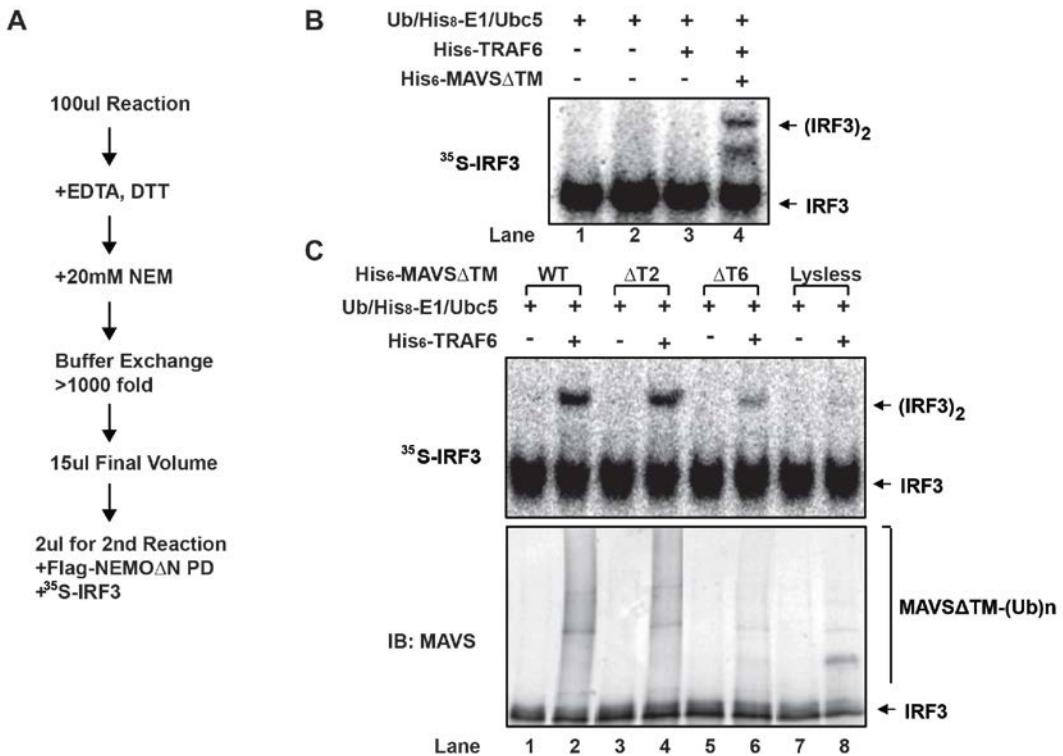


Figure 34. 2-STEP Purified assay Revealed Ubiquitinated-MAVS as an IRF3 Activator.

(A) Experimental design of the 2-STEP assay derived from the one-STEP purified assay described in Figure 7D. TRAF6 and the Ubc13/Uev1A complex preferentially synthesize unanchored K63-linked polyubiquitin chains *in vitro*, while Ubc5 heavily polyubiquitinates TRAF6 (Retroski et al., 2007). Ubc5 is also important for the ubiquitination of RIP1 in TNF α -induced NF- κ B activation (Ea et al., 2004). These studies raise the possibility that Ubc5 may help to ubiquitinate certain targets. To further dissect the mechanism of IRF3 activation in this purified system, we separated the assay into a 2-step reaction: ubiquitination followed by phosphorylation. The ubiquitination reaction in the presence of MAVS Δ TM and the ubiquitin system is stopped by N-Ethylmaleimide (NEM) mediated ubiquitin enzyme inactivation before the phosphorylation reaction is carried out by adding the NEMO-TBK1 kinase complex and IRF3 (Figure 34A). We found that ubiquitinated MAVS is important for IRF3 activation in this 2-step assay, whose activity was abolished when the wild-type MAVS Δ TM

was replaced by MAVS without lysines (Lys-less) (Figure 34, B and C). However, *Mavs*^{-/-} MEF cells stably expressing lys-less MAVS still sufficiently supported IRF3 activation and cytokine production in response to virus (Zeng et al., 2009), suggesting there might be redundant ubiquitinated targets in cells. Indeed, both NEMO and IRF3 pulled down ubiquitinated TRAF2 in the MAVSΔTM + S100 assay as described above, indicating that possibly, TRAF2 functions as another ubiquitinated protein that leads to the activation of IRF3. However, reconstitution of TRAF2 (5KR) into DKO+shT6 cells also showed no defect in IRF3 activation. Nonetheless, in both purified and crude in vitro systems, NEMO, along with the associated kinases, was recruited to MAVS, in a ubiquitination-dependent manner. Interestingly, a recent study on sumoylation in DNA repair has proposed that massive sumoylation on many proteins may serve as a “glue” to enhance multiple protein-protein interactions within the complex, while the abolishment of sumoylation on individual proteins alone did not affect the pathway (Psakhye and Jentsch, 2012). Similarly, given the fact the multiple E3 ligases are involved downstream of MAVS, it is possible that multiple proteins are redundantly ubiquitinated to recruit the ubiquitin sensor NEMO to MAVS for kinase activation in vivo. But further systematic characterization of these ubiquitinated proteins will be needed to provide a more defined role of ubiquitination in MAVS-mediated kinase activation.

IRF3 Phosphorylation by TBK1

It has been assumed that the activation of a kinase subsequently leads to its substrate phosphorylation. In many studies, kinase phosphorylation is monitored or kinase activity

assayed using a surrogate substrate to recapitulate the phosphorylation of its physiological substrate. However, accumulating evidences have suggested that kinase activation is not always directly coupled to substrate phosphorylation. In some cases, additional specification is required in order for a kinase to phosphorylate a substrate efficiently and under the correct setting. Recently, NEMO was shown to interact with I κ B α to specify I κ B α phosphorylation by IKK α/β (Schrofelbauer et al., 2012; Yamamoto et al., 2001). Active form of IKK β introduced into *Nemo*^{-/-} cells failed to phosphorylate I κ B α .

The IKK-related kinase TBK1 is broadly activated by multiple stimuli such as IL1- β , TNF- α , insulin, DNA, and RNA. However, IRF3 activation is only restricted to STING-dependent DNA sensing pathway, MAVS-dependent RNA sensing pathway, and TRIF-dependent TLR 3/4 pathways. A recent study in our lab found that in the DNA sensing pathway, STING binds to both TBK1 and IRF3 to specify the substrate phosphorylation and mutations in STING that specifically disrupt STING-IRF3 interaction uncoupled TBK1 activation from IRF3 phosphorylation (Tanaka and Chen, 2012). Additionally, structural analysis of TBK1 suggested that it lacks additional substrate specification within its structure (Ma et al., 2012).

Through *in vivo* reconstitution of MAVS-dependent IRF3 activation by using both endogenous TBK1 and purified active form of TBK1, we obtained evidence that may explain

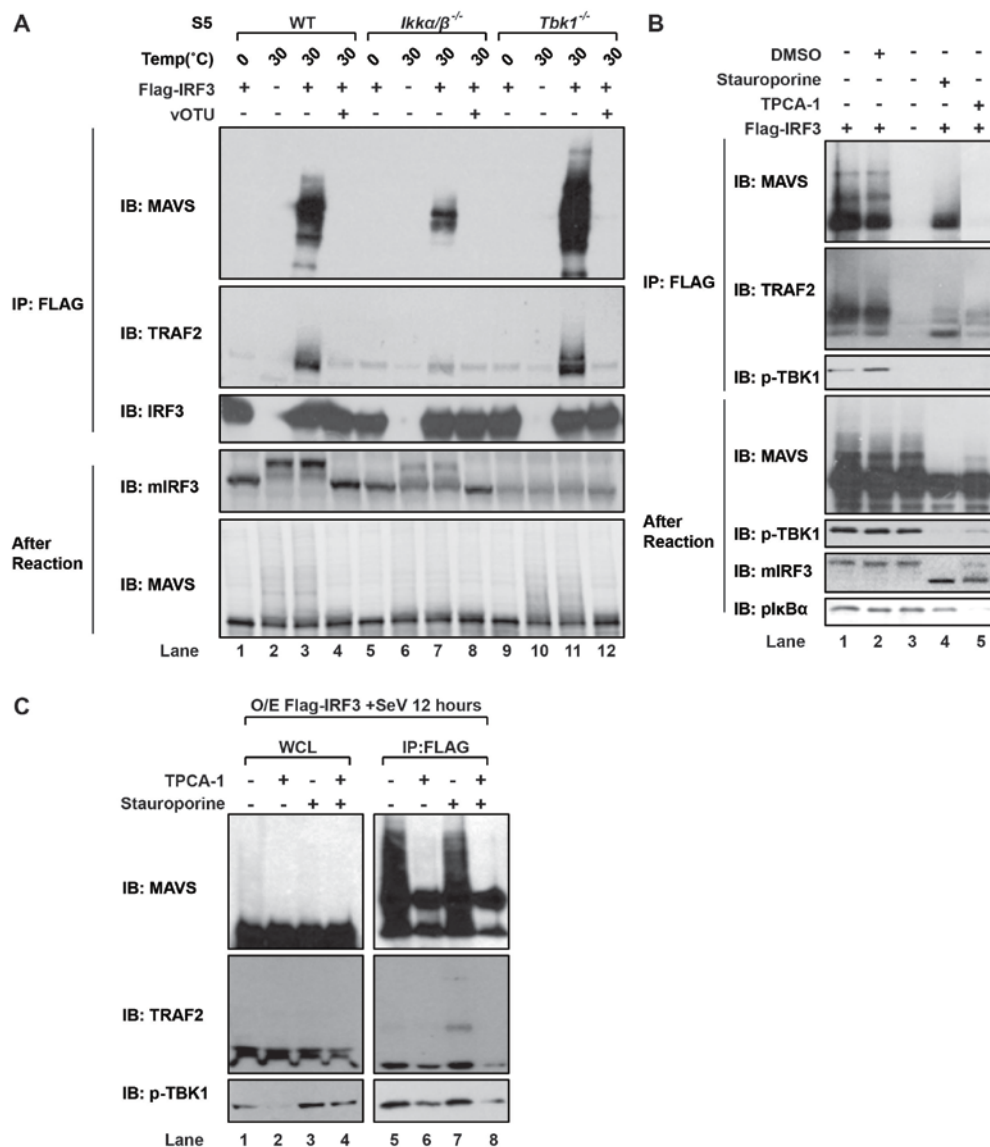


Figure 35. Both IKK and TBK1 may be Responsible for MAVS Phosphorylation in vitro and in vivo.

(A) Extracts from wild-type, *Ikka/β^{-/-}* and *Tbk1^{-/-}* MEF cells were incubated in the presence of His₆-MAVSΔTM. Flag-IRF3c was added on ice after the reaction and immunoprecipitated with M2 agarose. Co-immunoprecipitated proteins were analyzed by immunoblotting.

(B) DMSO, Staurosporine or TPCA-1 were incubated with MEF S5 in the presence of His₆-MAVSΔTM. IRF3-MAVS-TRAF2 complex formation was analyzed as described in (A).

(C) Cells treated with TPCA-1 or Saturoporine or both (1-hour prior to infection) were infected with Sendai virus for 12 hours. IRF3-MAVS-TBK1 complex formation was analyzed as described in Figure 30A.

the specific activation of IRF3 by TBK1 downstream of MAVS. We found that the MAVS bound to IRF3 is heavily phosphorylated and the interaction is sensitive to phosphatase treatment. Moreover, we show that NEMO recruits IKK α/β and TBK1 to MAVS through its ubiquitin-binding domain. These results suggest that phosphorylated MAVS may serve as an adaptor to specify IRF3 phosphorylation by TBK1. However, identification of a MAVS mutant defective in IRF3 binding without interfering with kinase activation is required to support the conclusion. Additionally, the kinase(s) responsible for this phosphorylation event is yet to be confirmed. In our in vitro IRF3 pull-down SILAC experiment, TBK1/IKK ε , IKK α/β , Plk1 were recruited to the IRF3-MAVS complex and serve as possible kinase candidates for MAVS phosphorylation.

Purified TBK1 can directly phosphorylate MAVS even when the amount present is insufficient for IRF3 phosphorylation in vitro. However, in extract from *Tbk1*^{-/-} cells, but not from *IKK α/β* ^{-/-} MEF cells, IRF3 is still able to efficiently phosphorylate MAVS (Figure 35A). Moreover, an IKK inhibitor, TPCA-1, greatly reduced IRF3-MAVS complex formation in WT cell extract (Figure 35B). Taken together, these results indicate that TBK1 and IKK α/β may redundantly phosphorylate MAVS in cells in response to virus. Furthermore, we found that the combination of IKK-inhibitor TPCA-1 and TBK1 inhibitor Stauroporine which does not affect IKK activity blocked IRF3-MAVS-TBK1 complex formation in 293 cells (Figure 35C). However, the kinase inhibitors are not specific: firstly, Stauroporine has inhibitory effect on many kinases, so a more specific TBK1 inhibitor needs to be tested; secondly, the IKK inhibitor has been suggested to promote A20 and NEMO

interaction (Skaug et al., 2011), thus the inhibitory effect could be due to enhanced negative regulation by A20. Additional experiments using *A20*^{-/-} or *CylD*^{-/-} cell extracts will further strengthen the conclusion.

CHAPTER IV

Methodology

Reagents

Rabbit antibodies against human IRF3, TRAF2, TRAF3, TRAF6, NEMO, IKK α/β and mouse antibodies against MAVS and ubiquitin were obtained from Santa Cruz Biotechnology; antibody against the Flag tag (M2), M2-conjugated agarose, anti-HA-conjugated agarose were purchased from Sigma; antibody against HA was from COVANCE; antibodies against p-IRF3 Ser³⁹⁶, p-TBK1 Ser¹⁷², p-I κ B α Ser^{32/36}, p-IKK α/β and p-STAT1 Tyr⁷⁰¹ were from Cell Signaling; Rabbit antibody against mouse IRF3 was from Invitrogen. Mouse Antibody against TBK1 was obtained from IMGENEX; antibody against TANK was from BioVision; Mouse antibody against RIP1 was from BD Biosciences; Mouse antibody against cIAP1 was from R&D Systems; Rabbit antibodies against human and mouse MAVS were generated as described before; Rabbit antibody against Sharpin was raised against full-length His₆ tagged mouse Sharpin purified from Sf9 cells. Sendai virus (Cantell strain Charles River Laboratories) was used at a final concentration of 100 hemagglutinating-units/ml. VSV (Δ M51)-GFP virus was from Dr. John Bell (Univeristy of Ottawa) and propagated in Vero cells. CHT Ceramic Hydroxyapatite column was from Biorad. Other chromatography columns were from GE Healthcare. Non-tagged ubiquitins were from Boston Biochem.

Expression constructs and recombinant proteins

For expression in mammalian cells, mouse cDNAs encoding N-terminal Flag or HA tagged

TRAF6 WT, TRAF6 C70A, TRAF6 (No-Lys), TRAF2 WT, TRAF2 C34A, TRAF2 Δ R (Δ aa34-72), TRAF2 Δ C (aa1-359), TRAF2 K31R, TRAF2 5KR (K31/148/195/313/481R), TRAF2 6KR (K31/38/148/195/313/481R) and TRAF5 WT were cloned into pcDNA3. Human cDNAs encoding N-terminal flag or HA tagged NEMO WT, K285/309R, 5KR (K285/309/325/342/344R), UBD mut (Y308S/H413A/C417A), and Δ N (aa 85-419) were cloned into pcDNA3 and PTY-EF1A-puroR-2a lenti-viral vectors. Human cDNA encoding N-terminal flag tagged IRF3 2A (S385/386A) was cloned into pcDNA3. Human MAVS WT, QN (Q145N), 2ED (E155D and E457D) and QN+2ED (Q145N, E155D and E457D) were cloned into pTY-EF1A-puroR-2a lenti-viral vectors. Various mutants were generated with the QuikChange Site-Directed Mutagenesis Kit (Stratagene). Flag or HA-tagged TRAF proteins were overexpressed in HEK293T cells while Flag or HA-tagged NEMO proteins were overexpressed in *Nemo*^{-/-} cells. Proteins were purified with M2 or anti-HA agarose, followed by Flag or HA peptide elution, respectively. For expression in *E.coli*, cDNAs encoding N-terminal His₆-flag tandem-tagged NEMO WT and K285/309R were inserted into pET23a; cDNAs encoding N-terminal His₆-tagged Ubiquitin WT, K63R and K63 only, and MAVS Δ TM (aa1-510 or 1-460) were also cloned into pET23a. cDNAs encoding Flag-tagged IRF3 full length (2A), aa1-384, aa1-189, aa190-427 (2A), aa190-384 and aa384-427 (2A) were cloned into pGEX4T1 in frame with a N-terminal GST tag. Vectors encoding ubiquitin mutants were transformed and expressed in *E. Coli* BL21 (DE3)-pJY2 strain to prevent misincorporation of Lys residues. Other vectors were transformed and expressed in *E. Coli* BL21(DE3)-pLysS strain. His₆-MAVS Δ TM (aa1-510 or 1-460) was purified in the presence of 4M Urea whereas other His₆-tagged proteins were purified under native condition, by

nickel affinity chromatography. GST-tagged proteins were purified under native condition with Glutathione agarose in PBS and eluted with an Elution buffer containing 10 mM glutathione and 50mM Tris-HCl (pH 8.0). Ubc5c, His₆-TRAF6, His₈-E1 and His₈-IRF3 were purified as described previously (Hou et al., 2011; Zeng et al., 2009).

Immunoblot Analysis

Cells were homogenized in buffer containing 20mM Tris-HCl (pH7.5), 150mM NaCl, 10% (v/v) glycerol, 1mM dithiothreitol (DTT), 1% (v/v) NP-40, 1mM Na₃VO₄, 20mM β-glycerol phosphate, and protease inhibitors cocktail (Roche). After incubation on ice for 10 minutes, the lysate was centrifuged at 20,000xg for 10 minutes. 20μg of supernatant was subjected to gel electrophoresis, followed by immunoblot analysis with antibodies as indicated in the figure legends.

Calcium Phosphate Precipitation Method

HEK293T cells were set up in 12-well plates or 10cm dishes at day 0. cDNAs were diluted in 37.5 μl H₂O and mixed with 12.5 μl of 1M CaCl₂. 50 μl of 2xHBS buffer containing 50mM HEPES (pH 7.05), 10mM KCl, 12mM Dextrose, 280mM NaCl and 1.5mM Na₂HPO₄ was added to the mixture, and the mixture was then added to cells drop by drop immediately after mixing.

Cell culture and Transfections

Cells were cultured at 37°C in an atmosphere of 5% (v/v) CO₂, HEK293T cells were cultured in Dulbecco's modified Eagle's medium (DMEM) supplemented with 10% (v/v) cosmic calf

serum (Hyclone) supplemented with penicillin (100 U/ml) and streptomycin (100 mg/ml). *Traf2*^{-/-} MEF cells and stable cells generated from these cells were cultured in DMEM supplemented with 20% (v/v) fetal bovine serum (Invitrogen) and antibiotics. Other MEF cells were cultured in DMEM supplemented with 10% (v/v) fetal bovine serum (Atlanta) and antibiotics.

For transient overexpression in HEK293T cells, cells were set up in 10cm culture dishes with 8% confluence on day 0. On day 1, 10 μ g of expression plasmids were transfected using calcium phosphate precipitation method. For SeV infection experiments, cells were infected with SeV for 12 hours before harvest. For protein purification, cells were harvested 48 hours post transfection.

For transient overexpression in MEF cells, a similar protocol to that described above was used, except the Lipofectamine 2000 (Invitrogen) was used instead of the calcium phosphate precipitation method.

Purification of NEMO-TBK1 complex

Nemo^{-/-} MEFs and MEFs stably expressing Flag-NEMO Δ N were lysed in hypotonic buffer [10mM Tris -HCl (pH 7.5), 10mM KCl, 1.5mM MgCl₂ and a protease cocktail (Roche)]. After centrifugation at 100,000g for 30 min, the supernatants from both types of cells were mixed at a ratio of 5:1, and the mixture was subjected to immunoprecipitation with M2 agarose at 4°C overnight. The agarose beads were washed three times with buffer B [10mM Tris-HCl (pH 7.5), 1M NaCl and 0.1% CHAPS], and the proteins were eluted with Flag

peptide (0.2 mg/ml) in buffer C [50mM Tris-HCl (pH 7.5), 0.1% CHAPS]. The eluted proteins containing endogenous TBK1 and TANK from MEFs were stored in buffer D [20mM Tris-HCl (pH 7.5), 50mM NaCl, 10% Glycerol and 0.1% CHAPS] after buffer exchange by repeated dilutions and subsequent concentration.

Biochemistry Assay for IRF3 Activation, I κ B α Phosphorylation, NEMO-MAVS and IRF3-MAVS complex in vitro

The procedure of the in vitro assay for IRF3 activation and I κ B α phosphorylation was described previously (Zeng et al., 2009). 20ng of His₆-MAVS Δ TM can be used to replace crude virus-infected P5. In the assays for the TRAF6 purification, the Q-A fraction was replaced with 0.05 μ g of Ubc5 in combination with 0.1 μ g His₈-E1, 5 μ g Ubiquitin, 0.02 μ g His₈-IRF3 and 1 μ l of NEMO-PD. After purification, 0.003-0.01 μ g of His₆-TRAF6 was added to replace the Heparin fraction. For IRF3 activation in vitro, some samples were subjected to SDS PAGE, and phosphorylation of IRF3 was determined by immunoblotting using antibodies against mouse or human IRF3.

To determine the NEMO-MAVS complex formation in vitro, a 100 μ l reaction with 200ng His₆-MAVS Δ TM, 200 μ g S5 or S100, 200ng Flag-NEMO purified from *Nemo*^{-/-} MEF cells and a buffer containing 20mM HEPES-KOH (pH 7.0), 2mM ATP and 5mM MgCl₂ was incubated at 30°C for 1 hr. The reactions were subjected to immunoprecipitation with M2 agarose at 4°C overnight supplemented with the additional 20mM Tris-HCl (pH 7.5), 100mM NaCl, 0.5%NP-40 and the protease cocktail. The agarose beads were washed three times with lysis buffer A [20mM Tris-HCl (pH 7.5), 100mM NaCl, 10% Glycerol and

0.5%NP-40], co-immunoprecipitated proteins on the beads were detected by immunoblotting with anti-MAVS, anti-NEMO or anti-TRAF2 antibodies.

To characterize the IRF3-MAVS complex formation in crude extracts, similar experiments to NEMO-MAVS complex were performed, except that Flag-IRF3 2A or GST-IRF3 proteins were added on ice after the reaction, and prior to the immunoprecipitation step. To determine the IRF3-MAVS complex formation in the presence of GST-TBK1 in purified system, the M2 agarose was pre-incubated in lysis buffer A containing 1 mg/ml BSA for 2 hours. The following immunoprecipitation was carried out in the buffer described above with additional 0.2 mg/ml BSA.

Biochemical Fractionation of Cytosolic Extract and Purification of TRAF6

Hela S100 was prepared as described previously from 50 L of cells purchased from National Cell culture Center. S100 was loaded onto 60 ml Q-Sepharose column equilibrated with buffer Q-A (20 mM Tris-HCl [pH 7.5], 10% glycerol and 0.02% CHAPS), and Eluate by 0.25 M NaCl was diluted and concentrated repeatedly to reduce the salt with buffer SP-A (20 mM HEPES-KOH [pH 6.5], 10% glycerol and 0.02% CHAPS). The sample was further loaded on SP-Sepharose. The flow through from the SP column was directly fractionated on a Heparin-Sepharose column with a linear gradient of NaCl (0-300 mM) in buffer SP-A, and active fractions eluted around 150 mM NaCl were pooled. After the salt was reduced by repeated dilution in buffer SP-A, the sample was fractionated on 2 ml CHT Ceramic Hydroxyapatite column with a linear gradient of KPO₄ (0-300 mM) in buffer CHT-A [5 mM KPO₄, 150 mM NaCl, pH 7.0]. Active fractions eluted around 150 mM KPO₄ were pooled

and precipitated with 30% ammonium sulfate. The pellet was resuspended with buffer Q-A and fractioned on 2.4 ml Superdex 200 PC 3.2/30 column in buffer Q-A containing 100 mM NaCl. Fractions containing proteins with a size of 300 KD were pooled and finally loaded onto MonoQ-Sepharose with a linear gradient of NaCl (150-350 mM) in buffer Q-A. In vitro assay for IRF3 dimerization was performed as described above following each step of chromatography. 50% of each MonoQ fractions were subjected to SDS-PAGE, and the proteins were visualized by silver staining. The protein bands were excised for analysis by tandem mass spectrometry. Later, 10% of each MonoQ fractions were subjected to immunoblotting with anti-TRAF6 antibody.

Lentiviral-mediated RNAi and Rescue with Transgene

The lentiviral knockdown vector, pTY-shRNA-EF1a-puroR-2a-GFP-Flag, was provided by Y. Zhang (University of North Carolina at Chapel Hill) and later was re-engineered into pTY- shRNA-EF1a-GFP-IRES-puroR. The shRNA sequences were cloned into the vectors with a U6 promoter. The rescue cDNAs were cloned into the vectors by replacing the GFP construct. Lentiviral infection and establishment of stable cells were described previously (He et al., 2011; Tanaka and Chen, 2012). The shRNA sequences are as follows (only the sense strand is shown): mouse TRAF6, 5'-GGATGATACTTACTAGTG-3'; mouse HOIP, 5'-GGCGCTCAGTGAAGTTAA-3'; mouse MAVS, 5'-GATCAAGTGACTCGAGTT-3';

RT-PCR and Real-time PCR (qPCR)

Total RNA from MEF cells was isolated using TRIzol (Invitrogen). 0.1 µg total RNA was reverse-transcribed into cDNA using iScript Kit (Biorad). The resulting cDNA was served as

the template for Quantitative-PCR analysis using SYBR Green Supermix (Biorad) and Real-Time PCR System (ABI). Primers for specific genes are listed as follows: Mouse β-actin, 5'-TGACGTTGACATCCGTAAAGACC-3' and 5'-AAGGGTGTAAAACGCAGCTCA-3'; Mouse IFN-β, 5'CCCTATGGAGATGACGGAGA-3' and 5'-CTGTCTGCTGGTGGAGTTCA-3'; Mouse IFN-α, 5'-ATTGGATTCCCCTGGAG-3' and 5'-TATGTCCTCACAGCCAGCAG-3'; Mouse CxCl10, 5'-GGTCTGAGTGGACTCAAGG-3' and 5'-GTGGCAATGATCTAACACCG-3'; Mouse IL6, 5'-TCCATCCAGTTGCCTCTTG-3' and 5'-GGTCTGTTGGGAGTGGTATC-3'; Mouse TRAF6, 5'-GCCCAGGCTGTTATAATGT-3' and 5'-CGGATCTGATGGCCTGTCT-3'; Mouse HOIP, 5'-TTATGCGAGACCCAAGTTC-3' and 5'-GCCTTGAGCCTGGTACTCTG-3';

SILAC Experiments

Wild-type MEF and *Nemo*^{-/-} MEF expressing Flag-NEMOΔN85 WT or UBDm were cultured in SILAC-DMEM medium lacking lysine and arginine. The medium was supplemented with dialyzed FBS, penicillin, streptomycin and amino acids L-lysine and L-arginine. The ‘light’ culture was supplemented with Lys0 (¹²C₆¹⁴N₂) and Arg0 (¹²C₆¹⁴N₄), and the ‘heavy’ culture with Lys8 (¹³C₆¹⁵N₂) and Arg10 (¹³C₆¹⁵N₄). All SILAC reagents were purchased from Pierce (Thermo Scientific). The in vitro and cell-based SILAC experiments were preformed according to the outline described in Figure 5 – supplement 1A and 1C, respectively. After SDS-PAGE and silver staining, 10 to 12 gel slices from each lane were excised and digested with trypsin in situ. Extracted peptides were fractionated on a homemade analytical column

(75 μm ID, 100 mm length) packed with C18 resin (100 Å, 3 μm , MICHROM Bioresources) using Dionex Ultimate 3000 nanoLC system (Thermo Scientific). The column was coupled in-line to a Q Exactive mass spectrometer (Thermo Scientific) equipped with a nano-electrospray ion source, which was set at a spray voltage of 2.3 kV. Peptides were eluted with a 78 min gradient as follows: 2–30% B in 68 min, 30–35% B in 4 min, 35–40% B in 2 min, 40–60% B in 3 min, and 60–80% B in 1 min (A = 0.1% formic acid; B = 100% acetonitrile in 0.1% formic acid). Full scan mass spectra were acquired from m/z 300–1500 with a resolution of 70,000 at m/z = 200 in the Orbitrap. MS/MS spectra (resolution: 17,500 at m/z = 200) were acquired in a data-dependent mode whereby the top 10 most abundant parent ions were subjected to further fragmentation by higher energy collision dissociation (HCD). SILAC data was processed using MaxQuant computational platform (Cox and Mann, 2008) version 1.3.0.5 which incorporates the Andromeda search engine (Cox et al., 2011). Proteins were identified by searching the mouse UniProt database supplemented with frequently observed contaminants. The first search tolerance was set at 20 ppm and main search deviation at 6 ppm. The required minimum peptide length was six amino acids. The false discovery rate (FDR) at both peptide and protein levels was set to 0.01. SILAC quantification of each protein group was based on at least two ratio counts.

CHAPTER V

BIBLIOGRAPHY

- Alvarez, S.E., Harikumar, K.B., Hait, N.C., Allegood, J., Strub, G.M., Kim, E.Y., Maceyka, M., Jiang, H.L., Luo, C., Kordula, T., *et al.* (2010). Sphingosine-1-phosphate is a missing cofactor for the E3 ubiquitin ligase TRAF2. *Nature* *465*, 1084-U1149.
- Barber, G.N. (2011). Innate immune DNA sensing pathways: STING, AIMII and the regulation of interferon production and inflammatory responses. *Current opinion in immunology* *23*, 10-20.
- Beck, G., and Habicht, G.S. (1996). Immunity and the invertebrates. *Scientific American* *275*, 60-63, 66.
- Belgnaoui, S.M., Paz, S., Samuel, S., Goulet, M.L., Sun, Q., Kikkert, M., Iwai, K., Dikic, I., Hiscott, J., and Lin, R.T. (2012). Linear Ubiquitination of NEMO Negatively Regulates the Interferon Antiviral Response through Disruption of the MAVS-TRAF3 Complex. *Cell Host Microbe* *12*, 211-222.
- Cao, Z., Xiong, J., Takeuchi, M., Kurama, T., and Goeddel, D.V. (1996). TRAF6 is a signal transducer for interleukin-1. *Nature* *383*, 443-446.
- Chen, Z., Hagler, J., Palombella, V.J., Melandri, F., Scherer, D., Ballard, D., and Maniatis, T. (1995). Signal-induced site-specific phosphorylation targets I kappa B alpha to the ubiquitin-proteasome pathway. *Genes Dev* *9*, 1586-1597.
- Chen, Z.J. (2005). Ubiquitin signalling in the NF-kappaB pathway. *Nat Cell Biol* *7*, 758-765.
- Chen, Z.J., and Sun, L.J. (2009). Nonproteolytic functions of ubiquitin in cell signaling. *Mol Cell* *33*, 275-286.
- Chiu, Y.H., MacMillan, J.B., and Chen, Z.J.J. (2009). RNA Polymerase III Detects Cytosolic DNA and Induces Type I Interferons through the RIG-I Pathway. *Cell* *138*, 576-591.

Chung, J.Y., Park, Y.C., Ye, H., and Wu, H. (2002). All TRAFs are not created equal: common and distinct molecular mechanisms of TRAF-mediated signal transduction. *J Cell Sci* *115*, 679-688.

Clark, K., Takeuchi, O., Akira, S., and Cohen, P. (2011). The TRAF-associated protein TANK facilitates cross-talk within the I kappa B kinase family during Toll-like receptor signaling. *P Natl Acad Sci USA* *108*, 17093-17098.

Cui, S., Eisenacher, K., Kirchhofer, A., Brzozka, K., Lammens, A., Lammens, K., Fujita, T., Conzelmann, K.K., Krug, A., and Hopfner, K.P. (2008). The C-terminal regulatory domain is the RNA 5'-triphosphate sensor of RIG-I. *Molecular Cell* *29*, 169-179.

Damgaard, R.B., Nachbur, U., Yabal, M., Wong, W.W., Fiil, B.K., Kastirr, M., Rieser, E., Rickard, J.A., Bankovacki, A., Peschel, C., *et al.* (2012). The ubiquitin ligase XIAP recruits LUBAC for NOD2 signaling in inflammation and innate immunity. *Mol Cell* *46*, 746-758.

Deng, L., Wang, C., Spencer, E., Yang, L., Braun, A., You, J., Slaughter, C., Pickart, C., and Chen, Z.J. (2000). Activation of the IkappaB kinase complex by TRAF6 requires a dimeric ubiquitin-conjugating enzyme complex and a unique polyubiquitin chain. *Cell* *103*, 351-361.

Dranoff, G. (2004). Cytokines in cancer pathogenesis and cancer therapy. *Nat Rev Cancer* *4*, 11-22.

Ea, C.K., Sun, L., Inoue, J., and Chen, Z.J.J. (2004). TIFA activates I kappa B kinase (IKK) by promoting oligomerization and ubiquitination of TRAF6. *P Natl Acad Sci USA* *101*, 15318-15323.

Fitzgerald, K.A., McWhirter, S.M., Faia, K.L., Rowe, D.C., Latz, E., Golenbock, D.T., Coyle, A.J., Liao, S.M., and Maniatis, T. (2003). IKKepsilon and TBK1 are essential components of the IRF3 signaling pathway. *Nat Immunol* *4*, 491-496.

Franchi, L., Wamer, N., Viani, K., and Nunez, G. (2009). Function of Nod-like receptors in microbial recognition and host defense. *Immunological reviews* *227*, 106-128.

Gack, M.U., Shin, Y.C., Joo, C.H., Urano, T., Liang, C., Sun, L.J., Takeuchi, O., Akira, S., Chen, Z.J., Inoue, S.S., *et al.* (2007). TRIM25 RING-finger E3 ubiquitin ligase is essential for RIG-I-mediated antiviral activity. *Nature* *446*, 916-U912.

Gerlach, B., Cordier, S.M., Schmukle, A.C., Emmerich, C.H., Rieser, E., Haas, T.L., Webb, A.I., Rickard, J.A., Anderton, H., Wong, W.W., *et al.* (2011). Linear ubiquitination prevents inflammation and regulates immune signalling. *Nature* *471*, 591-596.

Gitlin, L., Barchet, W., Gilfillan, S., Cella, M., Beutler, B., Flavell, R.A., Diamond, M.S., and Colonna, M. (2006). Essential role of mda-5 in type I IFN responses to polyriboinosinic:polyribocytidyl acid and encephalomyocarditis picornavirus. *Proc Natl Acad Sci U S A* *103*, 8459-8464.

Guo, B., and Cheng, G. (2007). Modulation of the interferon antiviral response by the TBK1/IKK α adaptor protein TANK. *J Biol Chem* *282*, 11817-11826.

Haas, T.L., Emmerich, C.H., Gerlach, B., Schmukle, A.C., Cordier, S.M., Rieser, E., Feltham, R., Vince, J., Warnken, U., Wenger, T., *et al.* (2009). Recruitment of the linear ubiquitin chain assembly complex stabilizes the TNF-R1 signaling complex and is required for TNF-mediated gene induction. *Mol Cell* *36*, 831-844.

Hayden, M.S., and Ghosh, S. (2008). Shared principles in NF- κ B signaling. *Cell* *132*, 344-362.

He, J., Anh, T.N., and Zhang, Y. (2011). KDM2b/JHDM1b, an H3K36me2-specific demethylase, is required for initiation and maintenance of acute myeloid leukemia. *Blood* *117*, 3869-3880.

Hornung, V., Ablasser, A., Charrel-Dennis, M., Bauernfeind, F., Horvath, G., Caffrey, D.R., Latz, E., and Fitzgerald, K.A. (2009). AIM2 recognizes cytosolic dsDNA and forms a caspase-1-activating inflammasome with ASC. *Nature* *458*, 514-518.

Hornung, V., Ellegast, J., Kim, S., Brzozka, K., Jung, A., Kato, H., Poeck, H., Akira, S., Conzelmann, K.K., Schlee, M., *et al.* (2006). 5'-triphosphate RNA is the ligand for RIG-I. *Science* *314*, 994-997.

Hou, F., Sun, L., Zheng, H., Skaug, B., Jiang, Q.X., and Chen, Z.J. (2011). MAVS forms functional prion-like aggregates to activate and propagate antiviral innate immune response. *Cell* 146, 448-461.

Ikeda, F., Deribe, Y.L., Skanland, S.S., Stieglitz, B., Grabbe, C., Franz-Wachtel, M., van Wijk, S.J., Goswami, P., Nagy, V., Terzic, J., *et al.* (2011). SHARPIN forms a linear ubiquitin ligase complex regulating NF-kappaB activity and apoptosis. *Nature* 471, 637-641.

Inn, K.S., Gack, M.U., Tokunaga, F., Shi, M.D., Wong, L.Y., Iwai, K., and Jung, J.U. (2011). Linear Ubiquitin Assembly Complex Negatively Regulates RIG-I- and TRIM25-Mediated Type I Interferon Induction. *Molecular Cell* 41, 354-365.

Inohara, N., Koseki, T., del Peso, L., Hu, Y., Yee, C., Chen, S., Carrio, R., Merino, J., Liu, D., Ni, J., *et al.* (1999). Nod1, an Apaf-1-like activator of caspase-9 and nuclear factor-kappaB. *J Biol Chem* 274, 14560-14567.

Ishikawa, H., and Barber, G.N. (2008). STING is an endoplasmic reticulum adaptor that facilitates innate immune signalling. *Nature* 455, 674-678.

Iwai, K., and Ishikawa, H. (2006). [Mechanism underlying ubiquitination of iron regulatory protein 2 (IRP2)]. Tanpakushitsu kakusan koso Protein, nucleic acid, enzyme 51, 1287-1291.

Jiang, X., Kinch, L.N., Brautigam, C.A., Chen, X., Du, F., Grishin, N.V., and Chen, Z.J. (2012). Ubiquitin-induced oligomerization of the RNA sensors RIG-I and MDA5 activates antiviral innate immune response. *Immunity* 36, 959-973.

Jin, L., Waterman, P.M., Jonscher, K.R., Short, C.M., Reisdorph, N.A., and Cambier, J.C. (2008). MPYS, a novel membrane tetraspanner, is associated with major histocompatibility complex class II and mediates transduction of apoptotic signals. *Molecular and Cellular Biology* 28, 5014-5026.

Kato, H., Takeuchi, O., Mikamo-Satoh, E., Hirai, R., Kawai, T., Matsushita, K., Hiiragi, A., Dermody, T.S., Fujita, T., and Akira, S. (2008). Length-dependent recognition of double-stranded ribonucleic acids by retinoic acid-inducible gene-I and melanoma differentiation-associated gene 5. *The Journal of experimental medicine* 205, 1601-1610.

Kawai, T., Takahashi, K., Sato, S., Coban, C., Kumar, H., Kato, H., Ishii, K.J., Takeuchi, O., and Akira, S. (2005). IPS-1, an adaptor triggering RIG-I- and Mda5-mediated type I interferon induction. *Nat Immunol* 6, 981-988.

Kayagaki, N., Phung, Q., Chan, S., Chaudhari, R., Quan, C., O'Rourke, K.M., Eby, M., Pietras, E., Cheng, G.H., Bazan, J.F., *et al.* (2007). DUBA: A deubiquitinase that regulates type I interferon production. *Science* 318, 1628-1632.

Kirisako, T., Kamei, K., Murata, S., Kato, M., Fukumoto, H., Kanie, M., Sano, S., Tokunaga, F., Tanaka, K., and Iwai, K. (2006). A ubiquitin ligase complex assembles linear polyubiquitin chains. *EMBO J* 25, 4877-4887.

Kishore, N., Huynh, Q.K., Mathialagan, S., Hall, T., Rouw, S., Creely, D., Lange, G., Carroll, J., Reitz, B., Donnelly, A., *et al.* (2002). IKK-i and TBK-1 are enzymatically distinct from the homologous enzyme IKK-2 - Comparative analysis of recombinant human IKK-i, TBK-1, and IKK-2. *Journal of Biological Chemistry* 277, 13840-13847.

Kowalinski, E., Lunardi, T., McCarthy, A.A., Louber, J., Brunel, J., Grigorov, B., Gerlier, D., and Cusack, S. (2011). Structural basis for the activation of innate immune pattern-recognition receptor RIG-I by viral RNA. *Cell* 147, 423-435.

Lamothe, B., Besse, A., Webster, W.K., Campos, A.D., Wu, H., and Darnay, B.G. (2006). Site-specific TRAF6 auto-ubiquitination via Lys63 linkages connects RANK to osteoclastogenesis. *J Bone Miner Res* 21, S24-S24.

Le Bon, A., and Tough, D.F. (2002). Links between innate and adaptive immunity via type I interferon. *Current opinion in immunology* 14, 432-436.

Li, S., Wang, L., and Dorf, M.E. (2009). PKC phosphorylation of TRAF2 mediates IKKalpha/beta recruitment and K63-linked polyubiquitination. *Mol Cell* 33, 30-42.

Li, S.T., Wang, L.Y., Berman, M., Kong, Y.Y., and Dorf, M.E. (2011a). Mapping a Dynamic Innate Immunity Protein Interaction Network Regulating Type I Interferon Production. *Immunity* 35, 426-440.

Li, X.D., and Chen, Z.J. (2012). Sequence specific detection of bacterial 23S ribosomal RNA by TLR13. *eLife* 1, e00102.

Li, X.D., Chiu, Y.H., Ismail, A.S., Behrendt, C.L., Wight-Carter, M., Hooper, L.V., and Chen, Z.J. (2011b). Mitochondrial antiviral signaling protein (MAVS) monitors commensal bacteria and induces an immune response that prevents experimental colitis. *Proc Natl Acad Sci U S A* *108*, 17390-17395.

Lin, L., and Ghosh, S. (1996). A glycine-rich region in NF-kappa B p105 functions as a processing signal for the generation of the p50 subunit. *Molecular and Cellular Biology* *16*, 2248-2254.

Ling, L., and Goeddel, D.V. (2000). T6BP, a TRAF6-interacting protein involved in IL-1 signaling. *P Natl Acad Sci USA* *97*, 9567-9572.

Lomaga, M.A., Yeh, W.C., Sarosi, I., Duncan, G.S., Furlonger, C., Ho, A., Morony, S., Capparelli, C., Van, G., Kaufman, S., *et al.* (1999). TRAF6 deficiency results in osteopetrosis and defective interleukin-1, CD40, and LPS signaling. *Genes Dev* *13*, 1015-1024.

Luo, D.H., Ding, S.C., Vela, A., Kohlway, A., Lindenbach, B.D., and Pyle, A.M. (2011). Structural Insights into RNA Recognition by RIG-I. *Cell* *147*, 409-422.

Ma, X.L., Helgason, E., Phung, Q.T., Quan, C.L., Iyer, R.S., Lee, M.W., Bowman, K.K., Starovasnik, M.A., and Dueber, E.C. (2012). Molecular basis of Tank-binding kinase 1 activation by transautophosphorylation. *P Natl Acad Sci USA* *109*, 9378-9383.

Maelfait, J., Roose, K., Bogaert, P., Sze, M., Saelens, X., Pasparakis, M., Carpentier, I., van Loo, G., and Beyaert, R. (2012). A20 (Tnfaip3) Deficiency in Myeloid Cells Protects against Influenza A Virus Infection. *Plos Pathog* *8*.

Mao, A.P., Li, S., Zhong, B., Li, Y., Yan, J., Li, Q., Teng, C.W., and Shu, H.B. (2010). Virus-triggered Ubiquitination of TRAF3/6 by cIAP1/2 Is Essential for Induction of Interferon-beta (IFN-beta) and Cellular Antiviral Response. *Journal of Biological Chemistry* *285*, 9470-9476.

McWhirter, S.M., Teneover, B.R., and Maniatis, T. (2005). Connecting mitochondria and innate immunity. *Cell* *122*, 645-647.

Meylan, E., Curran, J., Hofmann, K., Moradpour, D., Binder, M., Bartenschlager, R., and Tschopp, R. (2005). Cardif is an adaptor protein in the RIG-I antiviral pathway and is targeted by hepatitis C virus. *Nature* *437*, 1167-1172.

Mushegian, A., and Medzhitov, R. (2001). Evolutionary perspective on innate immune recognition. *The Journal of cell biology* *155*, 705-710.

Niu, J., Shi, Y., Iwai, K., and Wu, Z.H. (2011). LUBAC regulates NF-kappaB activation upon genotoxic stress by promoting linear ubiquitination of NEMO. *EMBO J* *30*, 3741-3753.

O'Neill, L.A., and Bowie, A.G. (2007). The family of five: TIR-domain-containing adaptors in Toll-like receptor signalling. *Nat Rev Immunol* *7*, 353-364.

O'Neill, L.A., and Bowie, A.G. (2010). Sensing and signaling in antiviral innate immunity. *Curr Biol* *20*, R328-333.

Oganesyan, G., Saha, S.K., Guo, B.C., He, J.Q., Shahangian, A., Zarnegar, B., Perry, A., and Cheng, G.H. (2006). Critical role of TRAF3 in the Toll-like receptor-dependent and -independent antiviral response. *Nature* *439*, 208-211.

Ogura, Y., Inohara, N., Benito, A., Chen, F.F., Yamaoka, S., and Nunez, G. (2001). Nod2, a Nod1/Apaf-1 family member that is restricted to monocytes and activates NF-kappa B. *Journal of Biological Chemistry* *276*, 4812-4818.

Oldenburg, M., Kruger, A., Ferstl, R., Kaufmann, A., Nees, G., Sigmund, A., Bathke, B., Lauterbach, H., Suter, M., Dreher, S., *et al.* (2012). TLR13 recognizes bacterial 23S rRNA devoid of erythromycin resistance-forming modification. *Science* *337*, 1111-1115.

Ou, Y.H., Torres, M., Ram, R., Formstecher, E., Roland, C., Cheng, T., Brekken, R., Wurz, R., Tasker, A., Polverino, T., *et al.* (2011). TBK1 directly engages Akt/PKB survival signaling to support oncogenic transformation. *Mol Cell* *41*, 458-470.

Panne, D., McWhirter, S.M., Maniatis, T., and Harrison, S.C. (2007). Interferon regulatory factor 3 is regulated by a dual phosphorylation-dependent switch. *Journal of Biological Chemistry* *282*, 22816-22822.

- Park, Y.C., Burkitt, V., Villa, A.R., Tong, L., and Wu, H. (1999). Structural basis for self-association and receptor recognition of human TRAF2. *Nature* *398*, 533-538.
- Paz, S., Vilasco, M., Werden, S.J., Arguello, M., Joseph-Pillai, D., Zhao, T., Nguyen, T.L., Sun, Q., Meurs, E.F., Lin, R., *et al.* (2011). A functional C-terminal TRAF3-binding site in MAVS participates in positive and negative regulation of the IFN antiviral response. *Cell Res* *21*, 895-910.
- Pertel, T., Hausmann, S., Morger, D., Zuger, S., Guerra, J., Lascano, J., Reinhard, C., Santoni, F.A., Uchil, P.D., Chatel, L., *et al.* (2011). TRIM5 is an innate immune sensor for the retrovirus capsid lattice. *Nature* *472*, 361-365.
- Petroski, M.D., Zhou, X.L., Dong, G.Q., Daniel-Issakani, S., Payan, D.G., and Huang, J.N. (2007). Substrate modification with lysine 63-linked ubiquitin chains through the UBC13-UEV1A ubiquitin-conjugating enzyme. *Journal of Biological Chemistry* *282*, 29936-29945.
- Pichlmair, A., and Reis e Sousa, C. (2007). Innate recognition of viruses. *Immunity* *27*, 370-383.
- Pichlmair, A., Schulz, O., Tan, C.P., Naslund, T.I., Liljestrom, P., Weber, F., and Reis e Sousa, C. (2006). RIG-I-mediated antiviral responses to single-stranded RNA bearing 5'-phosphates. *Science* *314*, 997-1001.
- Piwko, W., and Jentsch, S. (2006). Proteasome-mediated protein processing by bidirectional degradation initiated from an internal site. *Nature Structural & Molecular Biology* *13*, 691-697.
- Pomerantz, J.L., and Baltimore, D. (2002). Two pathways to NF-kappaB. *Mol Cell* *10*, 693-695.
- Psakhye, I., and Jentsch, S. (2012). Protein Group Modification and Synergy in the SUMO Pathway as Exemplified in DNA Repair. *Cell* *151*, 807-820.
- Qin, B.Y., Liu, C., Lam, S.S., Srinath, H., Delston, R., Correia, J.J., Derynck, R., and Lin, K. (2003). Crystal structure of IRF-3 reveals mechanism of autoinhibition and virus-induced phosphoactivation. *Nat Struct Biol* *10*, 913-921.

Rahighi, S., Ikeda, F., Kawasaki, M., Akutsu, M., Suzuki, N., Kato, R., Kensche, T., Uejima, T., Bloor, S., Komander, D., *et al.* (2009). Specific Recognition of Linear Ubiquitin Chains by NEMO Is Important for NF- κ B Activation. *Cell* *136*, 1098-1109.

Roach, J.C., Glusman, G., Rowen, L., Kaur, A., Purcell, M.K., Smith, K.D., Hood, L.E., and Aderem, A. (2005). The evolution of vertebrate Toll-like receptors. *Proc Natl Acad Sci U S A* *102*, 9577-9582.

Rothenfusser, S., Goutagny, N., DiPerna, G., Gong, M., Monks, B.G., Schoenemeyer, A., Yamamoto, M., Akira, S., and Fitzgerald, K.A. (2005). The RNA helicase Lgp2 inhibits TLR-independent sensing of viral replication by retinoic acid-inducible gene-I. *J Immunol* *175*, 5260-5268.

Ryzhakov, G., and Randow, F. (2007). SINTBAD, a novel component of innate antiviral immunity, shares a TBK1-binding domain with NAP1 and TANK. *EMBO J* *26*, 3180-3190.

Saha, S.K., Pietras, E.M., He, J.Q., Kang, J.R., Liu, S.Y., Oganesyan, G., Shahangian, A., Zarnegar, B., Shiba, T.L., Wang, Y., *et al.* (2006). Regulation of antiviral responses by a direct and specific interaction between TRAF3 and Cardif. *EMBO J* *25*, 3257-3263.

Sasai, M., Shingai, M., Funami, K., Yoneyama, M., Fujita, T., Matsumoto, M., and Seya, T. (2006). NAK-associated protein 1 participates in both the TLR3 and the cytoplasmic pathways in type IIFN induction. *J Immunol* *177*, 8676-8683.

Satoh, T., Kato, H., Kumagai, Y., Yoneyama, M., Sato, S., Matsushita, K., Tsujimura, T., Fujita, T., Akira, S., and Takeuchi, O. (2010). LGP2 is a positive regulator of RIG-I- and MDA5-mediated antiviral responses. *P Natl Acad Sci USA* *107*, 1512-1517.

Sauer, J.D., Sotelo-Troha, K., von Moltke, J., Monroe, K.M., Rae, C.S., Brubaker, S.W., Hyodo, M., Hayakawa, Y., Woodward, J.J., Portnoy, D.A., *et al.* (2011). The N-ethyl-N-nitrosourea-induced Goldenticket mouse mutant reveals an essential function of Sting in the *in vivo* interferon response to *Listeria monocytogenes* and cyclic dinucleotides. *Infection and immunity* *79*, 688-694.

- Scherer, D.C., Brockman, J.A., Chen, Z.J., Maniatis, T., and Ballard, D.W. (1995). Signal-Induced Degradation of I-Kappa-B-Alpha Requires Site-Specific Ubiquitination. *P Natl Acad Sci USA* *92*, 11259-11263.
- Schrofelbauer, B., Polley, S., Behar, M., Ghosh, G., and Hoffmann, A. (2012). NEMO Ensures Signaling Specificity of the Pleiotropic IKK beta by Directing Its Kinase Activity toward I kappa B alpha. *Molecular Cell* *47*, 111-121.
- Seth, R.B., Sun, L., Ea, C.K., and Chen, Z.J. (2005). Identification and characterization of MAVS, a mitochondrial antiviral signaling protein that activates NF-kappaB and IRF 3. *Cell* *122*, 669-682.
- Sharma, S., tenOever, B.R., Grandvaux, N., Zhou, G.P., Lin, R.T., and Hiscott, J. (2003). Triggering the interferon antiviral response through an IKK-related pathway. *Science* *300*, 1148-1151.
- Skaug, B., Chen, J., Du, F., He, J., Ma, A., and Chen, Z.J. (2011). Direct, noncatalytic mechanism of IKK inhibition by A20. *Mol Cell* *44*, 559-571.
- Spencer, E., Jiang, J., and Chen, Z.J. (1999). Signal-induced ubiquitination of IkappaBalphabeta by the F-box protein Slimb/beta-TrCP. *Genes Dev* *13*, 284-294.
- Stetson, D.B., and Medzhitov, R. (2006). Type I interferons in host defense. *Immunity* *25*, 373-381.
- Sun, L.J., Deng, L., Ea, C.K., Xia, Z.P., and Chen, Z.J.J. (2004). The TRAF6 ubiquitin ligase and TAK1 kinase mediate IKK activation by BCL10 and MALT1 in T lymphocytes. *Molecular Cell* *14*, 289-301.
- Takahasi, K., Suzuki, N.N., Horiuchi, M., Mori, M., Suhara, W., Okabe, Y., Fukuhara, Y., Terasawa, H., Akira, S., Fujita, T., *et al.* (2003). X-ray crystal structure of IRF-3 and its functional implications. *Nat Struct Biol* *10*, 922-927.
- Takeuchi, O., and Akira, S. (2008). MDA5/RIG-I and virus recognition. *Current opinion in immunology* *20*, 17-22.

Takeuchi, O., and Akira, S. (2010). Pattern recognition receptors and inflammation. *Cell* 140, 805-820.

Tamura, T., Yanai, H., Savitsky, D., and Taniguchi, T. (2008). The IRF family transcription factors in immunity and oncogenesis. *Annual review of immunology* 26, 535-584.

Tanaka, Y., and Chen, Z.J. (2012). STING Specifies IRF3 Phosphorylation by TBK1 in the Cytosolic DNA Signaling Pathway. *Sci Signal* 5, ra20.

Tang, E.D., and Wang, C.Y. (2010). TRAF5 is a downstream target of MAVS in antiviral innate immune signaling. *PLoS One* 5, e9172.

Taniguchi, T., Ogasawara, K., Takaoka, A., and Tanaka, N. (2001). IRF family of transcription factors as regulators of host defense. *Annual review of immunology* 19, 623-655.

Tokunaga, F., Nakagawa, T., Nakahara, M., Saeki, Y., Taniguchi, M., Sakata, S., Tanaka, K., Nakano, H., and Iwai, K. (2011). SHARPIN is a component of the NF-kappaB-activating linear ubiquitin chain assembly complex. *Nature* 471, 633-636.

Tokunaga, F., Sakata, S., Saeki, Y., Satomi, Y., Kirisako, T., Kamei, K., Nakagawa, T., Kato, M., Murata, S., Yamaoka, S., et al. (2009). Involvement of linear polyubiquitylation of NEMO in NF-kappaB activation. *Nat Cell Biol* 11, 123-132.

Traenckner, E.B., Pahl, H.L., Henkel, T., Schmidt, K.N., Wilk, S., and Baeuerle, P.A. (1995). Phosphorylation of human I kappa B-alpha on serines 32 and 36 controls I kappa B-alpha proteolysis and NF-kappa B activation in response to diverse stimuli. *EMBO J* 14, 2876-2883.

Tseng, P.H., Matsuzawa, A., Zhang, W., Mino, T., Vignali, D.A., and Karin, M. (2010). Different modes of ubiquitination of the adaptor TRAF3 selectively activate the expression of type I interferons and proinflammatory cytokines. *Nat Immunol* 11, 70-75.

Venkataraman, T., Valdes, M., Elsby, R., Kakuta, S., Caceres, G., Saijo, S., Iwakura, Y., and Barber, G.N. (2007). Loss of DExD/H box RNA helicase LGP2 manifests disparate antiviral responses. *J Immunol* 178, 6444-6455.

Vitour, D., Dabo, S., Ahmadi Pour, M., Vilasco, M., Vidalain, P.O., Jacob, Y., Mezel-Lemoine, M., Paz, S., Arguello, M., Lin, R., *et al.* (2009). Polo-like kinase 1 (PLK1) regulates interferon (IFN) induction by MAVS. *J Biol Chem* *284*, 21797-21809.

Wang, C., Deng, L., Hong, M., Akkaraju, G.R., Inoue, J., and Chen, Z.J.J. (2001). TAK1 is a ubiquitin-dependent kinase of MKK and IKK. *Nature* *412*, 346-351.

Wang, L., Li, S., and Dorf, M.E. (2012). NEMO Binds Ubiquitinated TANK-Binding Kinase 1 (TBK1) to Regulate Innate Immune Responses to RNA Viruses. *PLoS One* *7*, e43756.

Xia, Z.P., Sun, L., Chen, X., Pineda, G., Jiang, X., Adhikari, A., Zeng, W., and Chen, Z.J. (2009). Direct activation of protein kinases by unanchored polyubiquitin chains. *Nature* *461*, 114-119.

Xie, X., Zhang, D., Zhao, B., Lu, M.K., You, M., Condorelli, G., Wang, C.Y., and Guan, K.L. (2011). IkappaB kinase epsilon and TANK-binding kinase 1 activate AKT by direct phosphorylation. *Proc Natl Acad Sci U S A* *108*, 6474-6479.

Xu, L.G., Wang, Y.Y., Han, K.J., Li, L.Y., Zhai, Z.H., and Shu, H.B. (2005). VISA is an adapter protein required for virus-triggered IFN-beta signaling. *Molecular Cell* *19*, 727-740.

Xu, M., Skaug, B., Zeng, W., and Chen, Z.J. (2009). A ubiquitin replacement strategy in human cells reveals distinct mechanisms of IKK activation by TNFalpha and IL-1beta. *Mol Cell* *36*, 302-314.

Yamamoto, Y., Kim, D.W., Kwak, Y.T., Prajapati, S., Verma, U., and Gaynor, R.B. (2001). IKK gamma/NEMO facilitates the recruitment of the I kappa B proteins into the I kappa B kinase complex. *Journal of Biological Chemistry* *276*, 36327-36336.

Yan, N., Regalado-Magdos, A.D., Stiggebout, B., Lee-Kirsch, M.A., and Lieberman, J. (2010). The cytosolic exonuclease TREX1 inhibits the innate immune response to human immunodeficiency virus type 1. *Nat Immunol* *11*, 1005-1013.

Ye, H., Arron, J.R., Lamothe, B., Cirilli, M., Kobayashi, T., Shevde, N.K., Segal, D., Dzivenu, O.K., Vologodskiaia, M., Yim, M., *et al.* (2002a). Distinct molecular mechanism for initiating TRAF6 signalling. *Nature* 418, 443-447.

Ye, H., Cirilli, M., and Wu, H. (2002b). The use of construct variation and diffraction data analysis in the crystallization of the TRAF domain of human tumor necrosis factor receptor associated factor 6. *Acta Crystallogr D* 58, 1886-1888.

Yeh, W.C., Shahinian, A., Speiser, D., Kraunus, J., Billia, F., Wakeham, A., de la Pompa, J.L., Ferrick, D., Hum, B., Iscove, N., *et al.* (1997). Early lethality, functional NF- κ B activation, and increased sensitivity to TNF-induced cell death in TRAF2-deficient mice. *Immunity* 7, 715-725.

Yin, Q., Lamothe, B., Darnay, B.G., and Wu, H. (2009). Structural basis for the lack of E2 interaction in the RING domain of TRAF2. *Biochemistry-US* 48, 10558-10567.

Yoneyama, M., and Fujita, T. (2008). Structural mechanism of RNA recognition by the RIG-I-like receptors. *Immunity* 29, 178-181.

Yoneyama, M., Kikuchi, M., Matsumoto, K., Imaizumi, T., Miyagishi, M., Taira, K., Foy, E., Loo, Y.M., Gale, M., Jr., Akira, S., *et al.* (2005). Shared and unique functions of the DExD/H-box helicases RIG-I, MDA5, and LGP2 in antiviral innate immunity. *J Immunol* 175, 2851-2858.

Yoneyama, M., Kikuchi, M., Natsukawa, T., Shinobu, N., Imaizumi, T., Miyagishi, M., Taira, K., Akira, S., and Fujita, T. (2004). The RNA helicase RIG-I has an essential function in double-stranded RNA-induced innate antiviral responses. *Nature Immunology* 5, 730-737.

Zeng, W., Xu, M., Liu, S., Sun, L., and Chen, Z.J. (2009). Key role of Ubc5 and lysine-63 polyubiquitination in viral activation of IRF3. *Mol Cell* 36, 315-325.

Zeng, W.W., Sun, L.J., Jiang, X.M., Chen, X., Hou, F.J., Adhikari, A., Xu, M., and Chen, Z.J.J. (2010). Reconstitution of the RIG-I Pathway Reveals a Signaling Role of Unanchored Polyubiquitin Chains in Innate Immunity. *Cell* 141, 315-330.

Zhao, T., Yang, L., Sun, Q., Arguello, M., Ballard, D.W., Hiscott, J., and Lin, R. (2007). The NEMO adaptor bridges the nuclear factor-kappaB and interferon regulatory factor signaling pathways. *Nat Immunol* 8, 592-600.

Alvarez, S.E., Harikumar, K.B., Hait, N.C., Allegood, J., Strub, G.M., Kim, E.Y., Maceyka, M., Jiang, H.L., Luo, C., Kordula, T., *et al.* (2010). Sphingosine-1-phosphate is a missing cofactor for the E3 ubiquitin ligase TRAF2. *Nature* 465, 1084-U1149.

Barber, G.N. (2011). Innate immune DNA sensing pathways: STING, AIMII and the regulation of interferon production and inflammatory responses. *Current opinion in immunology* 23, 10-20.

Beck, G., and Habicht, G.S. (1996). Immunity and the invertebrates. *Scientific American* 275, 60-63, 66.

Belgnaoui, S.M., Paz, S., Samuel, S., Goulet, M.L., Sun, Q., Kikkert, M., Iwai, K., Dikic, I., Hiscott, J., and Lin, R.T. (2012). Linear Ubiquitination of NEMO Negatively Regulates the Interferon Antiviral Response through Disruption of the MAVS-TRAF3 Complex. *Cell Host Microbe* 12, 211-222.

Cao, Z., Xiong, J., Takeuchi, M., Kurama, T., and Goeddel, D.V. (1996). TRAF6 is a signal transducer for interleukin-1. *Nature* 383, 443-446.

Chen, Z., Hagler, J., Palombella, V.J., Melandri, F., Scherer, D., Ballard, D., and Maniatis, T. (1995). Signal-induced site-specific phosphorylation targets I kappa B alpha to the ubiquitin-proteasome pathway. *Genes Dev* 9, 1586-1597.

Chen, Z.J. (2005). Ubiquitin signalling in the NF-kappaB pathway. *Nat Cell Biol* 7, 758-765.

Chen, Z.J., and Sun, L.J. (2009). Nonproteolytic functions of ubiquitin in cell signaling. *Mol Cell* 33, 275-286.

Chiu, Y.H., MacMillan, J.B., and Chen, Z.J.J. (2009). RNA Polymerase III Detects Cytosolic DNA and Induces Type I Interferons through the RIG-I Pathway. *Cell* *138*, 576-591.

Chung, J.Y., Park, Y.C., Ye, H., and Wu, H. (2002). All TRAFs are not created equal: common and distinct molecular mechanisms of TRAF-mediated signal transduction. *J Cell Sci* *115*, 679-688.

Clark, K., Takeuchi, O., Akira, S., and Cohen, P. (2011). The TRAF-associated protein TANK facilitates cross-talk within the I kappa B kinase family during Toll-like receptor signaling. *P Natl Acad Sci USA* *108*, 17093-17098.

Cox, J., and Mann, M. (2008). MaxQuant enables high peptide identification rates, individualized p.p.b.-range mass accuracies and proteome-wide protein quantification. *Nature biotechnology* *26*, 1367-1372.

Cox, J., Neuhauser, N., Michalski, A., Scheltema, R.A., Olsen, J.V., and Mann, M. (2011). Andromeda: a peptide search engine integrated into the MaxQuant environment. *Journal of proteome research* *10*, 1794-1805.

Cui, S., Eisenacher, K., Kirchhofer, A., Brzozka, K., Lammens, A., Lammens, K., Fujita, T., Conzelmann, K.K., Krug, A., and Hopfner, K.P. (2008). The C-terminal regulatory domain is the RNA 5'-triphosphate sensor of RIG-I. *Molecular Cell* *29*, 169-179.

Damgaard, R.B., Nachbur, U., Yabal, M., Wong, W.W., Fiil, B.K., Kastirr, M., Rieser, E., Rickard, J.A., Bankovacki, A., Peschel, C., et al. (2012). The ubiquitin ligase XIAP recruits LUBAC for NOD2 signaling in inflammation and innate immunity. *Mol Cell* *46*, 746-758.

Deng, L., Wang, C., Spencer, E., Yang, L., Braun, A., You, J., Slaughter, C., Pickart, C., and Chen, Z.J. (2000). Activation of the IkappaB kinase complex by TRAF6 requires a dimeric ubiquitin-conjugating enzyme complex and a unique polyubiquitin chain. *Cell* *103*, 351-361.

Dranoff, G. (2004). Cytokines in cancer pathogenesis and cancer therapy. *Nat Rev Cancer* *4*, 11-22.

Ea, C.K., Sun, L., Inoue, J., and Chen, Z.J.J. (2004). TIFA activates I kappa B kinase (IKK) by promoting oligomerization and ubiquitination of TRAF6. *P Natl Acad Sci USA* *101*, 15318-15323.

Fitzgerald, K.A., McWhirter, S.M., Faia, K.L., Rowe, D.C., Latz, E., Golenbock, D.T., Coyle, A.J., Liao, S.M., and Maniatis, T. (2003). IKKepsilon and TBK1 are essential components of the IRF3 signaling pathway. *Nat Immunol* *4*, 491-496.

Franchi, L., Wamer, N., Viani, K., and Nunez, G. (2009). Function of Nod-like receptors in microbial recognition and host defense. *Immunological reviews* *227*, 106-128.

Gack, M.U., Shin, Y.C., Joo, C.H., Urano, T., Liang, C., Sun, L.J., Takeuchi, O., Akira, S., Chen, Z.J., Inoue, S.S., *et al.* (2007). TRIM25 RING-finger E3 ubiquitin ligase is essential for RIG-I-mediated antiviral activity. *Nature* *446*, 916-U912.

Gerlach, B., Cordier, S.M., Schmukle, A.C., Emmerich, C.H., Rieser, E., Haas, T.L., Webb, A.I., Rickard, J.A., Anderton, H., Wong, W.W., *et al.* (2011). Linear ubiquitination prevents inflammation and regulates immune signalling. *Nature* *471*, 591-596.

Gitlin, L., Barchet, W., Gilfillan, S., Cella, M., Beutler, B., Flavell, R.A., Diamond, M.S., and Colonna, M. (2006). Essential role of mda-5 in type I IFN responses to polyriboinosinic:polyribocytidylic acid and encephalomyocarditis picornavirus. *Proc Natl Acad Sci U S A* *103*, 8459-8464.

Guo, B., and Cheng, G. (2007). Modulation of the interferon antiviral response by the TBK1/IKK adaptor protein TANK. *J Biol Chem* *282*, 11817-11826.

Haas, T.L., Emmerich, C.H., Gerlach, B., Schmukle, A.C., Cordier, S.M., Rieser, E., Feltham, R., Vince, J., Warnken, U., Wenger, T., *et al.* (2009). Recruitment of the linear ubiquitin chain assembly complex stabilizes the TNF-R1 signaling complex and is required for TNF-mediated gene induction. *Mol Cell* *36*, 831-844.

Hayden, M.S., and Ghosh, S. (2008). Shared principles in NF-kappa B signaling. *Cell* *132*, 344-362.

He, J., Anh, T.N., and Zhang, Y. (2011). KDM2b/JHDM1b, an H3K36me2-specific demethylase, is required for initiation and maintenance of acute myeloid leukemia. *Blood* *117*, 3869-3880.

Hornung, V., Ablasser, A., Charrel-Dennis, M., Bauernfeind, F., Horvath, G., Caffrey, D.R., Latz, E., and Fitzgerald, K.A. (2009). AIM2 recognizes cytosolic dsDNA and forms a caspase-1-activating inflammasome with ASC. *Nature* *458*, 514-518.

Hornung, V., Ellegast, J., Kim, S., Brzozka, K., Jung, A., Kato, H., Poeck, H., Akira, S., Conzelmann, K.K., Schlee, M., *et al.* (2006). 5'-triphosphate RNA is the ligand for RIG-I. *Science* *314*, 994-997.

Hou, F., Sun, L., Zheng, H., Skaug, B., Jiang, Q.X., and Chen, Z.J. (2011). MAVS forms functional prion-like aggregates to activate and propagate antiviral innate immune response. *Cell* *146*, 448-461.

Ikeda, F., Deribe, Y.L., Skanland, S.S., Stieglitz, B., Grabbe, C., Franz-Wachtel, M., van Wijk, S.J., Goswami, P., Nagy, V., Terzic, J., *et al.* (2011). SHARPIN forms a linear ubiquitin ligase complex regulating NF-kappaB activity and apoptosis. *Nature* *471*, 637-641.

Inn, K.S., Gack, M.U., Tokunaga, F., Shi, M.D., Wong, L.Y., Iwai, K., and Jung, J.U. (2011). Linear Ubiquitin Assembly Complex Negatively Regulates RIG-I- and TRIM25-Mediated Type I Interferon Induction. *Molecular Cell* *41*, 354-365.

Inohara, N., Koseki, T., del Peso, L., Hu, Y., Yee, C., Chen, S., Carrio, R., Merino, J., Liu, D., Ni, J., *et al.* (1999). Nod1, an Apaf-1-like activator of caspase-9 and nuclear factor-kappaB. *J Biol Chem* *274*, 14560-14567.

Ishikawa, H., and Barber, G.N. (2008). STING is an endoplasmic reticulum adaptor that facilitates innate immune signalling. *Nature* *455*, 674-678.

Iwai, K., and Ishikawa, H. (2006). [Mechanism underlying ubiquitination of iron regulatory protein 2 (IRP2)]. *Tanpakushitsu kakusan koso Protein, nucleic acid, enzyme* *51*, 1287-1291.

Jiang, X., Kinch, L.N., Brautigam, C.A., Chen, X., Du, F., Grishin, N.V., and Chen, Z.J. (2012). Ubiquitin-induced oligomerization of the RNA sensors RIG-I and MDA5 activates antiviral innate immune response. *Immunity* 36, 959-973.

Jin, L., Waterman, P.M., Jonscher, K.R., Short, C.M., Reisdorph, N.A., and Cambier, J.C. (2008). MPYS, a novel membrane tetraspanner, is associated with major histocompatibility complex class II and mediates transduction of apoptotic signals. *Molecular and Cellular Biology* 28, 5014-5026.

Kato, H., Takeuchi, O., Mikamo-Satoh, E., Hirai, R., Kawai, T., Matsushita, K., Hiirogi, A., Dermody, T.S., Fujita, T., and Akira, S. (2008). Length-dependent recognition of double-stranded ribonucleic acids by retinoic acid-inducible gene-I and melanoma differentiation-associated gene 5. *The Journal of experimental medicine* 205, 1601-1610.

Kawai, T., Takahashi, K., Sato, S., Coban, C., Kumar, H., Kato, H., Ishii, K.J., Takeuchi, O., and Akira, S. (2005). IPS-1, an adaptor triggering RIG-I- and Mda5-mediated type I interferon induction. *Nat Immunol* 6, 981-988.

Kayagaki, N., Phung, Q., Chan, S., Chaudhari, R., Quan, C., O'Rourke, K.M., Eby, M., Pietras, E., Cheng, G.H., Bazan, J.F., *et al.* (2007). DUBA: A deubiquitinase that regulates type I interferon production. *Science* 318, 1628-1632.

Kirisako, T., Kamei, K., Murata, S., Kato, M., Fukumoto, H., Kanie, M., Sano, S., Tokunaga, F., Tanaka, K., and Iwai, K. (2006). A ubiquitin ligase complex assembles linear polyubiquitin chains. *EMBO J* 25, 4877-4887.

Kishore, N., Huynh, Q.K., Mathialagan, S., Hall, T., Rouw, S., Creely, D., Lange, G., Caroll, J., Reitz, B., Donnelly, A., *et al.* (2002). IKK-i and TBK-1 are enzymatically distinct from the homologous enzyme IKK-2 - Comparative analysis of recombinant human IKK-i, TBK-1, and IKK-2. *Journal of Biological Chemistry* 277, 13840-13847.

Kowalinski, E., Lunardi, T., McCarthy, A.A., Louber, J., Brunel, J., Grigorov, B., Gerlier, D., and Cusack, S. (2011). Structural basis for the activation of innate immune pattern-recognition receptor RIG-I by viral RNA. *Cell* 147, 423-435.

Lamothe, B., Besse, A., Webster, W.K., Campos, A.D., Wu, H., and Darnay, B.G. (2006). Site-specific TRAF6 auto-ubiquitination via Lys63 linkages connects RANK to osteoclastogenesis. *J Bone Miner Res* 21, S24-S24.

Le Bon, A., and Tough, D.F. (2002). Links between innate and adaptive immunity via type I interferon. *Current opinion in immunology* *14*, 432-436.

Li, S., Wang, L., and Dorf, M.E. (2009). PKC phosphorylation of TRAF2 mediates IKKalpha/beta recruitment and K63-linked polyubiquitination. *Mol Cell* *33*, 30-42.

Li, S.T., Wang, L.Y., Berman, M., Kong, Y.Y., and Dorf, M.E. (2011a). Mapping a Dynamic Innate Immunity Protein Interaction Network Regulating Type I Interferon Production. *Immunity* *35*, 426-440.

Li, X.D., and Chen, Z.J. (2012). Sequence specific detection of bacterial 23S ribosomal RNA by TLR13. *eLife* *1*, e00102.

Li, X.D., Chiu, Y.H., Ismail, A.S., Behrendt, C.L., Wight-Carter, M., Hooper, L.V., and Chen, Z.J. (2011b). Mitochondrial antiviral signaling protein (MAVS) monitors commensal bacteria and induces an immune response that prevents experimental colitis. *Proc Natl Acad Sci U S A* *108*, 17390-17395.

Lin, L., and Ghosh, S. (1996). A glycine-rich region in NF-kappa B p105 functions as a processing signal for the generation of the p50 subunit. *Molecular and Cellular Biology* *16*, 2248-2254.

Ling, L., and Goeddel, D.V. (2000). T6BP, a TRAF6-interacting protein involved in IL-1 signaling. *P Natl Acad Sci USA* *97*, 9567-9572.

Liu, S., and Chen, Z.J. (2011). Expanding role of ubiquitination in NF-kappaB signaling. *Cell Res* *21*, 6-21.

Lomaga, M.A., Yeh, W.C., Sarosi, I., Duncan, G.S., Furlonger, C., Ho, A., Morony, S., Capparelli, C., Van, G., Kaufman, S., *et al.* (1999). TRAF6 deficiency results in osteopetrosis and defective interleukin-1, CD40, and LPS signaling. *Genes Dev* *13*, 1015-1024.

Luo, D.H., Ding, S.C., Vela, A., Kohlway, A., Lindenbach, B.D., and Pyle, A.M. (2011). Structural Insights into RNA Recognition by RIG-I. *Cell* *147*, 409-422.

Ma, X.L., Helgason, E., Phung, Q.T., Quan, C.L., Iyer, R.S., Lee, M.W., Bowman, K.K., Starovasnik, M.A., and Dueber, E.C. (2012). Molecular basis of Tank-binding kinase 1 activation by transautophosphorylation. *P Natl Acad Sci USA* *109*, 9378-9383.

Maelfait, J., Roose, K., Bogaert, P., Sze, M., Saelens, X., Pasparakis, M., Carpentier, I., van Loo, G., and Beyaert, R. (2012). A20 (Tnfaip3) Deficiency in Myeloid Cells Protects against Influenza A Virus Infection. *Plos Pathog* *8*.

Mao, A.P., Li, S., Zhong, B., Li, Y., Yan, J., Li, Q., Teng, C.W., and Shu, H.B. (2010). Virus-triggered Ubiquitination of TRAF3/6 by cIAP1/2 Is Essential for Induction of Interferon-beta (IFN-beta) and Cellular Antiviral Response. *Journal of Biological Chemistry* *285*, 9470-9476.

McWhirter, S.M., Tenoever, B.R., and Maniatis, T. (2005). Connecting mitochondria and innate immunity. *Cell* *122*, 645-647.

Meylan, E., Curran, J., Hofmann, K., Moradpour, D., Binder, M., Bartenschlager, R., and Tschoopp, R. (2005). Cardif is an adaptor protein in the RIG-I antiviral pathway and is targeted by hepatitis C virus. *Nature* *437*, 1167-1172.

Mushegian, A., and Medzhitov, R. (2001). Evolutionary perspective on innate immune recognition. *The Journal of cell biology* *155*, 705-710.

Niu, J., Shi, Y., Iwai, K., and Wu, Z.H. (2011). LUBAC regulates NF-kappaB activation upon genotoxic stress by promoting linear ubiquitination of NEMO. *EMBO J* *30*, 3741-3753.

O'Neill, L.A., and Bowie, A.G. (2007). The family of five: TIR-domain-containing adaptors in Toll-like receptor signalling. *Nat Rev Immunol* *7*, 353-364.

O'Neill, L.A., and Bowie, A.G. (2010). Sensing and signaling in antiviral innate immunity. *Curr Biol* *20*, R328-333.

Oganesyan, G., Saha, S.K., Guo, B.C., He, J.Q., Shahangian, A., Zarnegar, B., Perry, A., and Cheng, G.H. (2006). Critical role of TRAF3 in the Toll-like receptor-dependent and -independent antiviral response. *Nature* *439*, 208-211.

- Ogura, Y., Inohara, N., Benito, A., Chen, F.F., Yamaoka, S., and Nunez, G. (2001). Nod2, a Nod1/Apaf-1 family member that is restricted to monocytes and activates NF-kappa B. *Journal of Biological Chemistry* 276, 4812-4818.
- Oldenburg, M., Kruger, A., Ferstl, R., Kaufmann, A., Nees, G., Sigmund, A., Bathke, B., Lauterbach, H., Suter, M., Dreher, S., *et al.* (2012). TLR13 recognizes bacterial 23S rRNA devoid of erythromycin resistance-forming modification. *Science* 337, 1111-1115.
- Ou, Y.H., Torres, M., Ram, R., Formstecher, E., Roland, C., Cheng, T., Brekken, R., Wurz, R., Tasker, A., Polverino, T., *et al.* (2011). TBK1 directly engages Akt/PKB survival signaling to support oncogenic transformation. *Mol Cell* 41, 458-470.
- Panne, D., McWhirter, S.M., Maniatis, T., and Harrison, S.C. (2007). Interferon regulatory factor 3 is regulated by a dual phosphorylation-dependent switch. *Journal of Biological Chemistry* 282, 22816-22822.
- Park, Y.C., Burkitt, V., Villa, A.R., Tong, L., and Wu, H. (1999). Structural basis for self-association and receptor recognition of human TRAF2. *Nature* 398, 533-538.
- Paz, S., Vilasco, M., Werden, S.J., Arguello, M., Joseph-Pillai, D., Zhao, T., Nguyen, T.L., Sun, Q., Meurs, E.F., Lin, R., *et al.* (2011). A functional C-terminal TRAF3-binding site in MAVS participates in positive and negative regulation of the IFN antiviral response. *Cell Res* 21, 895-910.
- Pertel, T., Hausmann, S., Morger, D., Zuger, S., Guerra, J., Lascano, J., Reinhard, C., Santoni, F.A., Uchil, P.D., Chatel, L., *et al.* (2011). TRIM5 is an innate immune sensor for the retrovirus capsid lattice. *Nature* 472, 361-365.
- Petroski, M.D., Zhou, X.L., Dong, G.Q., Daniel-Issakani, S., Payan, D.G., and Huang, J.N. (2007). Substrate modification with lysine 63-linked ubiquitin chains through the UBC13-UEV1A ubiquitin-conjugating enzyme. *Journal of Biological Chemistry* 282, 29936-29945.
- Pichlmair, A., and Reis e Sousa, C. (2007). Innate recognition of viruses. *Immunity* 27, 370-383.

Pichlmair, A., Schulz, O., Tan, C.P., Naslund, T.I., Liljestrom, P., Weber, F., and Reis e Sousa, C. (2006). RIG-I-mediated antiviral responses to single-stranded RNA bearing 5'-phosphates. *Science* *314*, 997-1001.

Piwko, W., and Jentsch, S. (2006). Proteasome-mediated protein processing by bidirectional degradation initiated from an internal site. *Nature Structural & Molecular Biology* *13*, 691-697.

Pomerantz, J.L., and Baltimore, D. (2002). Two pathways to NF-kappaB. *Mol Cell* *10*, 693-695.

Psakhye, I., and Jentsch, S. (2012). Protein Group Modification and Synergy in the SUMO Pathway as Exemplified in DNA Repair. *Cell* *151*, 807-820.

Qin, B.Y., Liu, C., Lam, S.S., Srinath, H., Delston, R., Correia, J.J., Derynck, R., and Lin, K. (2003). Crystal structure of IRF-3 reveals mechanism of autoinhibition and virus-induced phosphoactivation. *Nat Struct Biol* *10*, 913-921.

Rahighi, S., Ikeda, F., Kawasaki, M., Akutsu, M., Suzuki, N., Kato, R., Kensche, T., Uejima, T., Bloor, S., Komander, D., *et al.* (2009). Specific Recognition of Linear Ubiquitin Chains by NEMO Is Important for NF-kappa B Activation. *Cell* *136*, 1098-1109.

Roach, J.C., Glusman, G., Rowen, L., Kaur, A., Purcell, M.K., Smith, K.D., Hood, L.E., and Aderem, A. (2005). The evolution of vertebrate Toll-like receptors. *Proc Natl Acad Sci U S A* *102*, 9577-9582.

Rothenfusser, S., Goutagny, N., DiPerna, G., Gong, M., Monks, B.G., Schoenemeyer, A., Yamamoto, M., Akira, S., and Fitzgerald, K.A. (2005). The RNA helicase Lgp2 inhibits TLR-independent sensing of viral replication by retinoic acid-inducible gene-I. *J Immunol* *175*, 5260-5268.

Ryzhakov, G., and Randow, F. (2007). SINTBAD, a novel component of innate antiviral immunity, shares a TBK1-binding domain with NAP1 and TANK. *EMBO J* *26*, 3180-3190.

Saha, S.K., Pietras, E.M., He, J.Q., Kang, J.R., Liu, S.Y., Oganesyan, G., Shahangian, A., Zarnegar, B., Shiba, T.L., Wang, Y., *et al.* (2006). Regulation of antiviral responses by a direct and specific interaction between TRAF3 and Cardif. *EMBO J* 25, 3257-3263.

Sasai, M., Shingai, M., Funami, K., Yoneyama, M., Fujita, T., Matsumoto, M., and Seya, T. (2006). NAK-associated protein 1 participates in both the TLR3 and the cytoplasmic pathways in type IIFN induction. *J Immunol* 177, 8676-8683.

Satoh, T., Kato, H., Kumagai, Y., Yoneyama, M., Sato, S., Matsushita, K., Tsujimura, T., Fujita, T., Akira, S., and Takeuchi, O. (2010). LGP2 is a positive regulator of RIG-I- and MDA5-mediated antiviral responses. *P Natl Acad Sci USA* 107, 1512-1517.

Sauer, J.D., Sotelo-Troha, K., von Moltke, J., Monroe, K.M., Rae, C.S., Brubaker, S.W., Hyodo, M., Hayakawa, Y., Woodward, J.J., Portnoy, D.A., *et al.* (2011). The N-ethyl-N-nitrosourea-induced Goldenticket mouse mutant reveals an essential function of Sting in the in vivo interferon response to Listeria monocytogenes and cyclic dinucleotides. *Infection and immunity* 79, 688-694.

Scherer, D.C., Brockman, J.A., Chen, Z.J., Maniatis, T., and Ballard, D.W. (1995). Signal-Induced Degradation of I-Kappa-B-Alpha Requires Site-Specific Ubiquitination. *P Natl Acad Sci USA* 92, 11259-11263.

Schrofelbauer, B., Polley, S., Behar, M., Ghosh, G., and Hoffmann, A. (2012). NEMO Ensures Signaling Specificity of the Pleiotropic IKK beta by Directing Its Kinase Activity toward I kappa B alpha. *Molecular Cell* 47, 111-121.

Seth, R.B., Sun, L., Ea, C.K., and Chen, Z.J. (2005). Identification and characterization of MAVS, a mitochondrial antiviral signaling protein that activates NF-kappaB and IRF 3. *Cell* 122, 669-682.

Sharma, S., tenOever, B.R., Grandvaux, N., Zhou, G.P., Lin, R.T., and Hiscott, J. (2003). Triggering the interferon antiviral response through an IKK-related pathway. *Science* 300, 1148-1151.

Skaug, B., Chen, J., Du, F., He, J., Ma, A., and Chen, Z.J. (2011). Direct, noncatalytic mechanism of IKK inhibition by A20. *Mol Cell* 44, 559-571.

- Spencer, E., Jiang, J., and Chen, Z.J. (1999). Signal-induced ubiquitination of IkappaBalph α by the F-box protein Slimb/beta-TrCP. *Genes Dev* 13, 284-294.
- Stetson, D.B., and Medzhitov, R. (2006). Type I interferons in host defense. *Immunity* 25, 373-381.
- Sun, L., Liu, S., and Chen, Z.J. (2010). SnapShot: pathways of antiviral innate immunity. *Cell* 140, 436-436 e432.
- Sun, L.J., Deng, L., Ea, C.K., Xia, Z.P., and Chen, Z.J.J. (2004). The TRAF6 ubiquitin ligase and TAK1 kinase mediate IKK activation by BCL10 and MALT1 in T lymphocytes. *Molecular Cell* 14, 289-301.
- Takahasi, K., Suzuki, N.N., Horiuchi, M., Mori, M., Suhara, W., Okabe, Y., Fukuhara, Y., Terasawa, H., Akira, S., Fujita, T., *et al.* (2003). X-ray crystal structure of IRF-3 and its functional implications. *Nat Struct Biol* 10, 922-927.
- Takeuchi, O., and Akira, S. (2008). MDA5/RIG-I and virus recognition. *Current opinion in immunology* 20, 17-22.
- Takeuchi, O., and Akira, S. (2010). Pattern recognition receptors and inflammation. *Cell* 140, 805-820.
- Tamura, T., Yanai, H., Savitsky, D., and Taniguchi, T. (2008). The IRF family transcription factors in immunity and oncogenesis. *Annual review of immunology* 26, 535-584.
- Tanaka, Y., and Chen, Z.J. (2012). STING Specifies IRF3 Phosphorylation by TBK1 in the Cytosolic DNA Signaling Pathway. *Sci Signal* 5, ra20.
- Tang, E.D., and Wang, C.Y. (2010). TRAF5 is a downstream target of MAVS in antiviral innate immune signaling. *PLoS One* 5, e9172.
- Taniguchi, T., Ogasawara, K., Takaoka, A., and Tanaka, N. (2001). IRF family of transcription factors as regulators of host defense. *Annual review of immunology* 19, 623-655.

Tokunaga, F., Nakagawa, T., Nakahara, M., Saeki, Y., Taniguchi, M., Sakata, S., Tanaka, K., Nakano, H., and Iwai, K. (2011). SHARPIN is a component of the NF-kappaB-activating linear ubiquitin chain assembly complex. *Nature* *471*, 633-636.

Tokunaga, F., Sakata, S., Saeki, Y., Satomi, Y., Kirisako, T., Kamei, K., Nakagawa, T., Kato, M., Murata, S., Yamaoka, S., *et al.* (2009). Involvement of linear polyubiquitylation of NEMO in NF-kappaB activation. *Nat Cell Biol* *11*, 123-132.

Traenckner, E.B., Pahl, H.L., Henkel, T., Schmidt, K.N., Wilk, S., and Baeuerle, P.A. (1995). Phosphorylation of human I kappa B-alpha on serines 32 and 36 controls I kappa B-alpha proteolysis and NF-kappa B activation in response to diverse stimuli. *EMBO J* *14*, 2876-2883.

Tseng, P.H., Matsuzawa, A., Zhang, W., Mino, T., Vignali, D.A., and Karin, M. (2010). Different modes of ubiquitination of the adaptor TRAF3 selectively activate the expression of type I interferons and proinflammatory cytokines. *Nat Immunol* *11*, 70-75.

Venkataraman, T., Valdes, M., Elsby, R., Kakuta, S., Caceres, G., Saijo, S., Iwakura, Y., and Barber, G.N. (2007). Loss of DExD/H box RNA helicase LGP2 manifests disparate antiviral responses. *J Immunol* *178*, 6444-6455.

Vitour, D., Dabo, S., Ahmadi Pour, M., Vilasco, M., Vidalain, P.O., Jacob, Y., Mezel-Lemoine, M., Paz, S., Arguello, M., Lin, R., *et al.* (2009). Polo-like kinase 1 (PLK1) regulates interferon (IFN) induction by MAVS. *J Biol Chem* *284*, 21797-21809.

Wang, C., Deng, L., Hong, M., Akkaraju, G.R., Inoue, J., and Chen, Z.J.J. (2001). TAK1 is a ubiquitin-dependent kinase of MKK and IKK. *Nature* *412*, 346-351.

Wang, L., Li, S., and Dorf, M.E. (2012). NEMO Binds Ubiquitinated TANK-Binding Kinase 1 (TBK1) to Regulate Innate Immune Responses to RNA Viruses. *PLoS One* *7*, e43756.

Xia, Z.P., Sun, L., Chen, X., Pineda, G., Jiang, X., Adhikari, A., Zeng, W., and Chen, Z.J. (2009). Direct activation of protein kinases by unanchored polyubiquitin chains. *Nature* *461*, 114-119.

Xie, X., Zhang, D., Zhao, B., Lu, M.K., You, M., Condorelli, G., Wang, C.Y., and Guan, K.L. (2011). IkappaB kinase epsilon and TANK-binding kinase 1 activate AKT by direct phosphorylation. *Proc Natl Acad Sci U S A* **108**, 6474-6479.

Xu, L.G., Wang, Y.Y., Han, K.J., Li, L.Y., Zhai, Z.H., and Shu, H.B. (2005). VISA is an adapter protein required for virus-triggered IFN-beta signaling. *Molecular Cell* **19**, 727-740.

Xu, M., Skaug, B., Zeng, W., and Chen, Z.J. (2009). A ubiquitin replacement strategy in human cells reveals distinct mechanisms of IKK activation by TNFalpha and IL-1beta. *Mol Cell* **36**, 302-314.

Yamamoto, Y., Kim, D.W., Kwak, Y.T., Prajapati, S., Verma, U., and Gaynor, R.B. (2001). IKK gamma/NEMO facilitates the recruitment of the I kappa B proteins into the I kappa B kinase complex. *Journal of Biological Chemistry* **276**, 36327-36336.

Yan, N., Regalado-Magdos, A.D., Stiggebout, B., Lee-Kirsch, M.A., and Lieberman, J. (2010). The cytosolic exonuclease TREX1 inhibits the innate immune response to human immunodeficiency virus type 1. *Nat Immunol* **11**, 1005-1013.

Ye, H., Arron, J.R., Lamothe, B., Cirilli, M., Kobayashi, T., Shevde, N.K., Segal, D., Dzivenu, O.K., Vologodskaya, M., Yim, M., *et al.* (2002a). Distinct molecular mechanism for initiating TRAF6 signalling. *Nature* **418**, 443-447.

Ye, H., Cirilli, M., and Wu, H. (2002b). The use of construct variation and diffraction data analysis in the crystallization of the TRAF domain of human tumor necrosis factor receptor associated factor 6. *Acta Crystallogr D* **58**, 1886-1888.

Yeh, W.C., Shahinian, A., Speiser, D., Kraunus, J., Billia, F., Wakeham, A., de la Pompa, J.L., Ferrick, D., Hum, B., Iscove, N., *et al.* (1997). Early lethality, functional NF-kappaB activation, and increased sensitivity to TNF-induced cell death in TRAF2-deficient mice. *Immunity* **7**, 715-725.

Yin, Q., Lamothe, B., Darnay, B.G., and Wu, H. (2009). Structural basis for the lack of E2 interaction in the RING domain of TRAF2. *Biochemistry-US* **48**, 10558-10567.

Yoneyama, M., and Fujita, T. (2008). Structural mechanism of RNA recognition by the RIG-I-like receptors. *Immunity* 29, 178-181.

Yoneyama, M., Kikuchi, M., Matsumoto, K., Imaizumi, T., Miyagishi, M., Taira, K., Foy, E., Loo, Y.M., Gale, M., Jr., Akira, S., *et al.* (2005). Shared and unique functions of the DExD/H-box helicases RIG-I, MDA5, and LGP2 in antiviral innate immunity. *J Immunol* 175, 2851-2858.

Yoneyama, M., Kikuchi, M., Natsukawa, T., Shinobu, N., Imaizumi, T., Miyagishi, M., Taira, K., Akira, S., and Fujita, T. (2004). The RNA helicase RIG-I has an essential function in double-stranded RNA-induced innate antiviral responses. *Nature Immunology* 5, 730-737.

Zeng, W., Xu, M., Liu, S., Sun, L., and Chen, Z.J. (2009). Key role of Ubc5 and lysine-63 polyubiquitination in viral activation of IRF3. *Mol Cell* 36, 315-325.

Zeng, W.W., Sun, L.J., Jiang, X.M., Chen, X., Hou, F.J., Adhikari, A., Xu, M., and Chen, Z.J.J. (2010). Reconstitution of the RIG-I Pathway Reveals a Signaling Role of Unanchored Polyubiquitin Chains in Innate Immunity. *Cell* 141, 315-330.

Zhao, T., Yang, L., Sun, Q., Arguello, M., Ballard, D.W., Hiscott, J., and Lin, R. (2007). The NEMO adaptor bridges the nuclear factor-kappaB and interferon regulatory factor signaling pathways. *Nat Immunol* 8, 592-600.

Zhong, B., Yang, Y., Li, S., Wang, Y.Y., Li, Y., Diao, F., Lei, C., He, X., Zhang, L., Tien, P., *et al.* (2008). The adaptor protein MITA links virus-sensing receptors to IRF3 transcription factor activation. *Immunity* 29, 538-550.